

## ***Supporting Information***

### **Outline**

<b>I. Experimental Part.....</b>	<b>2</b>
I.1. General methods.....	2
I.2. Synthetic procedures.....	3
I.3. NMR spectra .....	9
I.4. X-ray studies .....	23
I.5. Chiral HPLC separations .....	26
I.6. Photophysical studies .....	32
I.7. Optical rotations.....	35
I.8. Experimental electronic circular dichroism and UV-visible spectra .....	35
I.9. Circularly polarized luminescence spectra .....	36
I.10. References .....	37
<b>II. Computational Part .....</b>	<b>38</b>
II.1. Computational details .....	38
II.2. Additional computed data .....	39
II.3. Cartesian coordinates for optimized structures .....	51
II.4. References .....	65

# I. Experimental Part

## I.1. General methods

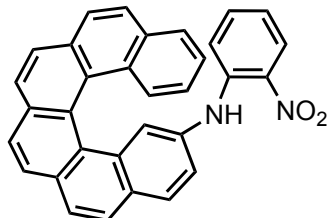
Experiments were performed using standard Schlenk techniques. Column chromatography purifications were performed in air over silica gel (Macherey Nagel 60 M, 0.04–0.063 mm). Irradiation reactions were conducted using a Heraeus TQ 150 mercury vapor lamp. All reactions were monitored by TLC analysis and visualizations were accomplished by irradiation with a UV light at 254 nm and 356 nm. THF was dried using Na/Benzophenone method. Dry toluene was obtained from an MB-SPS-800 distillation machine. Dry 1,4-dioxane over molecular sieves were purchased from Sigma-Aldrich and were directly used without further treatment. Cesium carbonate was dried in a 110°C oven for several days and stored at the same temperature. Other reagents or solvents were purchased from usual providers and were used as received unless otherwise stated. Microwave experiments were performed on an Anton-Paar Monowave 300 (with the technical support of the S2Wave platform, Univ. Rennes, 10A building).

<sup>1</sup>H and <sup>13</sup>C{<sup>1</sup>H} NMR spectra were recorded at room temperature either on a Bruker Avance I 300 MHz, Bruker Avance III 300 MHz or 400 MHz spectrometer equipped with a tunable BBFO probe, or a Bruker NEO 500 MHz spectrometer fitted with a TCI cryoprobe (Biosit platform – Université de Rennes I). NMR analyses of the stereoisomers of **1a** and **1b** were performed on a Bruker Avance NEO 900 MHz equipped with a CPTCI cryoprobe (UCCS-UGSF, UMR CNRS 8181-8576, Lille). Chemical shifts  $\delta$  are given in ppm and coupling constants  $J$  in Hz. <sup>1</sup>H and <sup>13</sup>C NMR chemical shifts were determined using residual signals of the deuterated solvents: deuterated dichloromethane (<sup>1</sup>H  $\delta$  = 5.32 ppm, <sup>13</sup>C  $\delta$  = 54.0 ppm) or deuterated chloroform (<sup>1</sup>H  $\delta$  = 7.26 ppm, <sup>13</sup>C  $\delta$  = 77.16 ppm). The terms s, d, t, q, hept, m indicate respectively singlet, doublet, triplet, quartet, heptuplet, multiplet; b stands for broad; dd is doublet of doublets, dt – doublet of triplets, td – triplet of doublets. Assignment of proton and carbon signals was based on COSY, NOESY, edited-HSQC, and HMBC experiments. <sup>1</sup>H dipolar couplings were studied using NOESY sequence, with 500 or 800 ms mixing time or ROESY sequence with 400 ms mixing time. High-resolution mass spectrometry (HR-MS) measurements were performed by the CRMPO, University of Rennes 1.

## I.2. Synthetic procedures

Racemic 2-bromo-[6]helicene (*rac*)-**2**<sup>[1]</sup> and pentahelicenic imidazolium **7**<sup>[2]</sup> were synthesized according to the literature.

### *N*-(2-Nitrophenyl)[6]helicen-11-amine (*rac*)-**3**



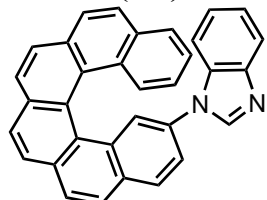
In a dried microwave reactor, were placed 2-bromo[6]helicene (*rac*)-**2** (183.3 mg, 0.45 mmol), *o*-nitroaniline (93.2 mg, 0.67 mmol), Pd(OAc)<sub>2</sub> (10.4 mg, 0.046 mmol), Xantphos (26.7 mg, 0.046 mmol) and dried Cs<sub>2</sub>CO<sub>3</sub> (295.1 mg, 0.90 mmol). The solids were dissolved in dried toluene (10 mL) and the reaction mixture was degassed by Ar bubbling for 10 min before being stirred and heated at 170°C for 30 min under microwave irradiation. The completion of the reaction was checked by TLC analysis and the reaction mixture was further filtered over a Celite pad washed with CH<sub>2</sub>Cl<sub>2</sub>. After evaporation under reduced pressure, the obtained crude was purified by column chromatography (SiO<sub>2</sub>, *n*-heptane / EtOAc = 9:1) to afford the desired product (*rac*)-**3** as a bright orange/red solid (133 mg, 64% yield).

**<sup>1</sup>H NMR (400 MHz, CDCl<sub>3</sub>)** δ = 8.82 (s, 1H), 8.09 (dd, *J* = 8.6, 1.6, 1H), 8.04 – 7.90 (m, 8H), 7.90 – 7.86 (m, 1H), 7.84 (dd, *J* = 8.5, 1.3, 1H), 7.64 (dd, *J* = 8.6, 1.1, 1H), 7.46 (d, *J* = 2.1, 1H), 7.30 (ddd, *J* = 8.0, 6.9, 1.2, 1H), 7.14 (td, *J* = 8.0, 1.8, 2H), 6.78 (ddd, *J* = 8.4, 6.8, 1.4, 1H), 6.66 (ddd, *J* = 8.4, 6.9, 1.3, 1H), 6.44 (dd, *J* = 8.6, 1.3, 1H).

**<sup>13</sup>C NMR (101 MHz, CDCl<sub>3</sub>)** δ = 142.5, 135.7, 135.5, 133.2, 133.1, 132.1, 131.8, 131.6, 131.1, 129.8, 129.7, 129.0, 128.1, 127.9, 127.5, 127.5, 127.5, 127.5, 127.4, 127.4, 127.3, 127.1, 126.5, 126.4, 126.2, 126.0, 124.8, 124.2, 122.3, 122.2, 117.5, 116.3.

**HR-MS (ESI, CH<sub>3</sub>OH / CH<sub>2</sub>Cl<sub>2</sub> = 90:10)** [M+K]<sup>+</sup> (C<sub>32</sub>H<sub>20</sub>N<sub>2</sub>O<sub>2</sub>K): calculated for 503.11564 m/z, found 503.1158 (Δ = 0 ppm).

### 1-([6]Helicen-11-yl)-1*H*-benzo[d]imidazole (*rac*)-**5**



In a 250 mL round-bottom flask, was placed (*rac*)-**3** (192 mg, 0.41 mmol) and tin(II) chloride dihydrate (460.1 mg, 2.03 mmol). The solids were further dissolved in EtOH (30 mL) and concentrated HCl was added (2/1, v/v). The red reaction mixture was then stirred vigorously while heated at reflux overnight. Over time, the red color changed to green-yellow progressively. The completion of the reaction was checked by TLC analysis. (If the reaction is not completed, equivalents of tin(II) chloride dihydrate, 10 mL of concentrated HCl and 5 mL of EtOAc can be additionally added to the reaction mixture. It can then be stirred for a longer time at reflux until the reaction mixture becomes green-yellow again and all the starting material is consumed according to TLC analysis.) After cooling down to room temperature, the reaction

was quenched by a slow addition of aqueous sat. NaHCO<sub>3</sub> until the bubbling stopped (about 120 mL). At the end, the solution should be bright yellow and heterogenous. The white precipitate was removed by filtration over a Celite pad washed excessively with EtOAc. The clear filtrate was then washed with aqueous sat. NaHCO<sub>3</sub> to ensure an alkaline pH and the combined aqueous layers were extracted with EtOAc three times. Finally, the gathered organic layers were dried with MgSO<sub>4</sub>, then filtered, and the solvent was evaporated under reduced pressure to afford a yellow wax corresponding to amino derivative (*rac*)-4 that was used directly in the next step without further purification.

The product obtained from previous step, (*rac*)-4, was placed in a 100 mL round-bottom flask and dissolved in triethyl orthoformate (3 mL). After addition of a catalytic amount of *p*-toluenesulfonic acid monohydrate (about 5 mg), the obtained reaction mixture was stirred at 80°C overnight. It was then cooled down to room temperature and diluted with CH<sub>2</sub>Cl<sub>2</sub>. The organic layer was washed with aqueous sat. NaHCO<sub>3</sub> three times and the aqueous layers were extracted twice with CH<sub>2</sub>Cl<sub>2</sub>. The combined organic layers were dried with MgSO<sub>4</sub>, then filtered, and the solvent was evaporated under reduced pressure. The obtained crude was further purified by column chromatography (SiO<sub>2</sub>, *n*-heptane / EtOAc = 8:2 to 1:1) to afford the desired product (*rac*)-5 as a beige solid (123 mg, 68% yield over 2 steps).

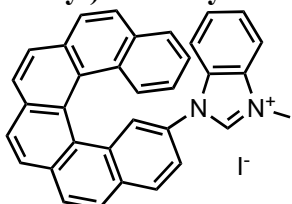
**<sup>1</sup>H NMR (500 MHz, CD<sub>2</sub>Cl<sub>2</sub>)** δ = 8.11 – 7.96 (m, 10H), 7.72 (d, *J* = 8.6, 1.1, 1H), 7.69 (d, *J* = 2.1, 1H), 7.66 (d, *J* = 8.1, 1H), 7.43 (dd, *J* = 8.4, 2.1, 1H), 7.38 (ddd, *J* = 8.0, 6.8, 1.2, 1H), 7.19 (ddd, *J* = 8.1, 7.1, 1.2, 1H), 7.13 (ddd, *J* = 7.5, 7.1, 0.8, 1H), 6.97 (d, *J* = 8.1, 1H), 6.84 (ddd, *J* = 8.4, 6.8, 1.4, 1H), 6.77 (s, 1H).

**<sup>13</sup>C NMR (126 MHz, CD<sub>2</sub>Cl<sub>2</sub>)** δ = 144.3, 143.5, 134.2, 133.9, 133.5, 132.7, 132.4, 131.5, 131.3, 130.1, 130.0, 128.5, 128.5, 128.3, 128.2, 128.0, 127.9, 127.8, 127.8, 127.8, 127.7, 127.4, 126.8, 125.7, 124.3, 123.9, 123.6, 122.8, 122.0, 120.4, 110.7. Due to overlapping, two signals cannot be seen.

**HR-MS (ESI, CH<sub>3</sub>OH / CH<sub>2</sub>Cl<sub>2</sub> = 90:10)** [M+H]<sup>+</sup> (C<sub>33</sub> H<sub>21</sub> N<sub>2</sub>): calculated for 445.16992 m/z, found 445.1697 (Δ = 0 ppm).

Enantiopure samples of (*M*)-(–) and (*P*)-(+)-5 were obtained by HPLC separations over a chiral stationary phase (*vide infra*).

#### (*M*)-(–) and (*P*)-(+)-1-[6]Helicen-11-yl)-3-methyl-1*H*-benzo[*d*]imidazol-3-i um iodide 6



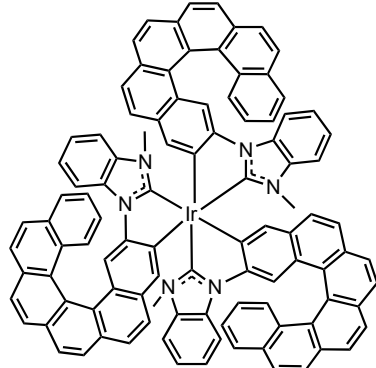
In a dried Schlenk tube, was placed (*M*)-(–)-5 (27.9 mg, 0.067 mmol) which was dissolved in acetonitrile (4 mL) after 3 cycles vacuum/argon. Under argon, was added an excess of methyl iodide. The reaction mixture was then sealed with a Teflon Cap and was heated at 95°C overnight. The resulting heterogenous mixture was finally allowed to cool down to room temperature, and the solvent was evaporated under vacuum. The resulting residue was transferred into a round-bottom flask by dissolution and evaporation of CH<sub>2</sub>Cl<sub>2</sub>. The solid was then washed with acetone, Et<sub>2</sub>O and EtOAc to afford pure iodide salt (*M*)-(–)-6 as a light-brown solid (36.5 mg, 99% yield: yield is slightly overestimated due to the hygroscopic nature of the salt). The procedure was reproduced with the other enantiomer, (*P*)-(+)-5 as starting material (0.089 mmol scale) and the corresponding salt (*P*)-(+)-6 was obtained in 90% yield.

**<sup>1</sup>H NMR (400 MHz, CD<sub>2</sub>Cl<sub>2</sub>)** δ = 9.31 (s, 1), 8.23 (d, *J* = 8.6, 1H), 8.20 (d, *J* = 8.6, 1H), 8.17 – 8.10 (m, 3), 8.10 – 8.00 (m, 2H), 7.97 – 7.92 (m, 2H), 7.91 – 7.87 (m, 2H), 7.78 – 7.71 (m, 3H), 7.68 (ddd, *J* = 8.4, 7.1, 1.0, 1H), 7.55 (ddd, *J* = 8.4, 7.1, 1.3, 1), 7.50 (t, *J* = 8.0, 6.8, 1.1, 1H), 6.95 (t, *J* = 8.5, 6.9, 1.4, 1H), 6.59 (d, *J* = 8.4, 1H), 4.27 (s, 3H).

**<sup>13</sup>C{<sup>1</sup>H} NMR** was not resolved enough due to low solubility of the compound.

**HR-MS (ESI, CH<sub>3</sub>OH / CH<sub>2</sub>Cl<sub>2</sub> = 90:10) [M+H]<sup>+</sup>** (C<sub>34</sub> H<sub>23</sub> N<sub>2</sub>): calculated for 459.18557 m/z, found 459.1861 ( $\Delta$  = 1 ppm).

### Enantiopure (*M*)-(–) and (*P*)-(+) tris-(*N*-([6]helicen-11-yl)-*N*-methyl-benzimidazol-2-ylidene)iridium(III) complex 1



In a dried Schlenk tube protected from light with aluminum foil, was placed (*M*)-(–)-6 (38.7 mg, 0.065 mmol) and Ag<sub>2</sub>O (5.2 mg, 0.022 mmol). After 3 vacuum/argon cycles, the solids were dissolved in distilled 1,4-dioxane (3 mL) and the reaction mixture was stirred at 60°C overnight in the dark. Then, [Ir(COD)Cl]<sub>2</sub> (7 mg, 0.010 mmol) was added into the Schlenk tube, the temperature was elevated to 120°C, and the mixture was stirred at this temperature for 24 h. Then, it was allowed to cool down to room temperature and further filtered over a Celite pad washed with CH<sub>2</sub>Cl<sub>2</sub>. After evaporation of the solvent under reduced pressure, <sup>1</sup>H-NMR analysis of the obtained crude confirmed the formation of the desired tris-NHC-helicene cyclometalated iridium(III) complex as a mixture of diastereoisomers (*mer*-(*M*,*A*<sub>Ir</sub>)-1a / *mer*-(*M*,*A*<sub>Ir</sub>)-1b / *fac*-(*M*,*A*<sub>Ir</sub>)-1c = 25 : 40 : 35 as determined by <sup>1</sup>H NMR) that were found to be neither separable by column chromatography nor preparative thin-layer chromatography. Thus, the mixture was purified and separated using chiral HPLC column chromatography (see ‘Chiral HPLC separations’ section for details) to afford pure *mer*-(*M*,*A*<sub>Ir</sub>)-1a (1.4 mg, 5% yield), pure *mer*-(*M*,*A*<sub>Ir</sub>)-1b (5.7 mg, 18% yield) and pure *fac*-(*M*,*A*<sub>Ir</sub>)-1c (0.6 mg, 2% yield), respectively. The procedure was reproduced with the other enantiomer, (*P*)-(+)-6 as starting material (0.076 mmol scale) and the corresponding complex was obtained as a diastereomeric mixture (*mer*-(*P*,*A*<sub>Ir</sub>)-1a / *mer*-(*P*,*A*<sub>Ir</sub>)-1b / *fac*-(*P*,*A*<sub>Ir</sub>)-1c = 19 : 39 : 42 as determined by <sup>1</sup>H NMR), further purified and separated using chiral HPLC column chromatography (see ‘Chiral HPLC separations’ section for details) to afford pure *mer*-(*P*,*A*<sub>Ir</sub>)-1a (2.2 mg, 6% yield), pure *mer*-(*P*,*A*<sub>Ir</sub>)-1b (4.8 mg, 13% yield) and pure *fac*-(*P*,*A*<sub>Ir</sub>)-1c (3.3 mg, 9% yield), respectively.

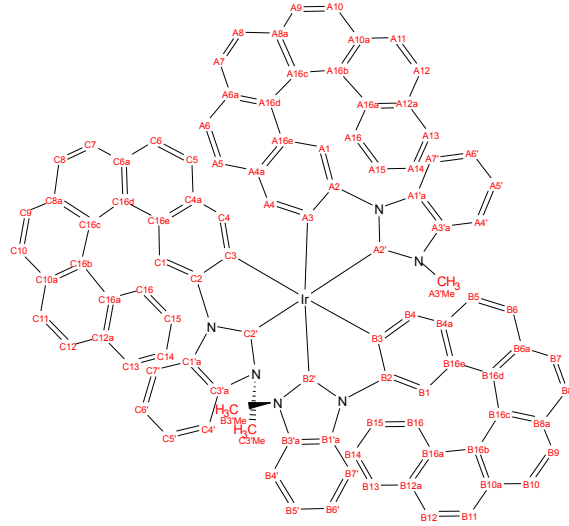
**HR-MS (MALDI, DCTB) [M]<sup>+</sup>** (C<sub>102</sub> H<sub>63</sub> N<sub>6</sub> <sup>193</sup>Ir): calculated for 1564.47381 m/z, found 1564.460 ( $\Delta$  = 9 ppm).

#### ***mer*-(*M*,*A*<sub>Ir</sub>)-1a / *mer*-(*P*,*A*<sub>Ir</sub>)-1a diastereoisomer:**

**<sup>1</sup>H NMR (900 MHz, CD<sub>2</sub>Cl<sub>2</sub>)** δ = 8.43 (s, 1H, A1), 8.42 (s, 1H, C1), 8.30 (s, 1H, B1), 8.17 – 8.15 (m, 1H, A11), 8.13 (d, *J* = 5.9, 1H, C11), 8.12 (s, 2H, A10, A9), 8.07 (d, *J* = 8.2, 1H, A7), 8.07 (d, *J* = 8.6, 1H, C10), 8.05 (d, *J* = 7.4, 1H, C9), 8.05 – 8.03 (m, 1H, B11), 8.03 (d, *J* = 8.2, 1H, A8), 8.00 (d, *J* = 8.2, 1H, C7), 7.99 (d, *J* = 8.5, 1H, B10), 7.98 (d, *J* = 7.8, 1H, B9), 7.95 – 7.94 (m, 1H, C8), 7.93 (d, *J* = 7.3, 1H, C12), 7.92 (d, *J* = 6.6, 1H, A12), 7.90 (d, *J* = 8.5, 1H,

**A6**), 7.86 (d,  $J = 8.8$ , 1H, **C6**), 7.83 (d,  $J = 8.7$ , 1H, **B8**), 7.80 (d,  $J = 8.8$ , 1H, **B7**), 7.79 (d,  $J = 7.7$ , 1H, **C16**), 7.79 (d,  $J = 8.2$ , 1H, **A16**), 7.76 (d,  $J = 8.8$ , 1H, **C5**), 7.75 (dd,  $J = 8.5$ , 0.8, 1H, **B12**), 7.67 (d,  $J = 8.4$ , 1H, **A5**), 7.57 (dd,  $J = 8.2$ , 1.3, 1H, **C13**), 7.55 – 7.53 (m, 1H, **A13**), 7.47 (d,  $J = 8.8$ , 2H, **B13**, **B6**), 7.45 – 7.43 (m, 1H, **B16**), 7.37 – 7.34 (m, 1H, **A4'**), 7.32 – 7.29 (m, 1H, **A5'**), 7.22 (s, 1H, **C4**), 7.18 (ddd,  $J = 7.7$ , 6.5, 1.0, 1H, **A14**), 7.15 (ddd,  $J = 8.1$ , 7.3, 1.1, 1H, **A6'**), 7.15 – 7.11 (m, 1H, **C5'**), 7.13 (d,  $J = 8.6$ , 1H, **B5**), 7.13 – 7.09 (m, 1H, **C14**), 7.07 (td,  $J = 7.7$ , 1.2, 1H, **C6'**), 7.04 (ddd,  $J = 8.0$ , 5.6, 1.3, 2H, **B14**, **B5'**), 6.97 – 6.96 (m, 1H, **C4'**), 6.96 (s, 1H, **B4**), 6.97 – 6.93 (m, 1H, **B6'**), 6.88 (dd,  $J = 8.7$ , 1.2, 1H, **B4'**), 6.75 (s, 1H, **A4**), 6.44 (d,  $J = 8.2$ , 1H, **A7'**), 6.32 – 6.30 (m, 1H, **C7'**), 6.28 (d,  $J = 8.2$ , 1H, **B7'**), 6.11 (ddd,  $J = 8.1$ , 6.7, 1.3, 1H, **C15**), 6.08 (ddd,  $J = 8.3$ , 6.8, 1.4, 1H, **A15**), 5.92 (ddd,  $J = 8.0$ , 6.3, 1.4, 1H, **B15**), 2.80 (s, 3H, **B3'Me**), 2.74 (s, 3H, **A3'Me**), 2.67 (s, 3H, **C3'Me**).

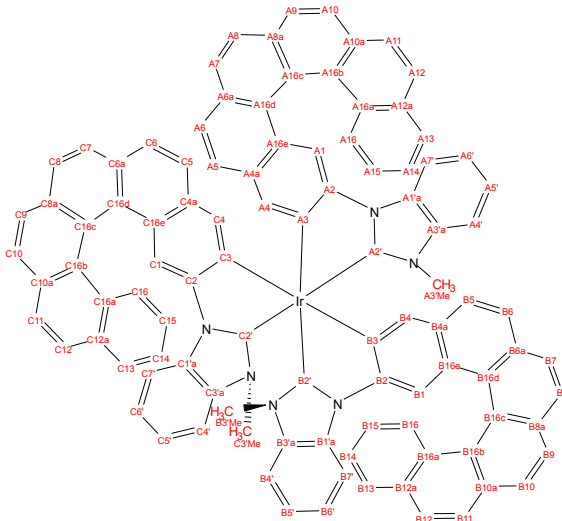
**<sup>13</sup>C NMR (226 MHz, CD<sub>2</sub>Cl<sub>2</sub>)** δ = 188.3 (**A2'**, C<sup>Carbene</sup>), 186.1 (**B2'**, C<sup>Carbene</sup>), 184.8 (**C2'**, C<sup>Carbene</sup>), 152.1 (**A3**), 151.3 (**C3**), 149.6 (**B2**), 149.1 (**C2**), 148.3 (**A2**), 147.8 (**B3**), 136.9 (**C4**), 136.1 (**C3'a**), 136.0 (**B3'a**), 135.9 (**A3'a**), 135.7 (**B4**), 134.2 (**A4**), 133.2 (**A8a**), 133.1 (**C8a**), 132.9 (**B8a**), 131.8 (**C12a**, **A12a**), 131.6 (**B12a**), 131.6 (**A10a**), 131.5 (**C10a**), 131.4 (**A1'a**), 131.3 (**C1'a**), 131.3 (**B10a**), 131.1 (**B1'a**), 130.4 (**A6a**), 130.3 (**A4a**), 130.2 (**C6a**), 130.0 (**C4a**), 129.9 (**B16a**), 129.8 (**B6a**), 129.7 (**A16a**), 129.6 (**C16a**), 129.3 (**B4a**), 128.7 (**C16d**), 128.7 (**A16d**), 128.6 (**C12**), 128.5 (**A12**), 128.3 (**B16d**), 128.2 (**A5**), 128.2 (**B12**), 127.9 (**C16b**, **A7**), 127.9 (**C7**, **A16b**), 127.7 (**C5**, **B16b**), 127.7 (**B7**), 127.3 (**A9**), 127.3 (**B16**), 127.2 (**C9**), 127.2 (**B9**), 127.1 (**B5**), 127.1 (**B13**), 127.1 (**C13**), 127.0 (**A13**), 127.0 (**A10**), 127.0 (**C10**), 126.9 (**C16**, **A16**), 126.8 (**B10**), 126.2 (**C14**), 126.1 (**A11**), 126.1 (**B11**), 125.9 (**C11**), 125.8 (**A14**), 125.5 (**A16e**), 125.4 (**C16e**, **B16e**), 125.4 (**B14**), 125.2 (**A8**), 125.0 (**C8**), 125.0 (**C15**), 124.9 (**B8**), 124.9 (**A15**), 124.0 (**B15**, **A16c**), 123.8 (**C6**, **C16c**), 123.6 (**A6**), 123.5 (**B6**), 123.5 (**B16c**), 122.4 (**B6'**), 122.2 (**C6'**), 122.1 (**A6'**), 121.9 (**A5'**), 121.8 (**B5'**), 121.8 (**C5'**), 111.8 (**A7'**), 111.5 (**C7'**), 111.0 (**B7'**), 109.5 (**A1**), 109.3 (**C1**), 109.3 (**C4'**), 109.2 (**B4'**), 108.9 (**B1**), 108.8 (**A4'**), 33.2 (**B3'Me**), 33.1 (**C3'Me**), 32.6 (**A3'Me**).



***mer-(M,Δ<sub>Ir</sub>)-1b / mer-(P,Δ<sub>Ir</sub>)-1b diastereoisomer:***

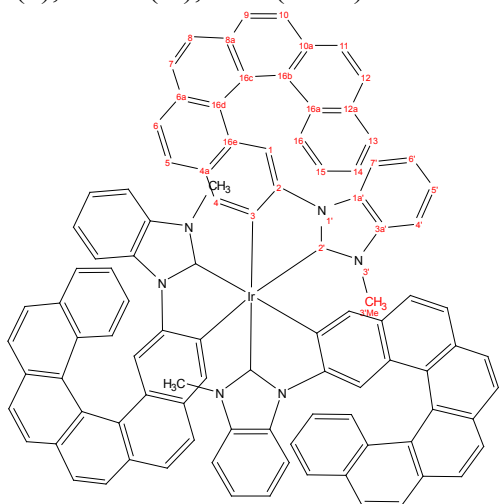
**<sup>1</sup>H NMR (900 MHz, CD<sub>2</sub>Cl<sub>2</sub>)** δ = 8.35 (s, 1H, **B1**), 8.28 (s, 1H, **A1**), 8.21 (s, 1H, **C1**), 8.20 (d, *J* = 8.1, 1H, **B11**), 8.17 – 8.14 (m, 1H, **C11**), 8.14 (dt, *J* = 8.4, 1.5, 2H, **A16**, **A11**), 8.09 (d, *J* = 8.5, 1H, **B10**), 8.07 (d, *J* = 8.5, 1H, **B9**), 8.03 – 8.00 (m, 1H, **C10**), 8.02 – 7.99 (m, 1H, **A10**), 7.98 (dd, *J* = 7.9, 1.0, 2H, **B12**, **B7**), 7.96 (dd, *J* = 7.4, 1.2, 1H, **C9**), 7.97 – 7.94 (m, 1H, **A9**), 7.94 (d, *J* = 7.9, 1H, **B8**), 7.95 – 7.92 (m, 1H, **B16**), 7.92 (d, *J* = 8.1, 1H, **A12**), 7.91 (d, *J* = 8.5, 1H, **C12**), 7.86 (dd, *J* = 8.4, 0.9, 1H, **B6**), 7.81 (d, *J* = 5.9, 1H, **B5**), 7.81 (d, *J* = 7.1, 1H, **C16**), 7.77 (dd, *J* = 7.9, 0.7, 1H, **A8**), 7.77 – 7.74 (m, 1H, **C8**), 7.75 – 7.72 (m, 1H, **A7**), 7.69 (dd, *J* = 7.8, 0.9, 1H, **C7**), 7.61 – 7.58 (m, 1H, **B13**), 7.55 (d, *J* = 7.7, 1H, **C13**), 7.55 (dd, *J* = 8.1, 1.3, 1H, **A13**), 7.44 (dd, *J* = 8.2, 0.8, 1H, **A6**), 7.41 (ddd, *J* = 7.8, 6.3, 1.1, 1H, **A14**), 7.37 – 7.34 (m, 1H, **C6**), 7.35 (s, 1H, **B4**), 7.33 (ddd, *J* = 8.2, 6.4, 1.4, 1H, **A15**), 7.32 – 7.29 (m, 2H, **C4'**, **C5'**), 7.25 (td, *J* = 7.8, 1.0, 1H, **B5'**), 7.21 – 7.14 (m, 5H, **B14**, **B4'**, **A5**, **C6'**, **B6'**), 7.13 (ddd, *J* = 7.8, 6.6, 1.1, 1H, **C14**), 7.09 (td, *J* = 7.6, 1.0, 1H, **A5'**), 7.06 (td, *J* = 7.6, 1.2, 1H, **A6'**), 7.01 – 6.98 (m, 1H, **C5**), 6.96 (dd, *J* = 7.9, 1.2, 1H, **A4'**), 6.79 (ddd, *J* = 8.3, 7.0, 1.5, 1H, **B15**), 6.75 (s, 1H, **A4**), 6.67 (ddd, *J* = 8.2, 6.6, 1.4, 1H, **C15**), 6.65 (s, 1H, **C4**), 6.31 (d, *J* = 8.3, 1H, **C7'**), 6.31 (d, *J* = 8.4, 1H, **B7'**), 6.24 – 6.21 (m, 1H, **A7'**), 3.14 (s, 3H, **C3'Me**), 3.08 (s, 3H, **B3'Me**), 2.83 (s, 3H, **A3'Me**).

**<sup>13</sup>C NMR (226 MHz, CD<sub>2</sub>Cl<sub>2</sub>)** δ = 188.5 (**A2'**, C<sup>Carbene</sup>), 186.5 (**B2'**, C<sup>Carbene</sup>), 185.0 (**C2'**, C<sup>Carbene</sup>), 151.9 (**A3**), 150.9 (**C3**), 150.5 (**B2**), 149.1 (**C2**), 148.6 (**A2**), 147.8 (**B3**), 137.1 (**B4**), 136.8 (**C3'a**), 136.6 (**B3'a**), 136.3 (**A3'a**), 135.5 (**C4**), 134.0 (**A4**), 133.6 (**B8a**), 133.5 (**A8a**), 133.5 (**C8a**), 132.5 (**B12a**), 132.4 (**A12a**), 132.4 (**C12a**), 132.0 (**C1'a**), 132.0 (**B1'a**), 131.9 (**A1'a**), 131.8 (**B10a**), 131.7 (**C10a**), 131.6 (**A10a**), 130.6 (**A4a**), 130.6 (**B6a**), 130.5 (**C16a**, **A16a**), 130.5 (**B4a**, **B16a**, **A6a**), 130.3 (**C4a**), 130.3 (**C6a**), 129.5 (**A16d**), 129.4 (**B16d**), 129.3 (**C16d**), 128.5 (**B12**), 128.5 (**A16b**), 128.5 (**B16b**), 128.4 (**A12**), 128.4 (**C12**), 128.3 (**C16b**), 128.3 (**B16**), 128.1 (**A16**), 128.1 (**C16**, **A13**), 128.1 (**B7**), 128.0 (**B13**), 128.0 (**C13**), 127.9 (**A7**), 127.9 (**B5**), 127.8 (**C7**), 127.5 (**B9**), 127.5 (**C9**, **A5**), 127.4 (**A9**), 127.2 (**B10**), 127.1 (**C5**, **B16e**), 127.0 (**C10**), 127.0 (**A10**), 126.6 (**C11**, **B11**), 126.5 (**A11**), 126.3 (**A16e**), 126.3 (**C16e**), 126.2 (**A14**), 125.9 (**B14**), 125.6 (**C14**), 125.5 (**A15**), 125.3 (**B8**), 125.0 (**C8**, **B15**, **A8**), 124.8 (**C15**), 124.1 (**B6**, **A16c**), 124.1 (**C6**), 124.0 (**A6**), 124.0 (**B16c**), 123.8 (**C16c**), 122.9 (**C6'**), 122.8 (**B6'**), 122.5 (**A6'**), 122.5 (**C5'**, **B5'**), 122.1 (**A5'**), 112.0 (**C7'**, **A7'**), 112.0 (**B7'**), 110.0 (**C1**), 109.9 (**C4'**), 109.7 (**B4'**), 109.7 (**B1**), 109.7 (**A4'**), 109.6 (**A1**), 34.8 (**B3'Me**), 34.7 (**C3'Me**), 32.9 (**A3'Me**).



***fac-(M,Δ<sub>Ir</sub>)-1c / fac-(P,Δ<sub>Ir</sub>)-1c diastereoisomer:***

**<sup>1</sup>H NMR (500 MHz, CD<sub>2</sub>Cl<sub>2</sub>)** δ = 8.42 (s, 1H, **1**), 8.11 (d, *J* = 8.5, 1H, **11**), 8.05 (s, 2H, **9**, **10**), 7.94 – 7.87 (m, 1H, **8**), 7.92 – 7.85 (m, 1H, **7**), 7.83 (d, *J* = 8.9, 1H, **12**), 7.56 (dd, *J* = 8.5, 1.0, 1H, **16**), 7.53 (d, *J* = 1.3, 1H, **13**), 7.51 (d, *J* = 8.6, 1H, **6**), 7.28 – 7.20 (m, 2H, **4'**, **5'**), 7.13 (d, *J* = 8.6, 1H, **5**), 7.10 (ddd, *J* = 8.4, 6.8, 1.8, 1H, **6'**), 7.04 (ddd, *J* = 8.0, 6.8, 1.1, 1H, **14**), 6.71 (s, 1H, **4**), 6.50 (d, *J* = 8.2, 1H, **7'**), 6.07 (ddd, *J* = 8.4, 6.8, 1.4, 1H, **15**), 2.90 (s, 3H, **3'Me**).  
**<sup>13</sup>C NMR (126 MHz, CD<sub>2</sub>Cl<sub>2</sub>)** δ = 190.6 (**2'**, C<sup>Carbene</sup>), 149.3 (**2**), 148.3 (**3**), 136.5 (**3'a'**), 134.6 (**4**), 133.6 (**8a**), 132.3 (**12a**), 132.1 (**1a'**), 131.8 (**10a**), 130.7 (**16a**), 130.7 (**6a**), 130.4 (**4a**), 129.0 (**16d**), 128.5 (**16b**), 128.4 (**12**), 128.2 (**7**), 128.0 (**5**), 128.0 (**16**), 127.7 (**10**), 127.5 (**13**), 127.1 (**9**), 126.6 (**11**), 126.4 (**16e**), 125.5 (**14**), 125.3 (**8**), 124.5 (**15**), 124.3 (**16c**), 123.9 (**6**), 122.7 (**6'**), 122.3 (**5'**), 111.9 (**7'**), 109.7 (**1**), 109.2 (**4'**), 33.7 (**3'Me**).



## NMR spectra

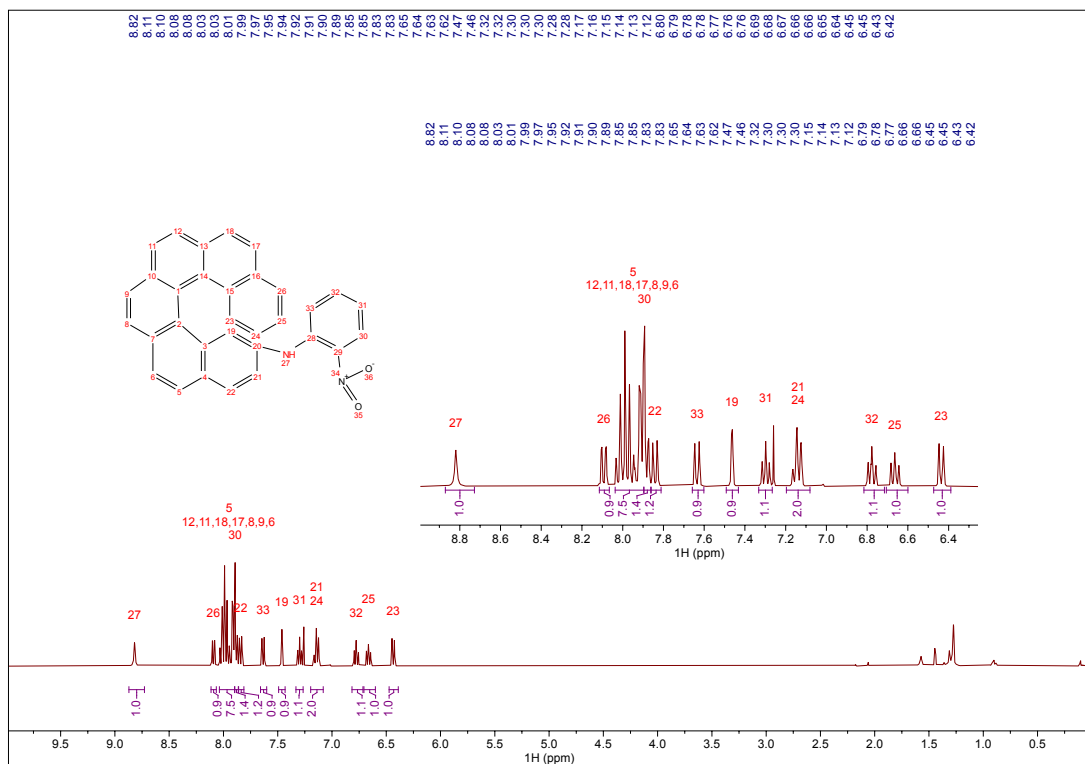


**Figure SI.1.**  $^1\text{H}$  NMR spectrum of (rac)-3 in  $\text{CDCl}_3$  at 298 K (400 MHz).

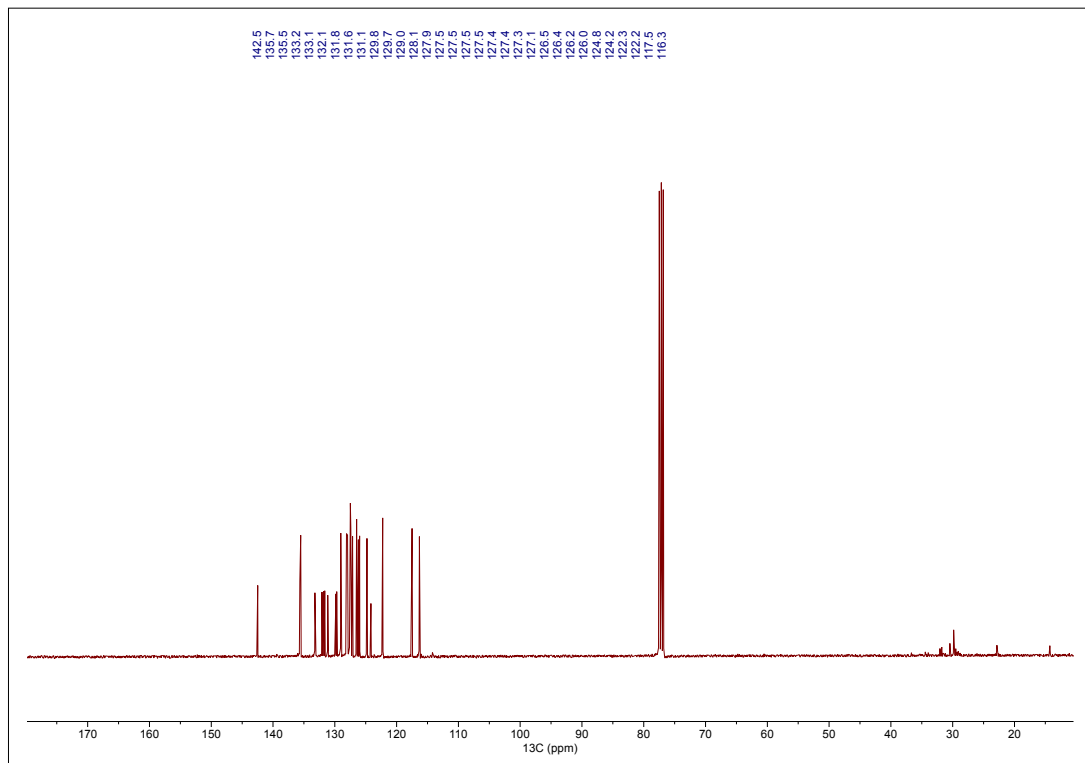


**Figure SI.2.**  $^{13}\text{C}$  NMR spectrum of (rac)-3 in  $\text{CDCl}_3$  at 298 K (101 MHz).

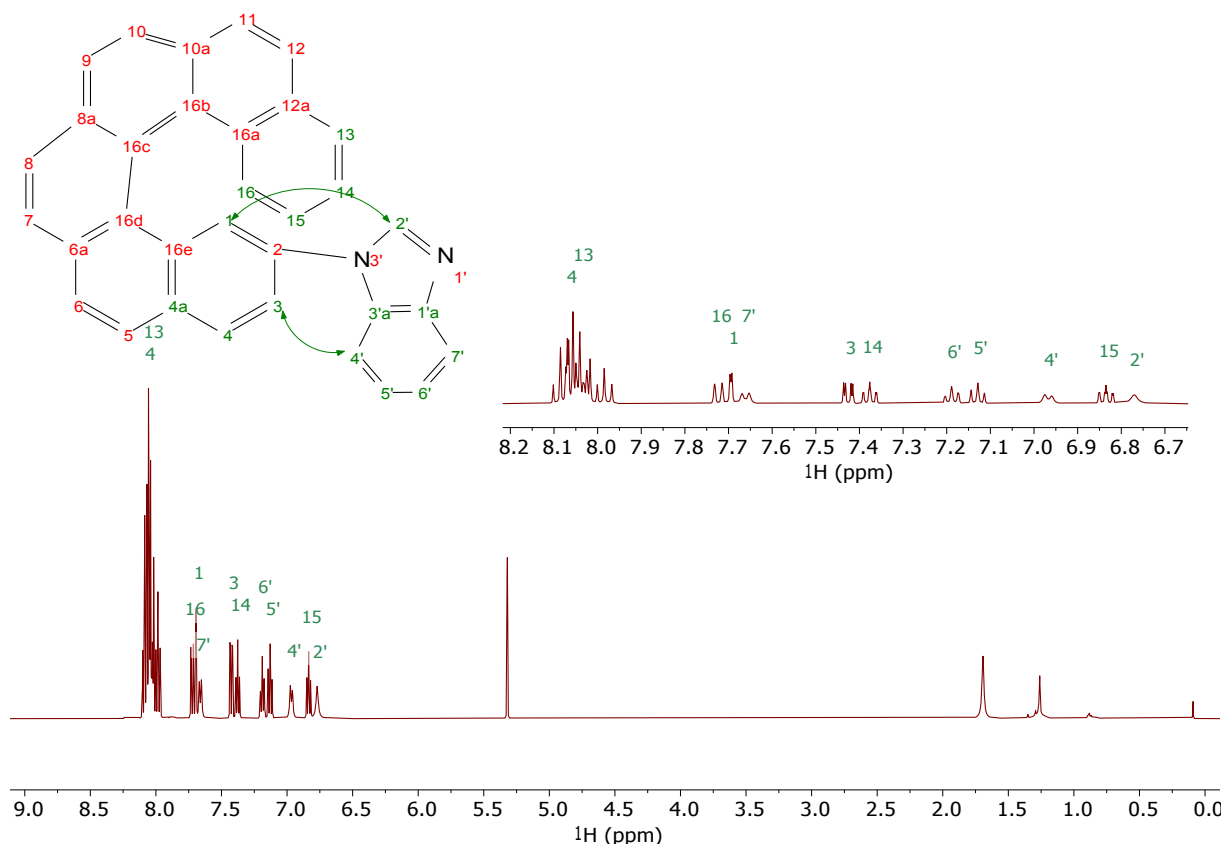


**Figure SI.3a.**  $^1\text{H}$  NMR spectrum of (rac)-5 in  $\text{CD}_2\text{Cl}_2$  at 298 K (500 MHz).

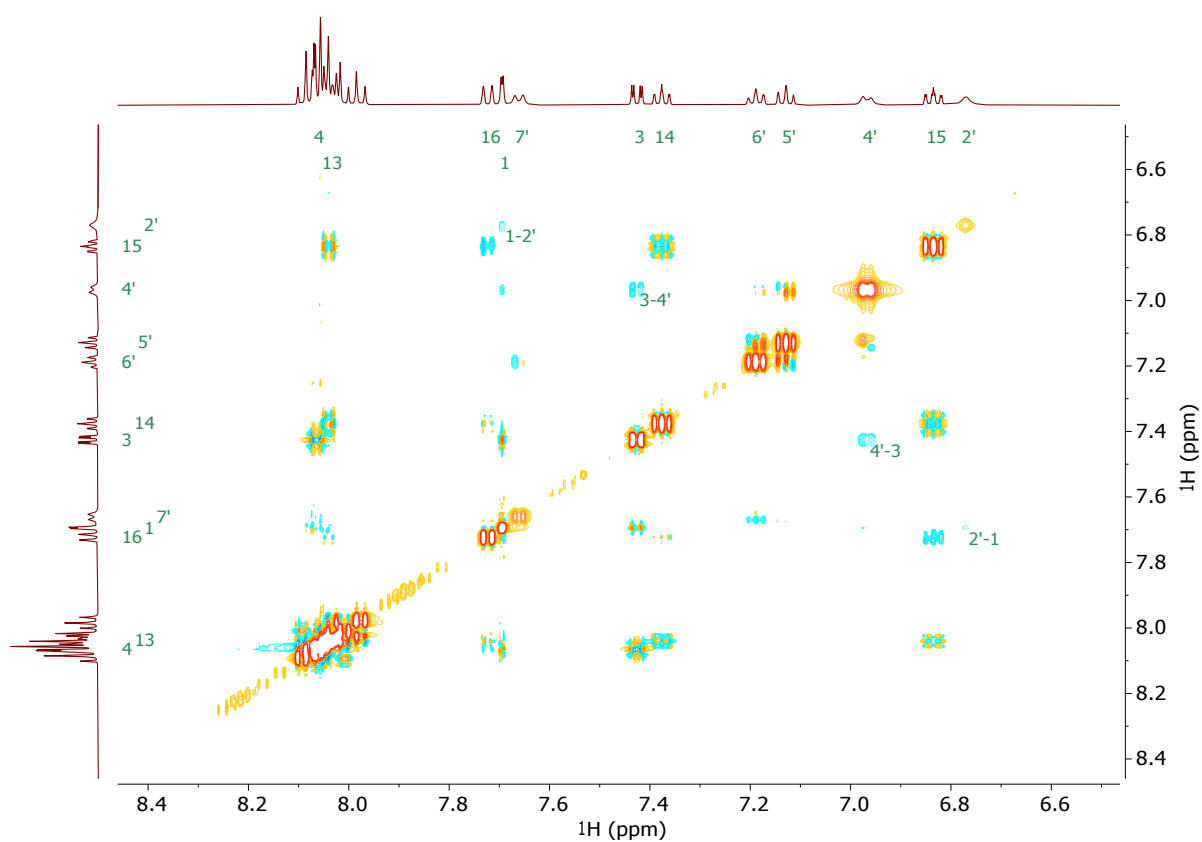


**Figure SI.4b.** NOESY spectrum of (rac)-5 in  $\text{CD}_2\text{Cl}_2$  at 290 K (500 MHz, mixing time 800ms)

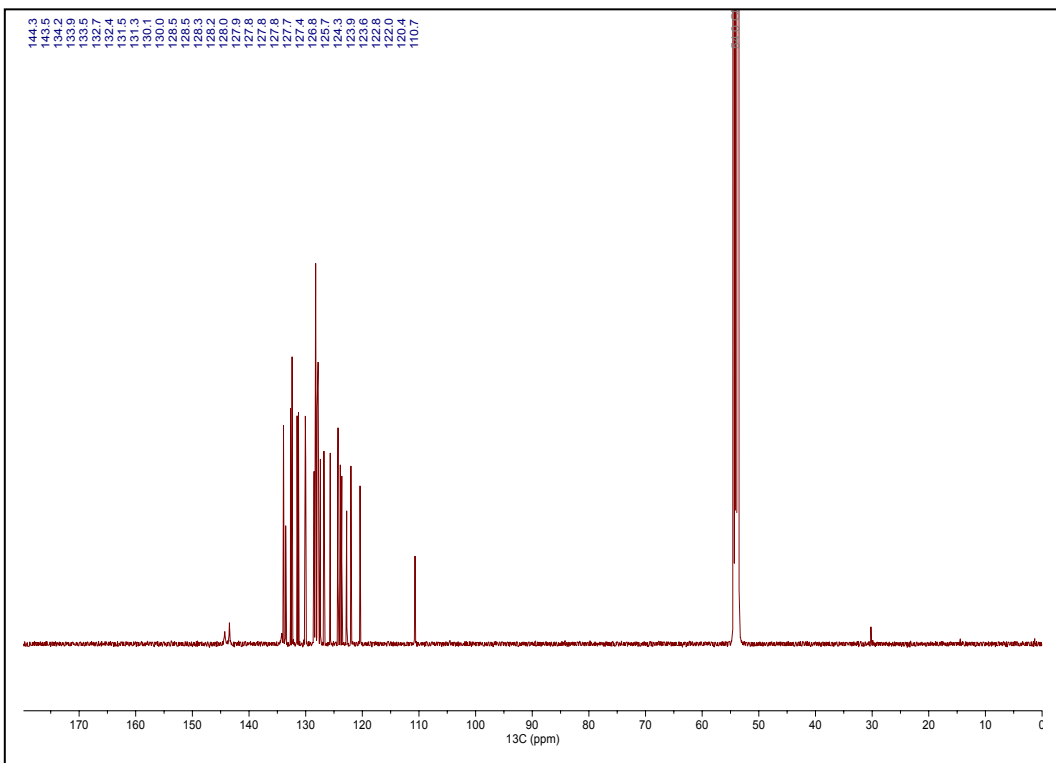


**Figure SI.5.**  $^{13}\text{C}$  NMR spectrum of (rac)-5 in  $\text{CDCl}_3$  at 298 K (126 MHz).

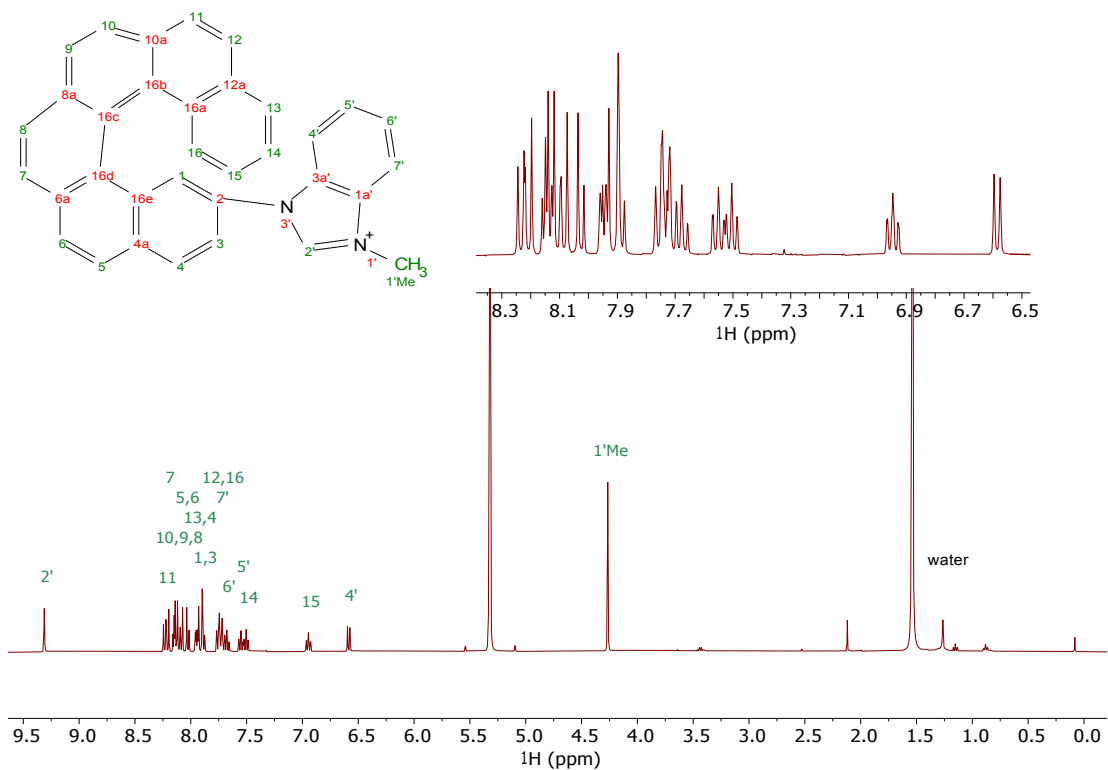


**Figure SI.6.**  $^1\text{H}$  NMR spectrum of (P)-(+)-6 in  $\text{CD}_2\text{Cl}_2$  at 298 K (400 MHz).

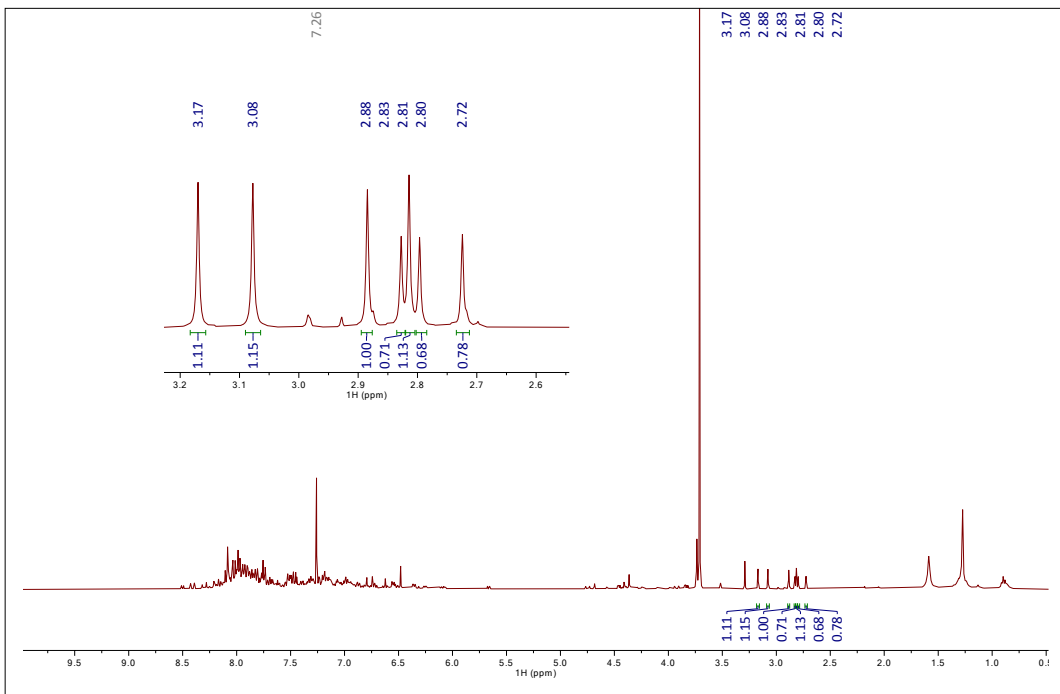


**Figure SI.7.** <sup>13</sup>C NMR spectrum of the crude mixture of complexes (M)-1a,b,c after the cyclometalation reaction ( $\text{CDCl}_3$  at 298 K, 400 MHz).

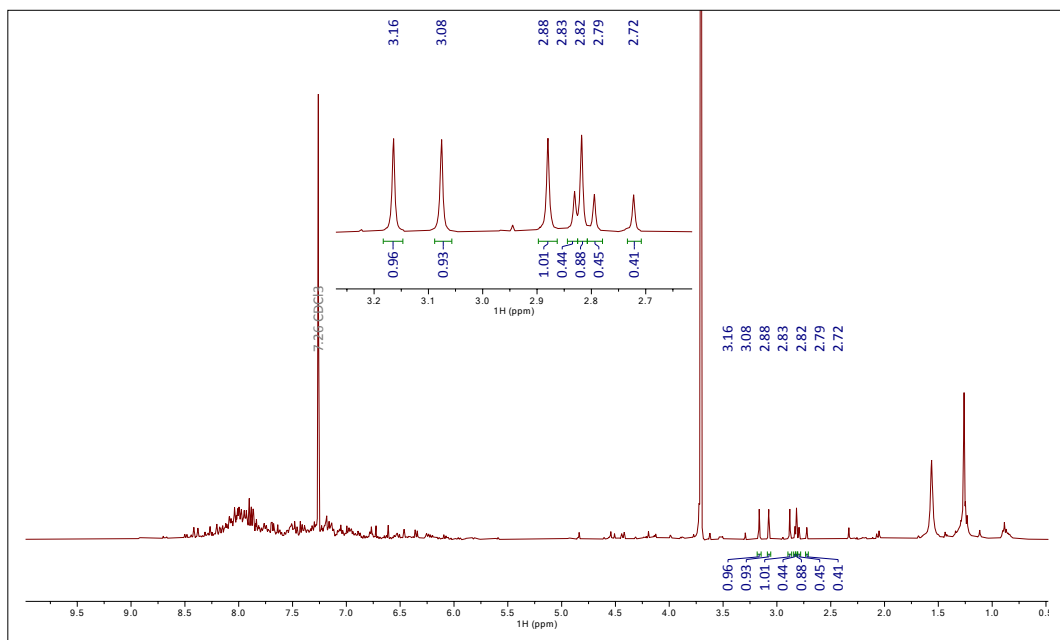


**Figure SI.8.** <sup>1</sup>H NMR spectrum of the crude mixture of complexes (P)-1a,b,c after the cyclometalation reaction ( $\text{CDCl}_3$  at 298 K, 400 MHz).

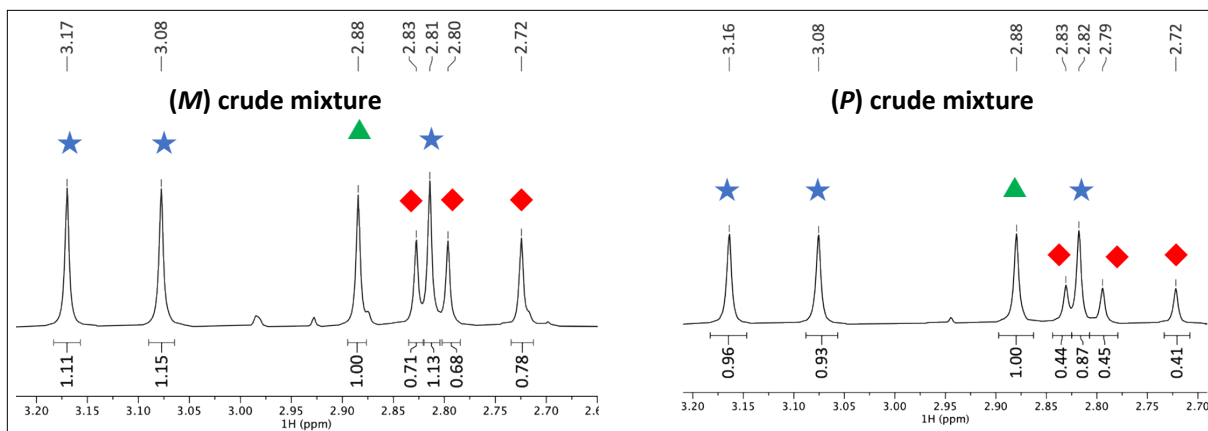


**Figure SI.9.** Partial <sup>1</sup>H NMR spectra (centered on the N-CH<sub>3</sub> area) of crude mixture of complexes (M)-1a,b,c and (P)-1a,b,c after cyclometalation reaction (CDCl<sub>3</sub> at 298 K, 400 MHz).

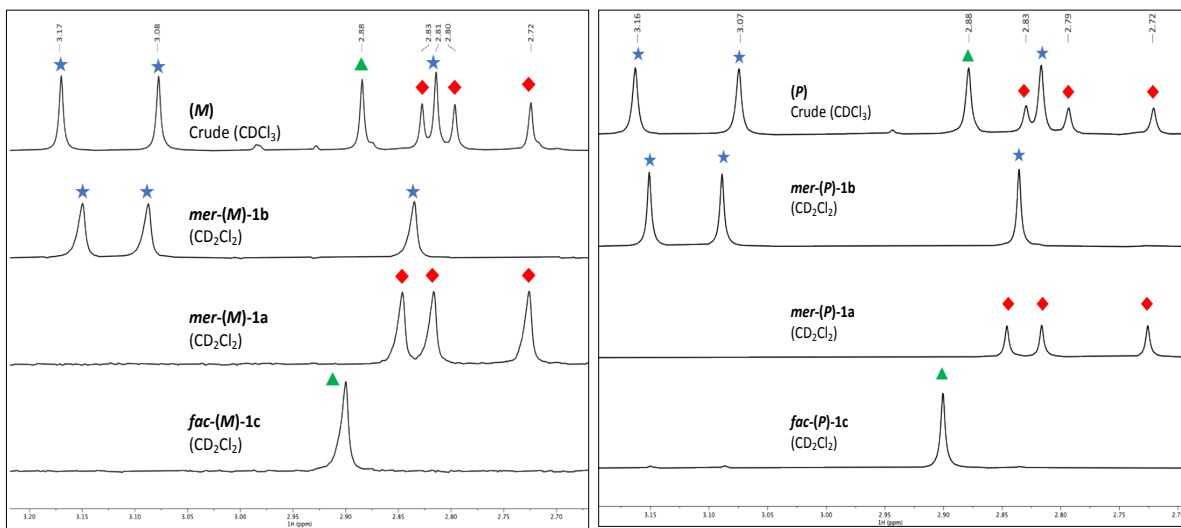


**Figure SI.10.** Partial <sup>1</sup>H NMR spectra (centered on the N-CH<sub>3</sub> area) of the chiral HPLC fractions of complexes (M)-1a,b,c (left) and (P)-1a,b,c (right) with comparison to the crude mixture.

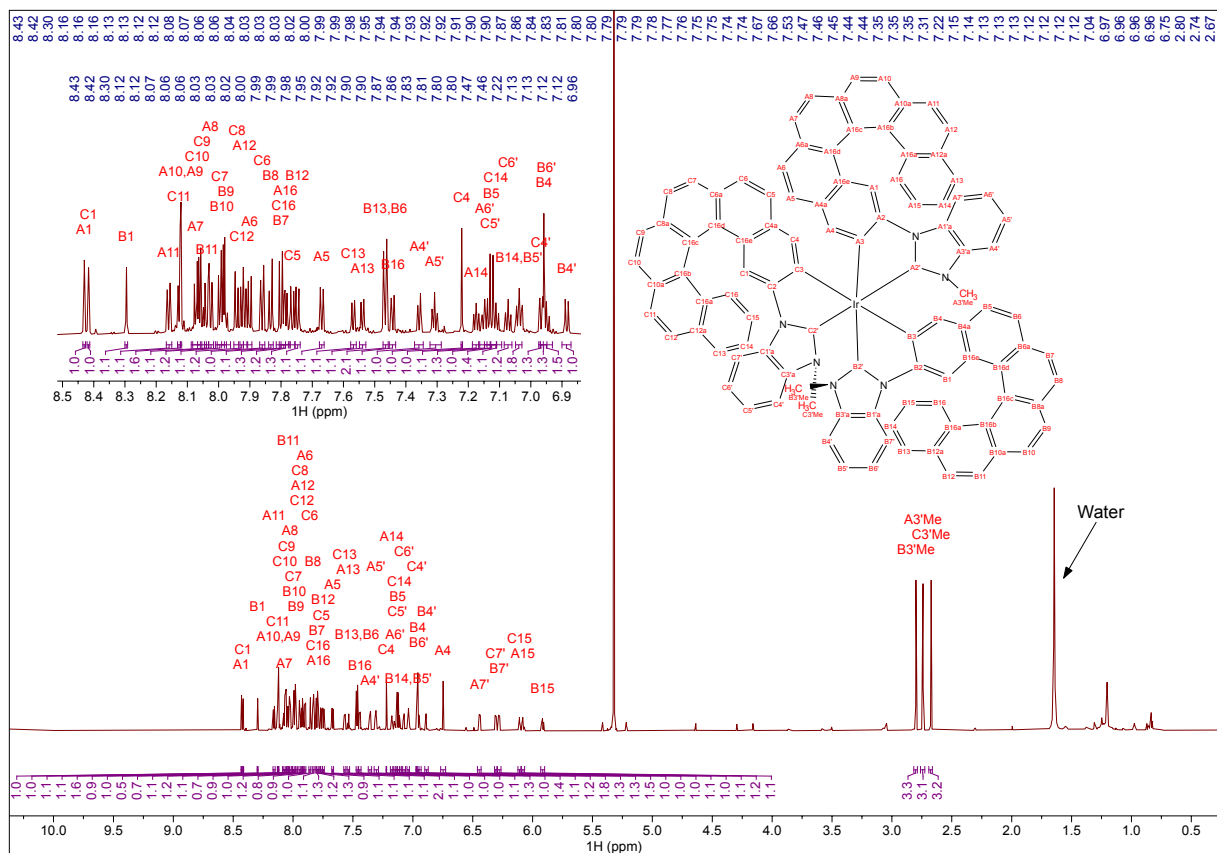


**Figure SI.11.**  $^1\text{H}$  NMR spectrum of mer-( $M, \Delta_{\text{Ir}}$ )-**1a** in  $\text{CD}_2\text{Cl}_2$  at 241 K (900 MHz). (Same spectrum obtained for mer-( $P, \Delta_{\text{Ir}}$ )-**1a**, not shown).

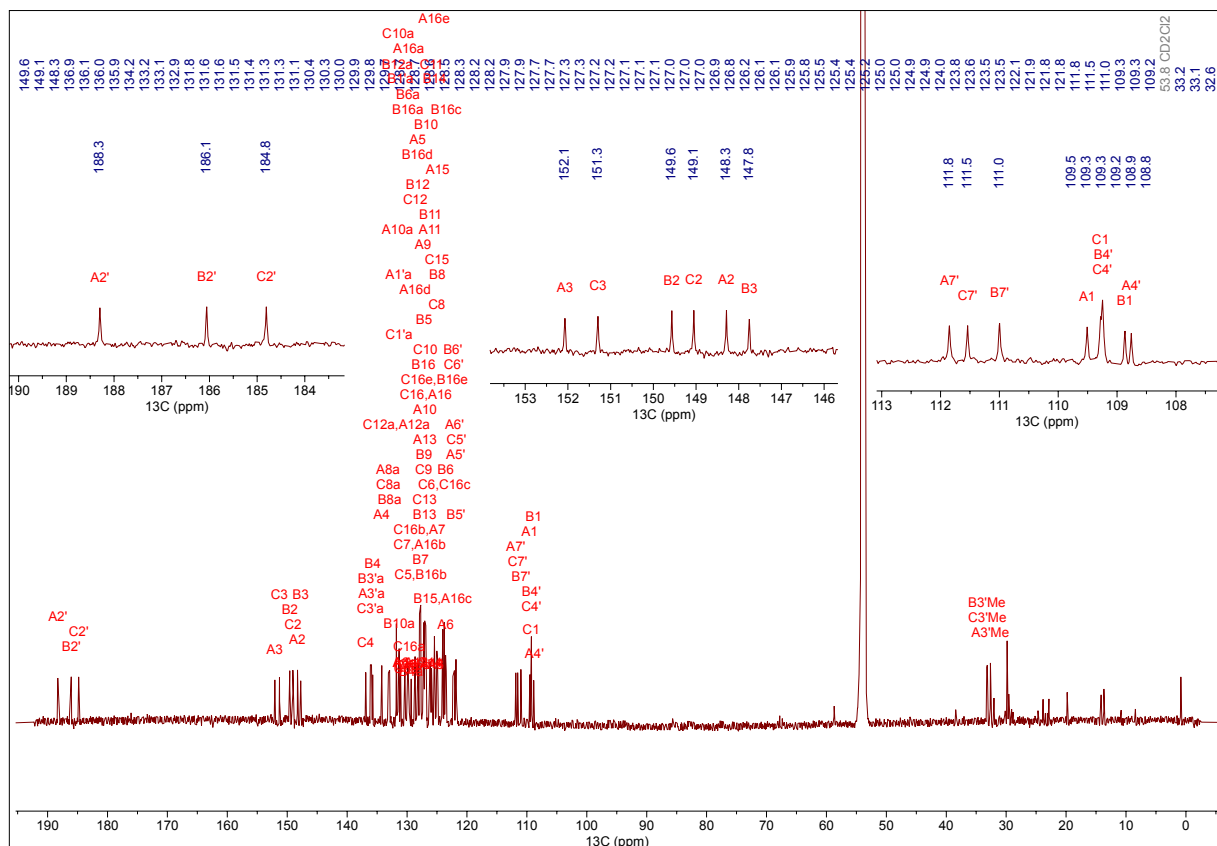


**Figure SI.12.**  $^{13}\text{C}$  NMR spectrum of *mer*-( $M,\text{A}_{\text{Iv}}$ )-**1a** in  $\text{CD}_2\text{Cl}_2$  at 241 K (226 MHz). (Same spectrum obtained for *mer*-( $P,\text{A}_{\text{Iv}}$ )-**1a**, not shown).

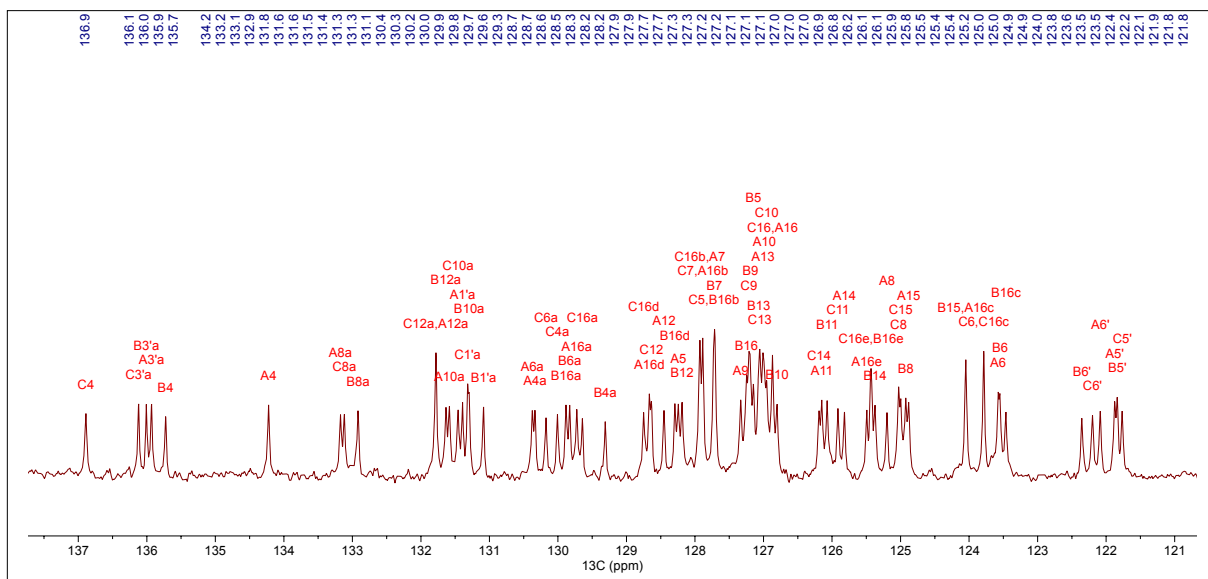


**Figure SI.13.** Part of the  $^{13}\text{C}$  NMR spectrum centered around 130 ppm of mer-( $M,\text{A}_{\text{Ig}}$ )-**1a** in  $\text{CD}_2\text{Cl}_2$  at 241 K (226 MHz). (Same spectrum obtained for mer-( $P,\text{A}_{\text{Ig}}$ )-**1a**, not shown).

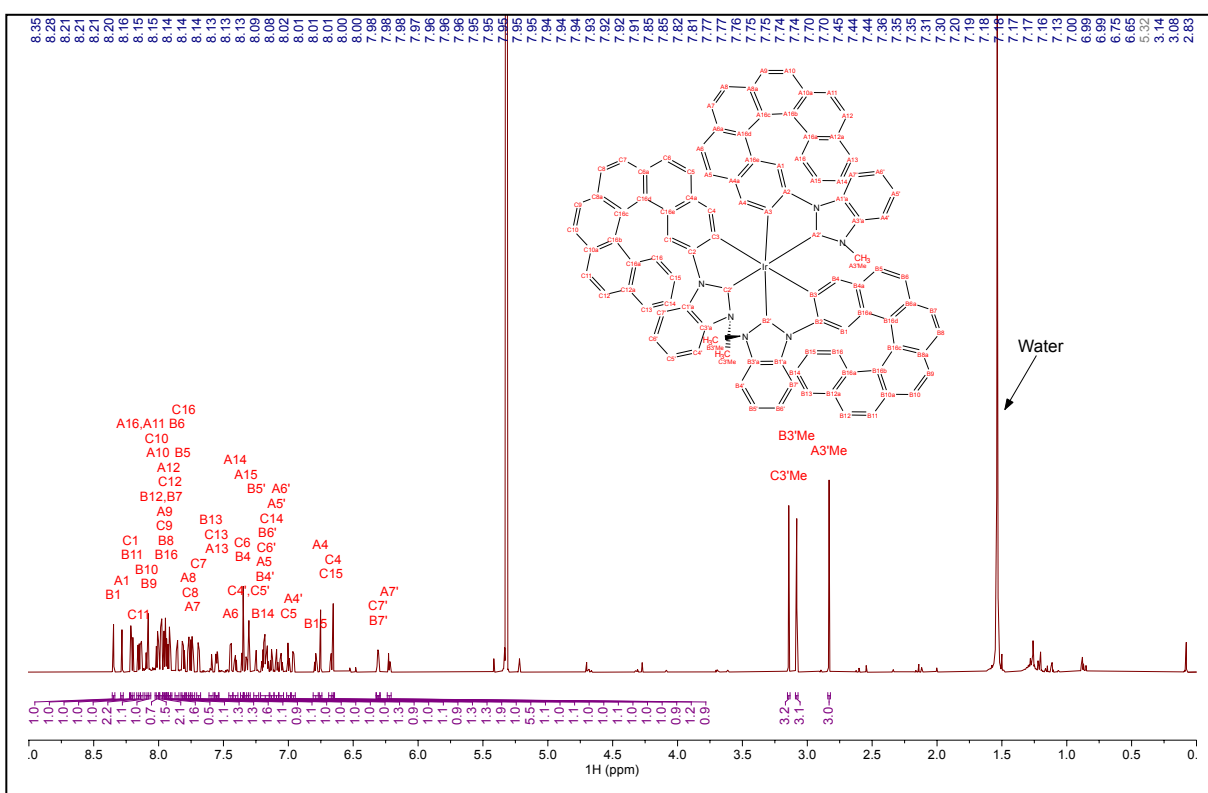


**Figure SI.14.**  $^1\text{H}$  NMR spectrum of *mer*-( $M, \Delta_{\text{I}b}$ )-**1b** in  $\text{CD}_2\text{Cl}_2$  at 293 K (900 MHz). (Same spectrum obtained for *mer*-( $P, \Delta_{\text{I}b}$ )-**1b**, not shown).

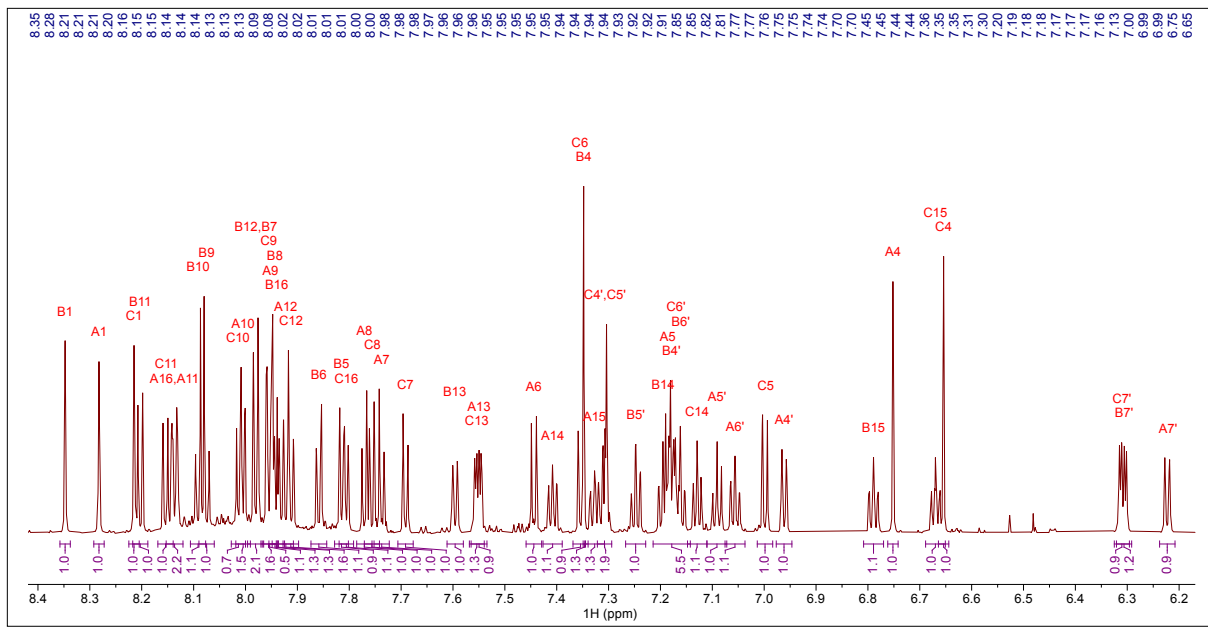


**Figure SI.15.** Part of the <sup>1</sup>H NMR spectrum centered around 7.3 ppm of mer-(M,Δ<sub>1r</sub>)-1b in  $\text{CD}_2\text{Cl}_2$  at 241 K (900 MHz). (Same spectrum obtained for mer-(P,Δ<sub>1r</sub>)-1b, not shown).

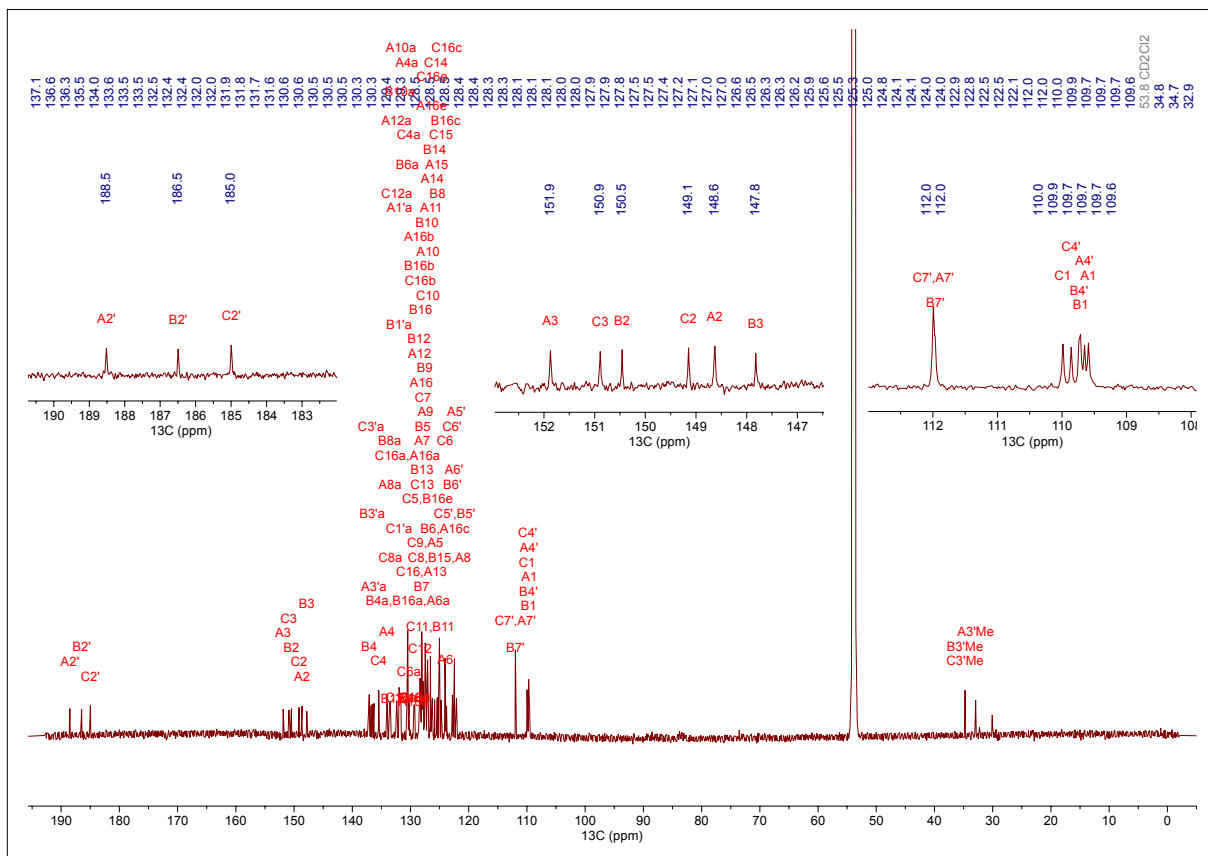


**Figure SI.16.** <sup>13</sup>C NMR spectrum of mer-(M,Δ<sub>1r</sub>)-1b in  $\text{CD}_2\text{Cl}_2$  at 293 K (226 MHz). (Same spectrum obtained for mer-(P,Δ<sub>1r</sub>)-1b, not shown).

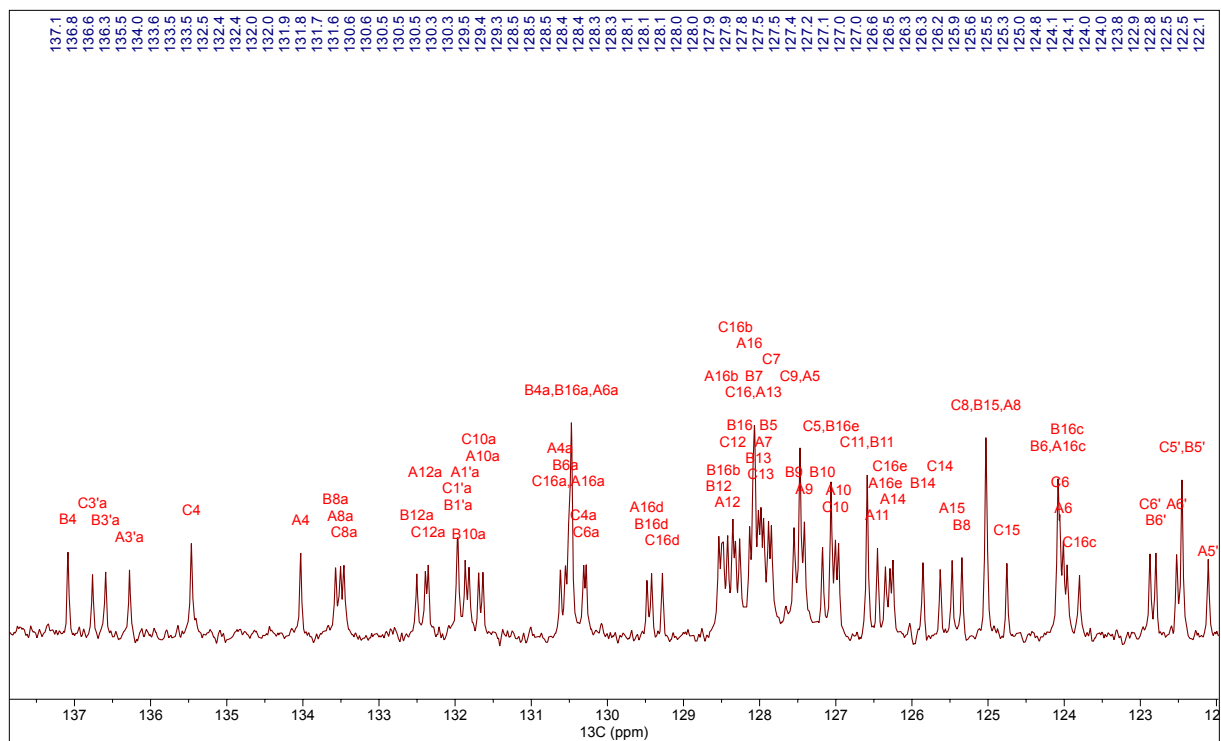


**Figure SI.17.** Part of the  $^{13}\text{C}$  NMR spectrum centered around 130 ppm of mer-( $M,\Delta_{\text{Ir}}$ )-1b in  $\text{CD}_2\text{Cl}_2$  at 293 K (226 MHz). (Same spectrum obtained for mer-( $P,\Delta_{\text{Ir}}$ )-1b, not shown).

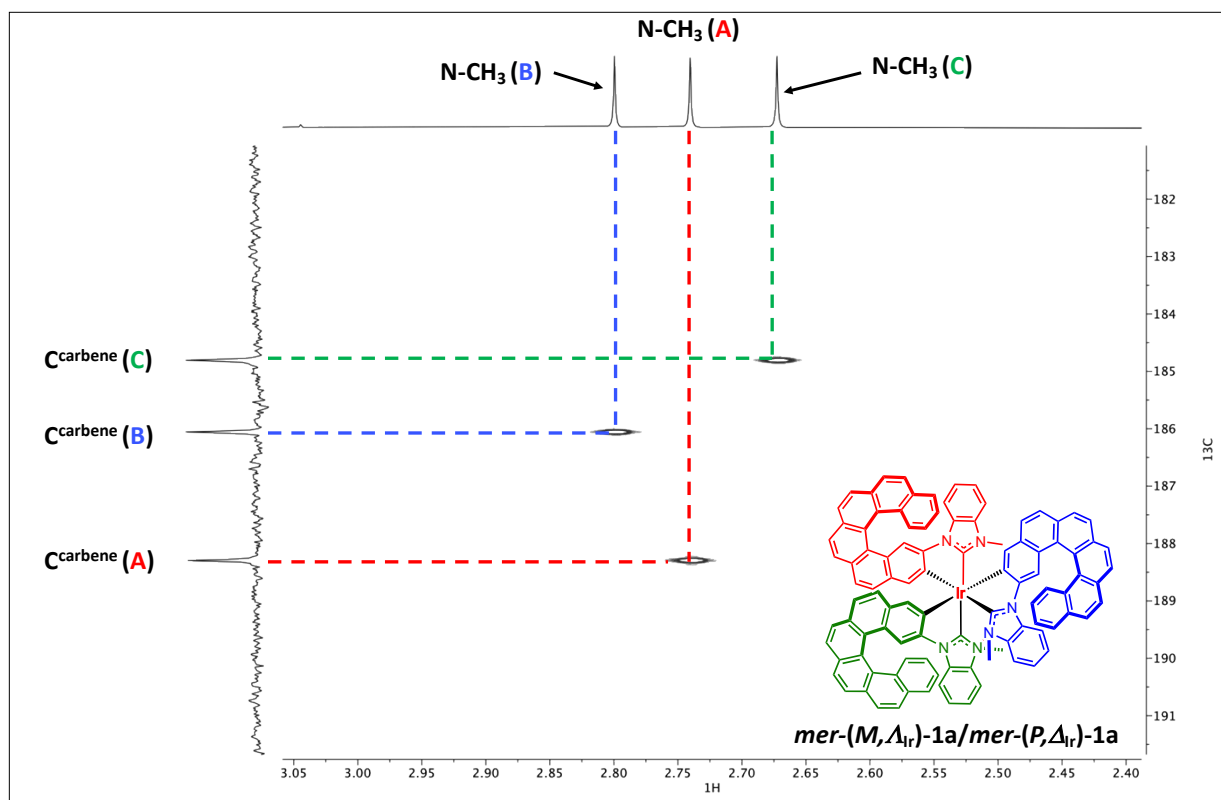


**Figure SI.18.**  $^1\text{H}$ - $^{13}\text{C}$  HMBC correlations for mer-( $M,\Delta_{\text{Ir}}$ )-1a showing the coupling between the inequivalent N-CH<sub>3</sub> groups and the distinct deshielded carbene atoms ( $\text{CD}_2\text{Cl}_2$ , 900 MHz  $^1\text{H}$ , 226 MHz  $^{13}\text{C}$ , 241 K).

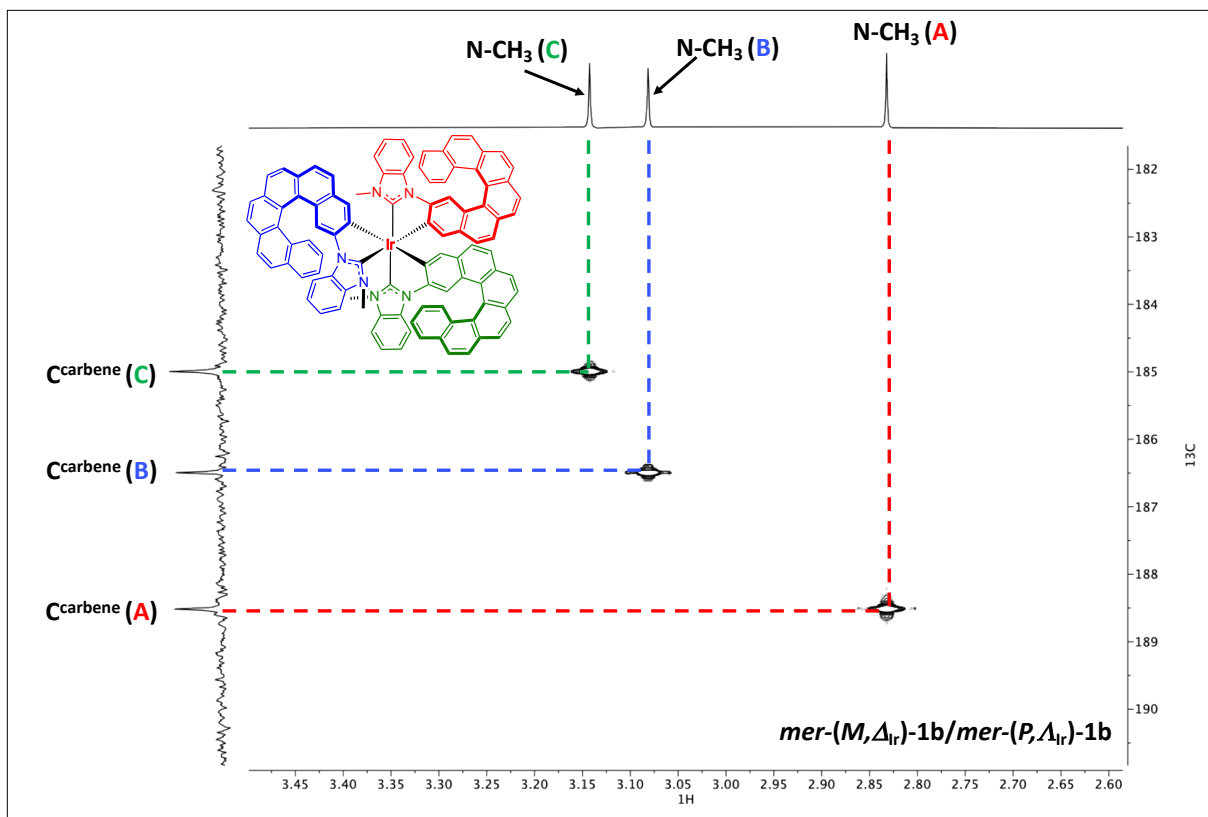


**Figure SI.19.** <sup>1</sup>H-<sup>13</sup>C HMBC correlations for *mer*-(*M*, $\Delta$ <sub>Ir</sub>)-1b showing the coupling between the inequivalent N-CH<sub>3</sub> groups and the distinct deshielded carbene atoms ( $CD_2Cl_2$ , 900 MHz <sup>1</sup>H, 226 MHz <sup>13</sup>C, 241 K).

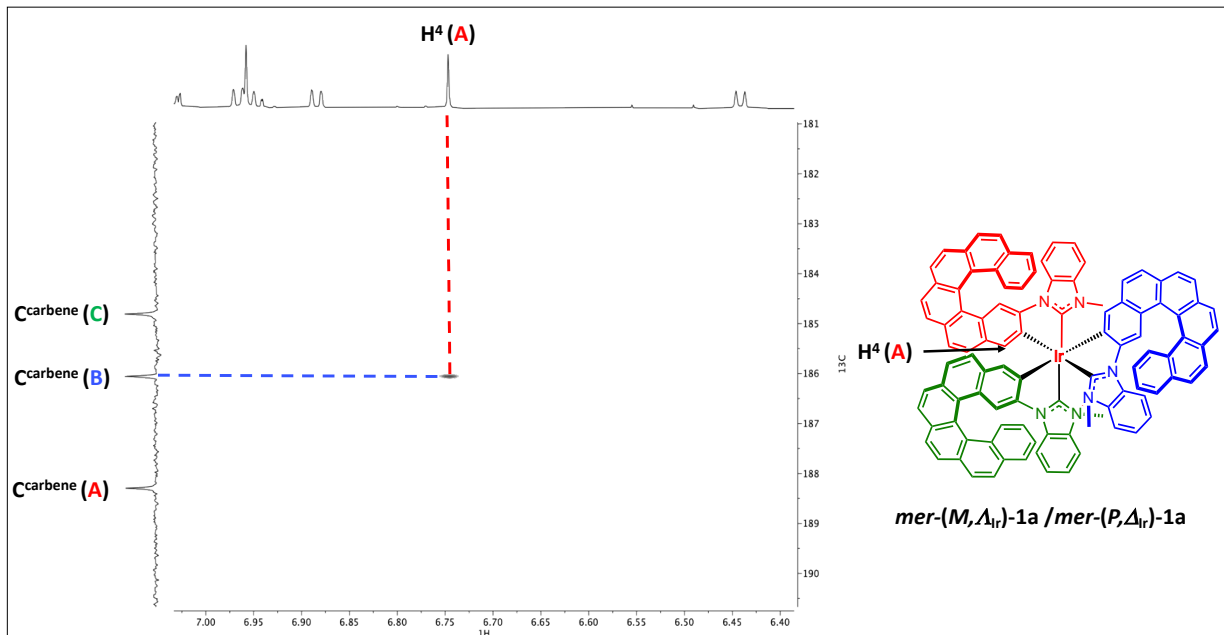


**Figure SI.20.** <sup>1</sup>H-<sup>13</sup>C HMBC correlations for *mer*-(*M*, $\Delta$ <sub>Ir</sub>)-1a showing the coupling between the proton H<sup>4</sup>(A) and the carbene of the ligand in trans position, B ( $CD_2Cl_2$ , 900 MHz <sup>1</sup>H, 226 MHz <sup>13</sup>C, 241 K).

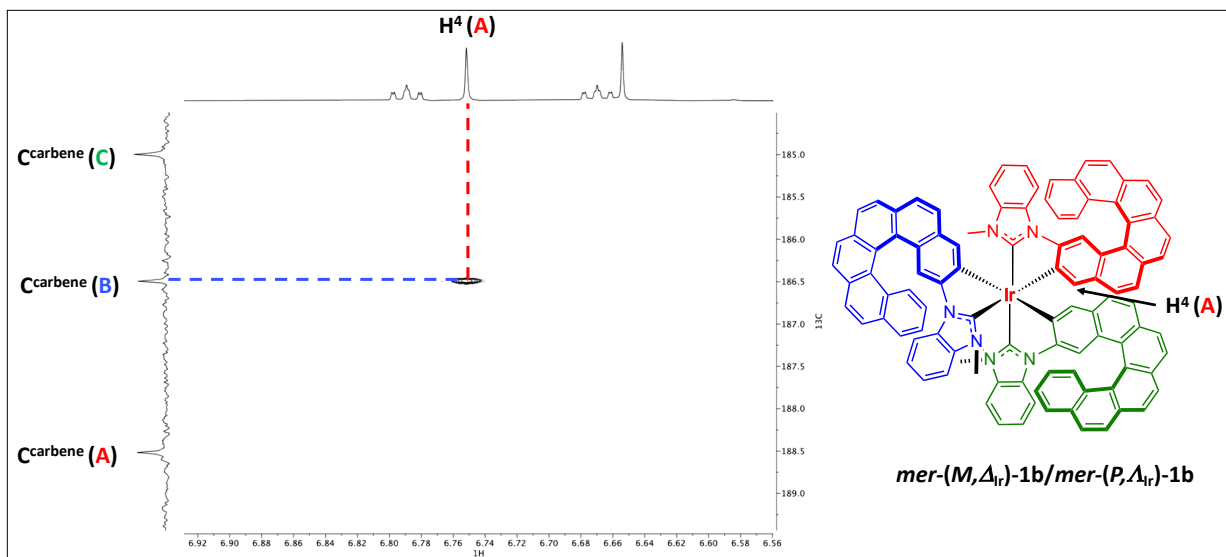


**Figure SI.21.**  $^1\text{H}$ - $^{13}\text{C}$  HMBC correlations for *mer*-( $M,\Delta_{\text{Ir}}$ )-**1b** showing the coupling between the proton  $H^4(\text{A})$  and the carbene of the ligand in trans position, **B** ( $\text{CD}_2\text{Cl}_2$ , 900 MHz  $^1\text{H}$ , 226 MHz  $^{13}\text{C}$ , 293 K).

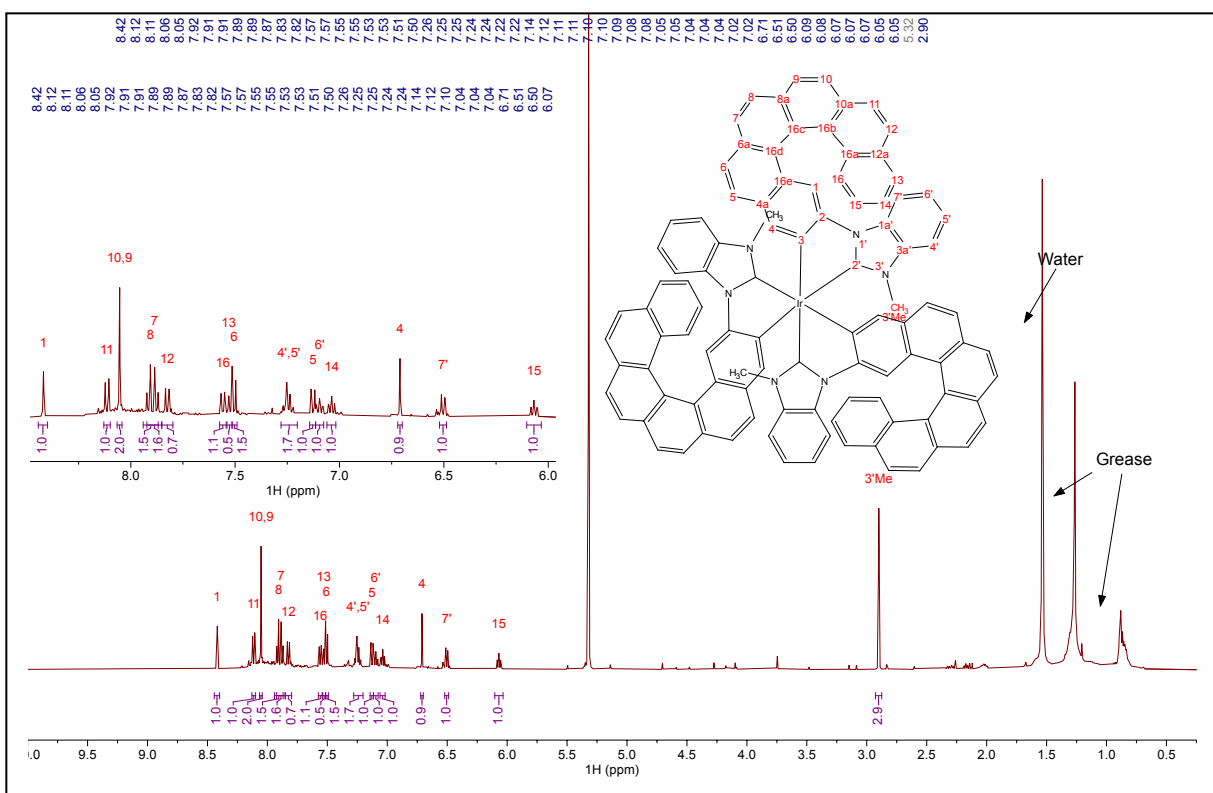


**Figure SI.22.**  $^1\text{H}$  NMR spectrum of *fac*-( $P,\Delta_{\text{Ir}}$ )-**1c** in  $\text{CD}_2\text{Cl}_2$  at 293 K (500 MHz).  
(Same spectrum obtained for *fac*-( $M,\Delta_{\text{Ir}}$ )-**1c**, not shown).

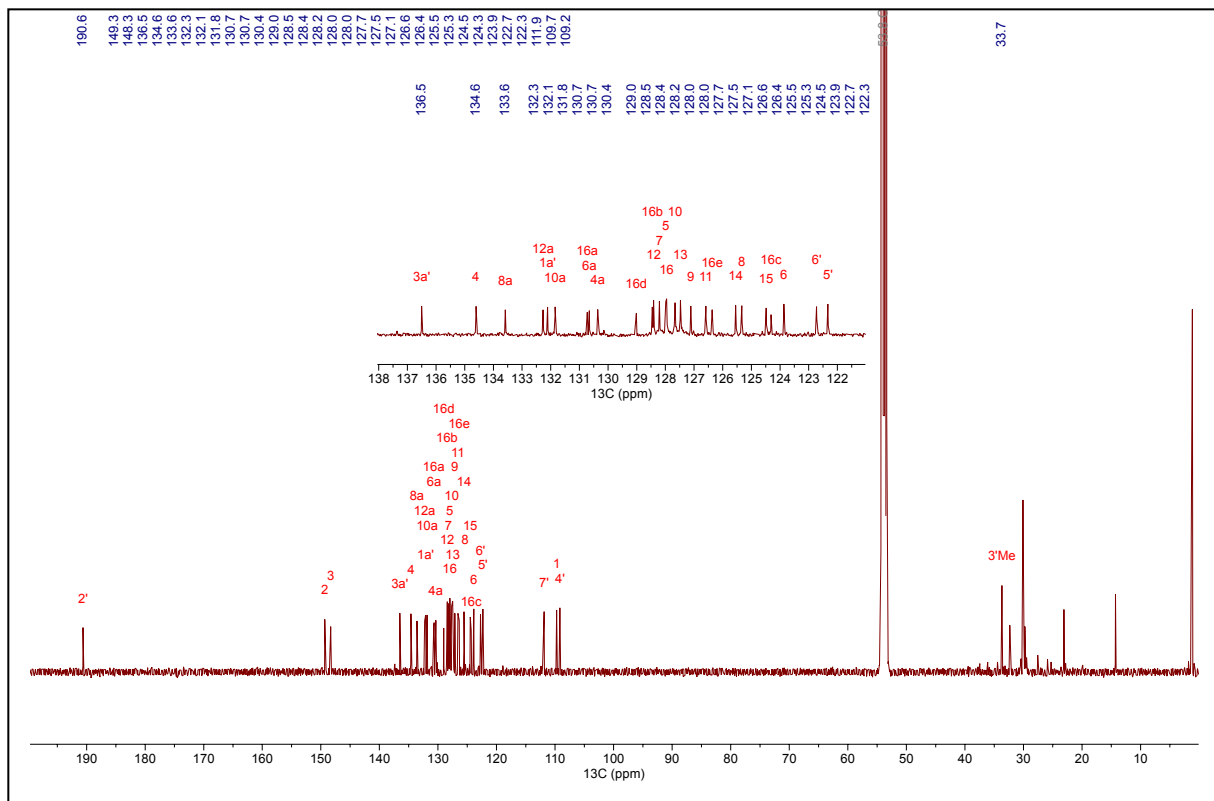


**Figure SI.23.**  $^{13}\text{C}$  NMR spectrum of  $\text{fac-}(P,\Delta_{\text{Ir}})\text{-1c}$  in  $\text{CD}_2\text{Cl}_2$  at 293 K (126 MHz).  
(Same spectrum obtained for  $\text{fac-}(M,\Delta_{\text{Ir}})\text{-1c}$ , not shown).

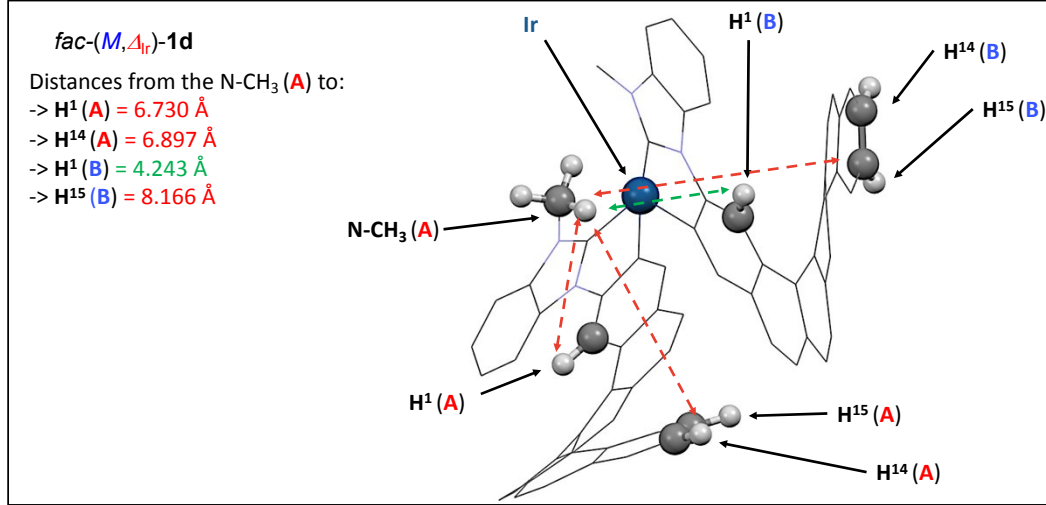


**Figure SI.24.** TPSS+D3/TZVP (continuum solvent model for dichloromethane) optimized geometry of  $\text{fac-}(M,\Delta_{\text{Ir}})\text{-1d}$  and selected distances (the third ligand and the majority of hydrogen atoms have been omitted for clarity).

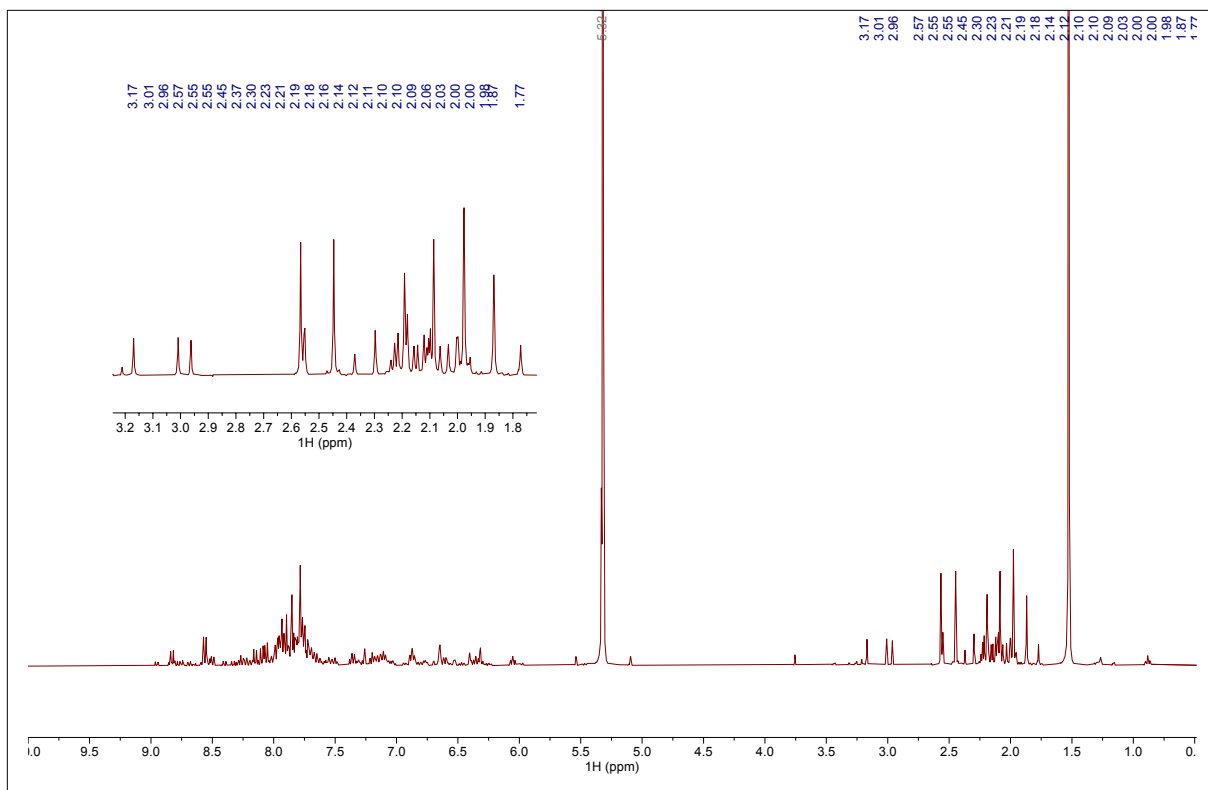


**Figure SI.25.**  $^1\text{H}$  NMR spectra of the diastereomeric mixture obtained after the cyclometalation of **7** and containing complexes **8a** and **8b** ( $\text{CDCl}_3$ , 298 K, 400 MHz).

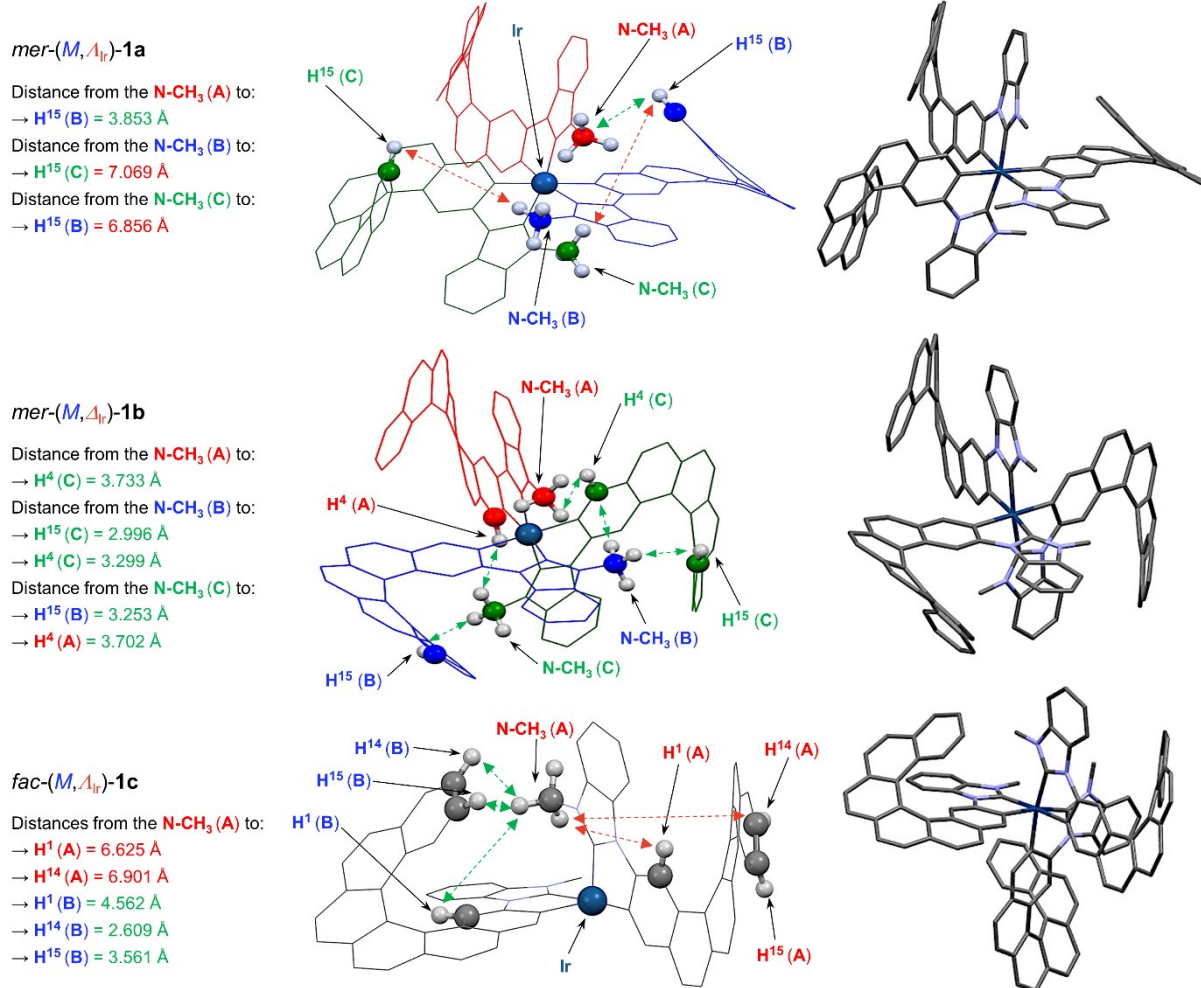


**Figure SI.26.** TPSS+D3/TZVP (continuum solvent model for dichloromethane) optimized geometries of *mer*-( $M, A_{lr}$ )-1a (top), *mer*-( $M, A_{lr}$ )-1b (middle), and *fac*-( $M, A_{lr}$ )-1c (bottom) isomers and selected distances (most hydrogen atoms and the third ligand of the *fac* isomer have been omitted for clarity). The three inequivalent [6]helicenic-NHC ligands are denoted **A**, **B** and **C** for clarity. On the right side of the figure, a corresponding ‘capped-sticks’ representation of each structure is shown in order to provide a clearer visualization of the 3D arrangement of the ligands.

### I.3. X-ray studies

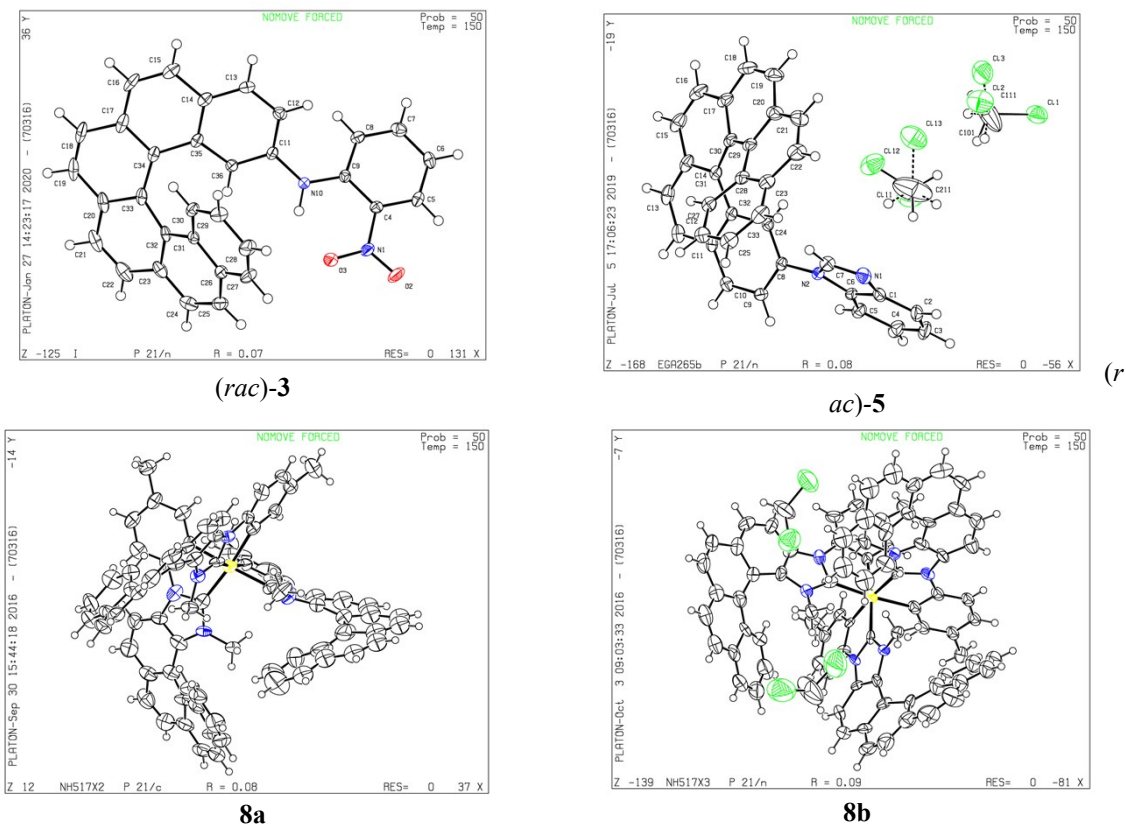


**Figure SI.27.** ORTEP figures for **3**, **5**, **8a** and **8b** (50% probability).

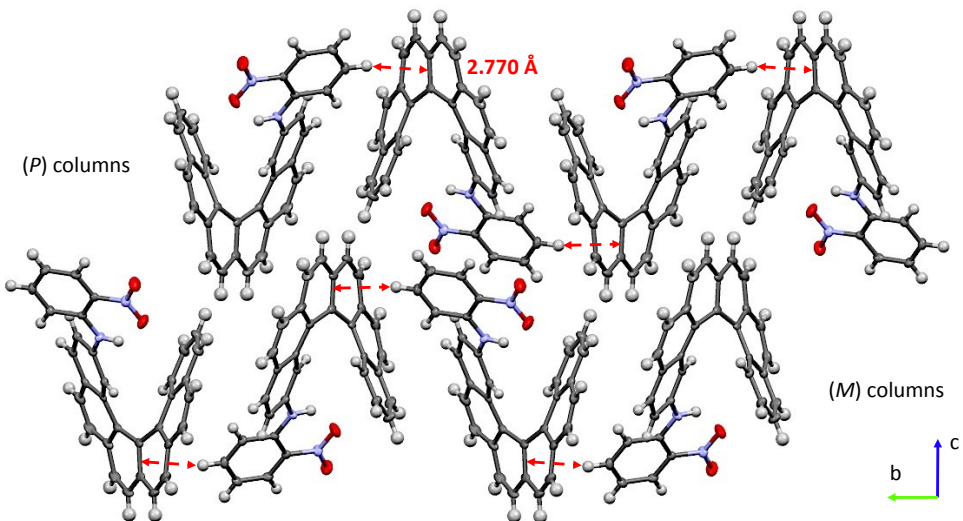


**Figure SI.28.** Supramolecular homochiral packing of **(rac)-3** along the **b** axis.

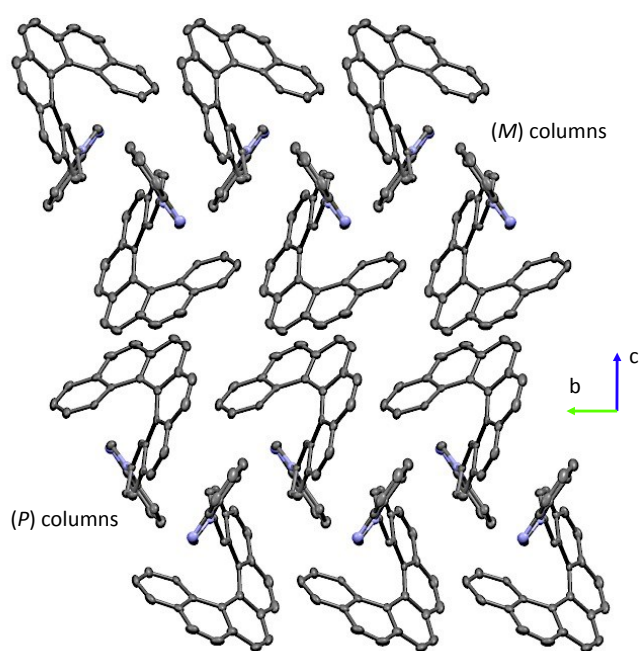


**Figure SI.29.** Supramolecular homochiral packing of (rac)-5 along the *b* axis. Hydrogen atoms have been omitted for clarity.

**Table SI.1.** X-ray crystallographic data for **3**, **5**, **8a** and **8b**.

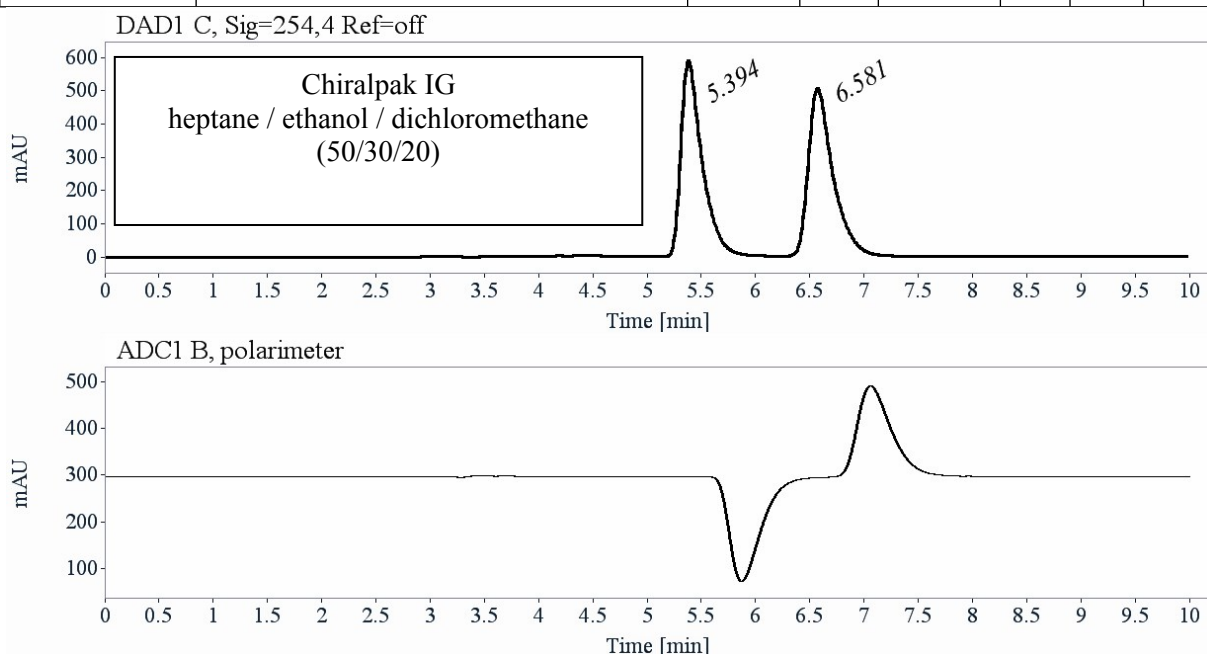
	(rac)-3	(rac)-5	8a	8b
<b>Empirical Formula</b>	C <sub>32</sub> H <sub>20</sub> N <sub>2</sub> O <sub>2</sub>	C <sub>33</sub> H <sub>20</sub> N <sub>2</sub> • 2 CH <sub>2</sub> Cl <sub>2</sub>	C <sub>81</sub> H <sub>57</sub> IrN <sub>6</sub>	C <sub>81</sub> H <sub>57</sub> IrN <sub>6</sub> • 2 CH <sub>2</sub> Cl <sub>2</sub>
<b>CCDC number</b>	2061016	2061046	2061047	2061048
<b>Formula Weight</b>	464.50	614.36	1306.60	1306.60
<b>Temperature (K)</b>	150	150(2)	150(2)	150(2)
<b>Wavelength (Å)</b>	0.71073	0.71073	0.71073	0.71073
<b>Crystal system</b>	s	monoclinic	monoclinic	monoclinic
<b>Space Group</b>	P <sub>2</sub> <sub>1</sub> /n	P <sub>2</sub> <sub>1</sub> /n	P <sub>2</sub> <sub>1</sub> /c	P <sub>2</sub> <sub>1</sub> /n
<b>a (Å)</b>	7.1750(7)	12.5677(12)	15.483(3)	15.548(5)
<b>b (Å)</b>	16.4043(15)	7.6881(8)	21.100(4)	22.223(8)
<b>c (Å)</b>	18.8242(15)	29.928(3)	23.328(4)	20.741(7)
<b>α (°)</b>	90	90	90	90
<b>β (°)</b>	92.833(4)	100.476(3)	109.463(6)	103.127(8)
<b>γ (°)</b>	90	90	90	90
<b>Volume (Å<sup>3</sup>)</b>	2212.9(3)	2843.5(5)	7186(2)	6979(4)
<b>Z</b>	4	4	4	4
<b>Color</b>	orange	yellow	yellow	yellow
<b>ρ<sub>calculated</sub> (g.cm<sup>-3</sup>)</b>	1.394	1.435	1.208	1.405
<b>Absorption coefficient (mm<sup>-1</sup>)</b>	0.088	0.446	1.903	2.116
<b>T<sub>min</sub></b>	0.670	0.727	0.892	0.498
<b>T<sub>max</sub></b>	0.995	0.919	0.718	0.628
<b>F (000)</b>	968	1264	2648	2984
<b>Crystal size (mm)</b>	0.390 x 0.075 x 0.060	0.530 x 0.220 x 0.190	0.320 x 0.280 x 0.060	0.450 x 0.260 x 0.220
<b>θ range for data collection (°)</b>	2.166 to 27.593	2.989 to 27.484	2.38 to 19.20	2.21 to 27.42
<b>Limiting indices</b>	-9 ≤ h ≤ 9 -21 ≤ k ≤ 18 -24 ≤ l ≤ 24	-16 ≤ h ≤ 16 -8 ≤ k ≤ 9 -38 ≤ l ≤ 38	-20 ≤ h ≤ 19 -27 ≤ k ≤ 26 -22 ≤ l ≤ 22	-20 ≤ h ≤ 20 -28 ≤ k ≤ 28 -26 ≤ l ≤ 26
<b>Data completeness</b>	98.4%	99%		
<b>Reflection collected</b>	19505	24608	49063	48312
<b>Reflections uniques</b>	5061 [R(int) = 0.1081]	6438 [R(int) = 0.0410]	16208	15867
<b>Data / restraints / parameters</b>	5061 / 0 / 328	6438 / 1 / 390	16208 / 1 / 727	15867 / 0 / 762
<b>Flack parameter</b>				
<b>Goodness-on-fit on F<sup>2</sup></b>	1.053	1.053	0.773	0.964
<b>Final R indices [I &gt; 2σ]</b>	R1 = 0.0732, wR2 = 0.1676	R1 = 0.0824, wR2 = 0.1850	R1 = 0.0753 wR2 = 0.1952	R1 = 0.0941 wR2 = 0.2068
<b>R indices (all data)</b>	R1 = 0.1043, wR2 = 0.1857	R1 = 0.1004, wR2 = 0.1961	R1 = 0.1710 wR2 = 0.2831	R1 = 0.2836 wR2 = 0.2777
<b>Largest diff peak and hole (eÅ<sup>-3</sup>)</b>	0.477 and -0.408	1.678 and -1.505	1.676 and -1.194	0.967 and 1.207

## I.4. Chiral HPLC separations

### Analytical chiral HPLC separation for (*rac*)-5

- The sample is dissolved in dichloromethane, injected on the chiral column, and detected with a UV detector at 254 nm and a polarimeter. The flow-rate is 1 mL/min.

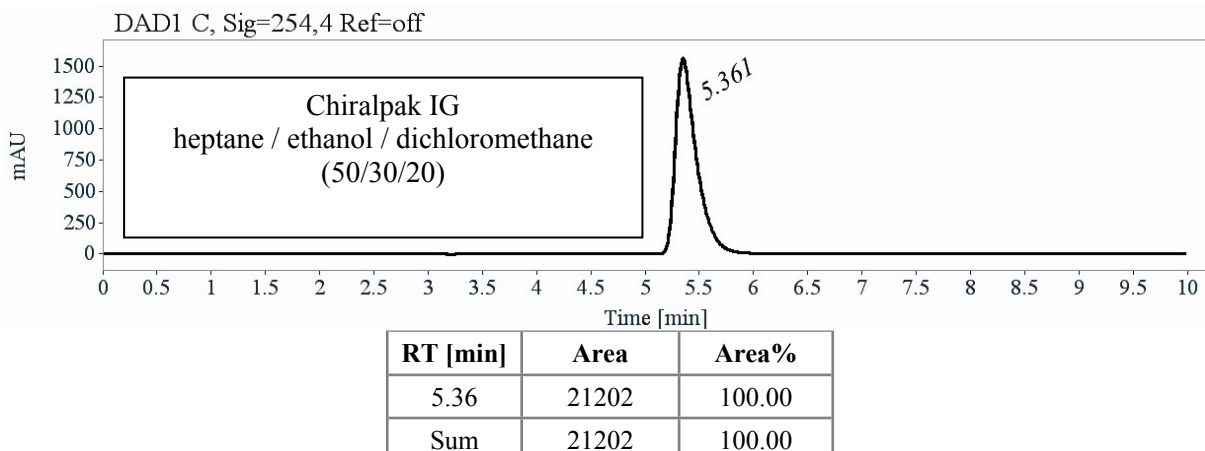
Column	Mobile Phase	t <sub>1</sub>	k <sub>1</sub>	t <sub>2</sub>	k <sub>2</sub>	$\alpha$	Rs
Chiraldak IG	heptane / ethanol / dichloromethane (50/30/20)	5.39 (-)	0.83	6.58 (+)	1.23	1.49	3.24



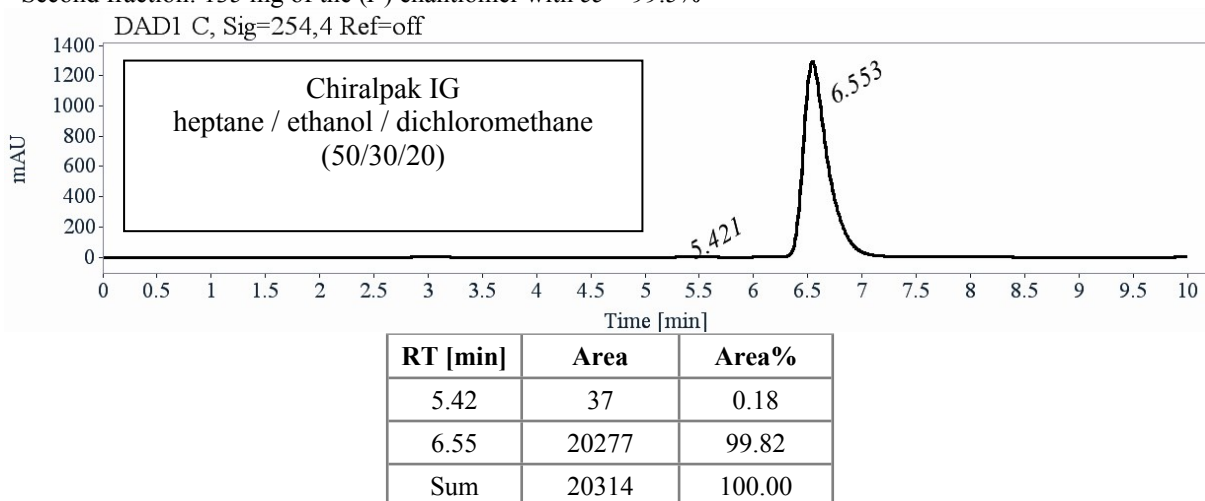
RT [min]	Area	Area%	Capacity Factor	Enantioselectivity	Resolution (USP)
5.39	8043	49.88	0.83		
6.58	8083	50.12	1.23	1.49	3.24
Sum	16126	100.00			

### Preparative separation for compound (*rac*)-5

- Sample preparation: About 285 mg of compound (*rac*)-5 is dissolved in 40 mL of dichloromethane and hexane (50/50).
- Chromatographic conditions: Chiraldak IG (250 x 10 mm), hexane / ethanol / dichloromethane (50/30/20) as a mobile phase, flow-rate = 5 mL/min, UV detection at 280 nm.
- Injections (stacked): 267 times 150  $\mu$ L, every 4 minutes.
- First fraction: 125 mg of the (*M*) enantiomer with ee > 99.5%

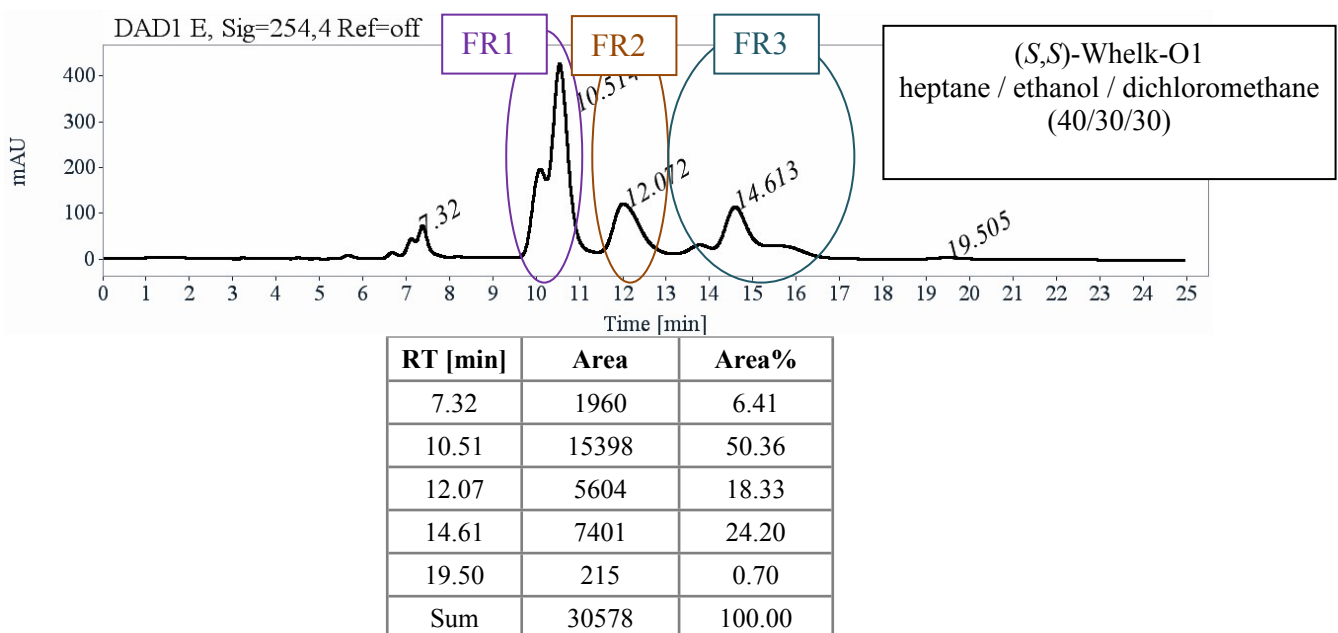


- Second fraction: 135 mg of the (*P*) enantiomer with *ee* > 99.5%



#### Analytical chiral HPLC separation for the diastereomeric mixture of *mer*-(*P*)-1a,b + *fac*-(*P*)-1c

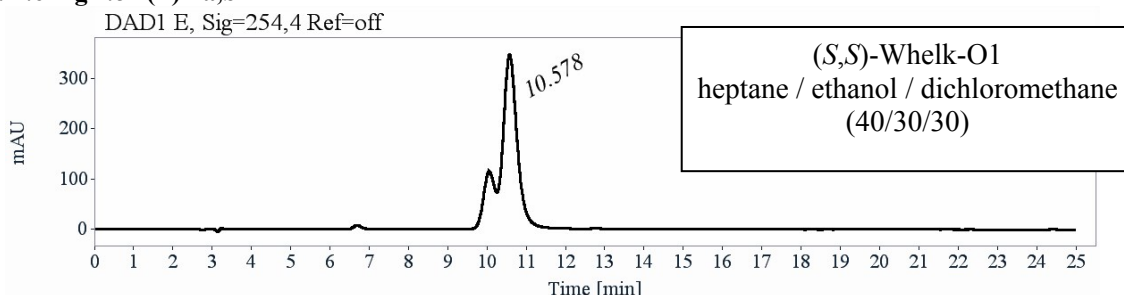
- The sample is dissolved in dichloromethane, injected on the chiral column, and detected with a UV detector at 254 nm and a circular dichroism detector at 254 nm. The flow-rate is 1 mL/min.



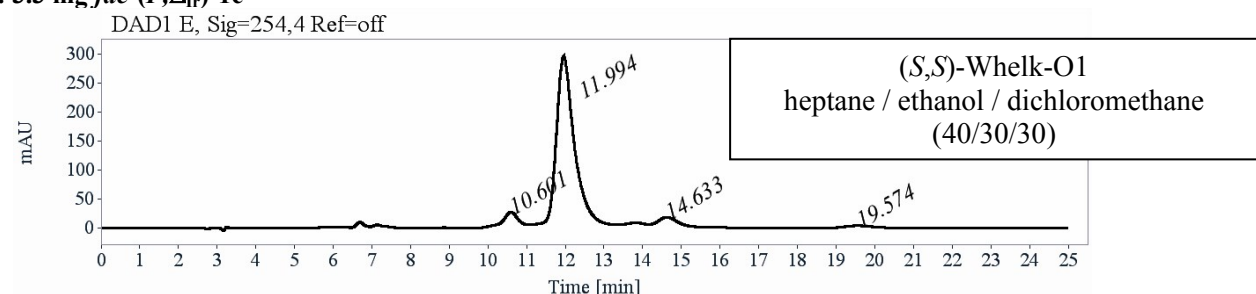
### Preparative separation for the diastereomeric mixture of *mer*-(*P*)-1a,b + *fac*-(*P*)-1c

- Sample preparation: About 25 mg of the diastereomeric mixture is dissolved in 5 mL of a mixture of dichloromethane and ethanol (60/40).
- Chromatographic conditions: (*S,S*)-Whelk-O1 (250 x 10 mm), hexane / ethanol / dichloromethane (40/30/30) as a mobile phase, flow-rate = 5 mL/min, UV detection at 254 nm.
- Injections (stacked): 17 times 300 µL, every 17.7 minutes.

#### **FR1: 7.6 mg *mer*-(*P*)-1a,b**

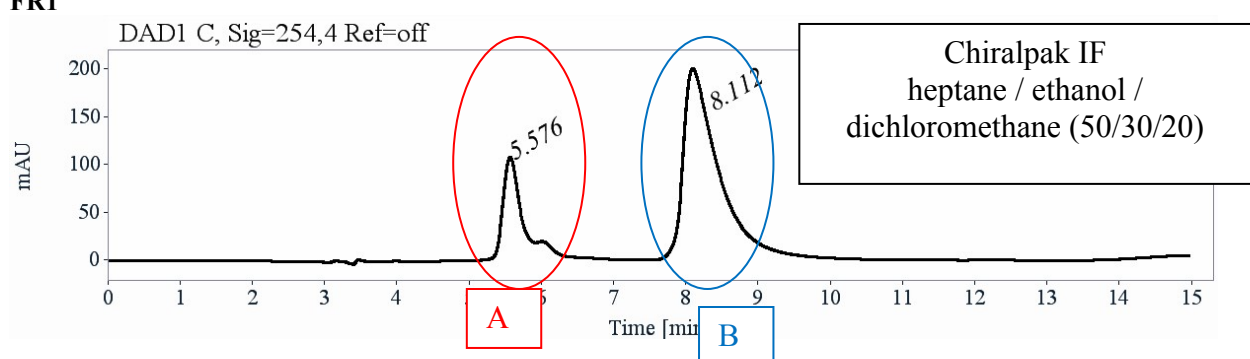


#### **FR2: 3.3 mg *fac*-(*P,Δ<sub>Ir</sub>*)-1c**



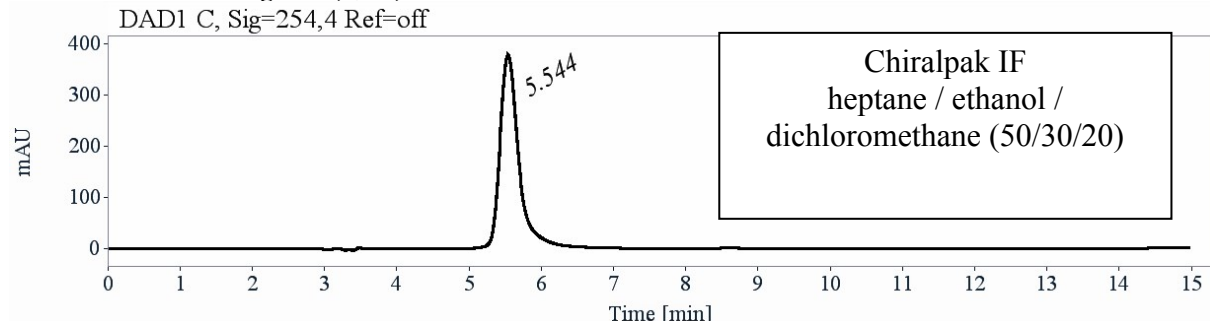
#### Preparative separation for the fraction FR1:

##### **FR1**

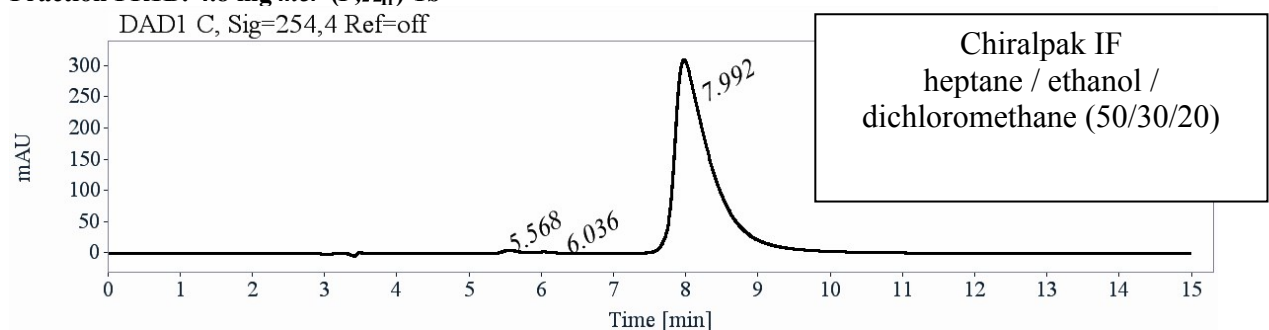


- Sample preparation: About 7 mg of the fraction **FR1** is dissolved in 1.5 mL of a mixture of dichloromethane and ethanol (60/40).
- Chromatographic conditions: Chiralpak IF (250 x 10 mm), hexane / ethanol / dichloromethane (50/30/20) as a mobile phase, flow-rate = 5 mL/min, UV detection at 254 nm.
- Injections (stacked): 15 times 100  $\mu$ L, every 10.5 minutes.

**Fraction FR1A: 2.2 mg *mer*-( $P,\Delta_{\text{L}}$ )-1a**

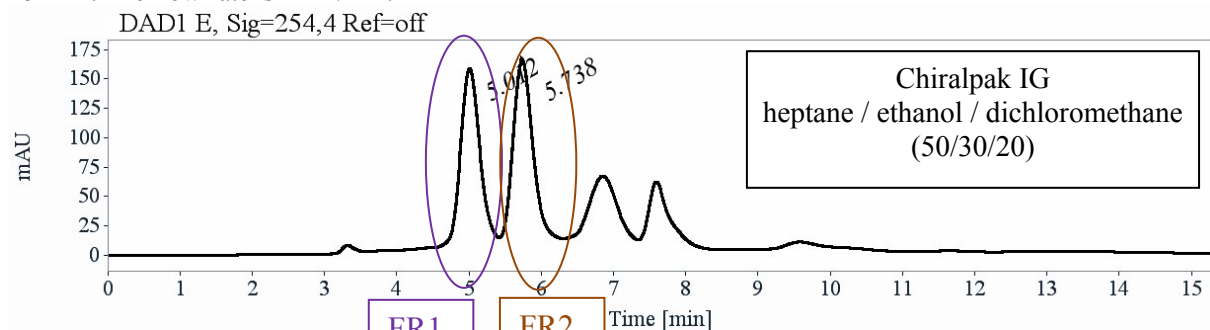


**Fraction FR1B: 4.8 mg *mer*-( $P,\Delta_{\text{L}}$ )-1b**



**Analytical chiral HPLC separation for the diastereomeric mixture of *mer*-(M)-1a,b + *fac*-(M)-1c**

- The sample is dissolved in dichloromethane, injected on the chiral column, and detected with a UV detector at 254 nm. The flow-rate is 1 mL/min.



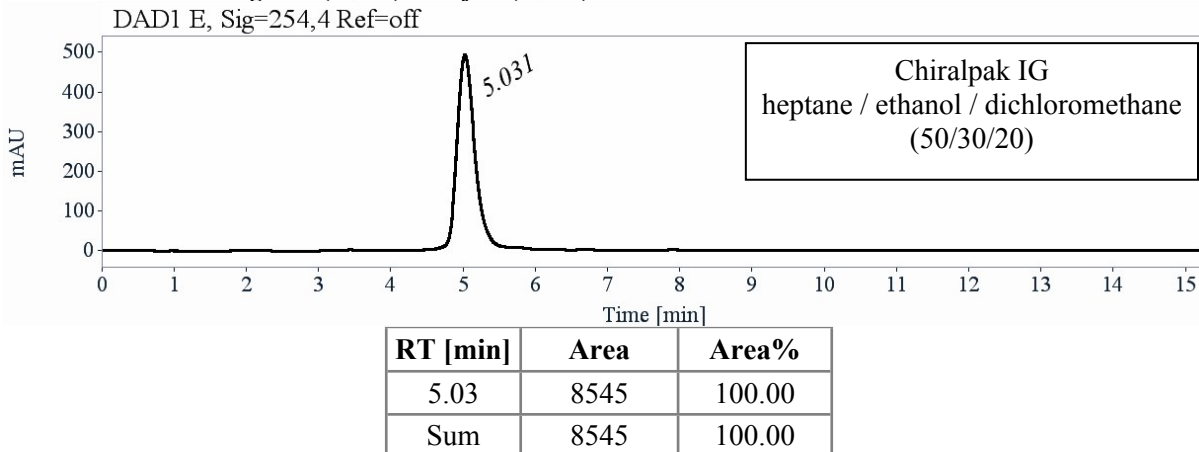
RT [min]	Area	Area%	Capacity Factor
5.01	2767	48.65	0.70
5.74	2921	51.35	0.95
Sum	5688	100.00	

**Preparative separation for the diastereomeric mixture of *mer*-(M)-1a,b + *fac*-(M)-1c**

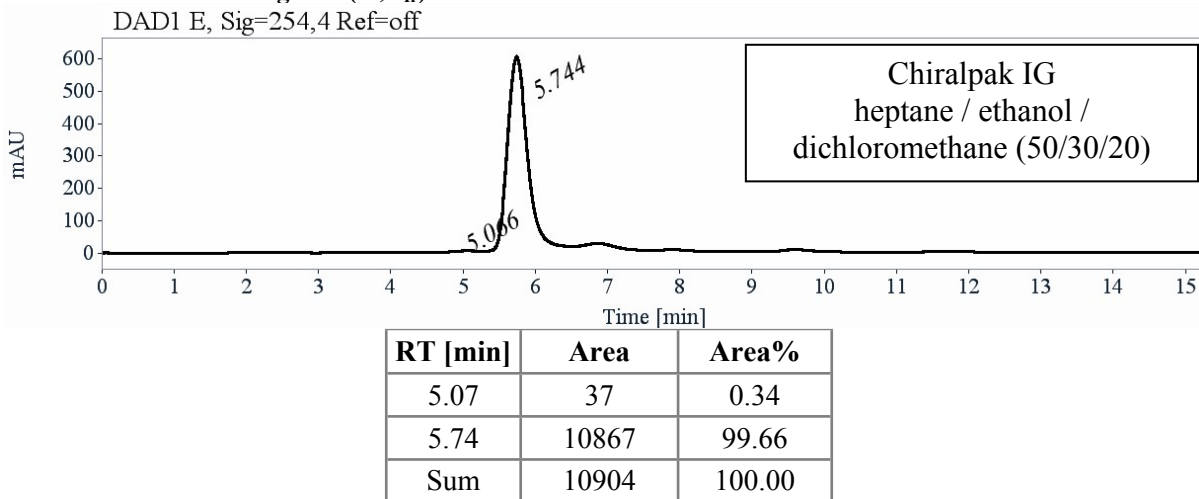
- Sample preparation: About 36 mg of the diastereomeric mixture is dissolved in 11.7 mL of a mixture of dichloromethane and ethanol (55/45).

- Chromatographic conditions: Chiraldak IG (250 x 10 mm), hexane / ethanol / dichloromethane (50/30/20) as a mobile phase, flow-rate = 5 mL/min, UV detection at 254 nm.
- Injections (stacked): 130 times 90  $\mu$ L, every 6.8 minutes.

• **First fraction: 5.4 mg *mer*-( $M,\Delta_{\text{Ir}}$ )-1a + *fac*-( $M,\Delta_{\text{Ir}}$ )-1c**

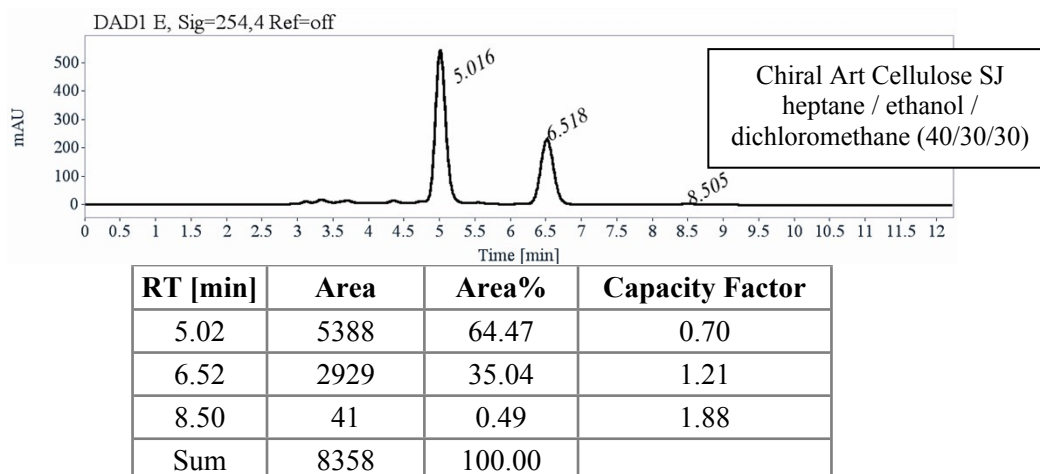


• **Second fraction: 5.7 mg *mer*-( $M,\Delta_{\text{Ir}}$ )-1b**



Analytical chiral HPLC separation for the fraction of *mer*-( $M,\Delta_{\text{Ir}}$ )-1a + *fac*-( $M,\Delta_{\text{Ir}}$ )-1c

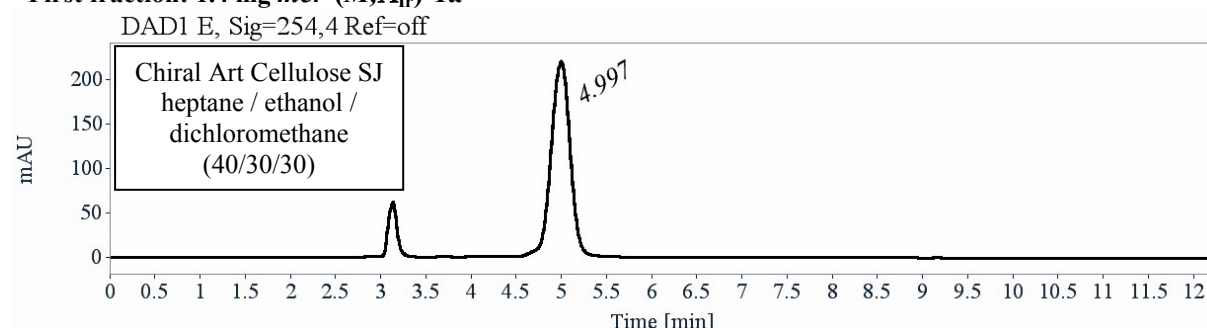
- The sample is dissolved in dichloromethane, injected on the chiral column, and detected with a UV detector at 254 nm. The flow-rate is 1 mL/min.



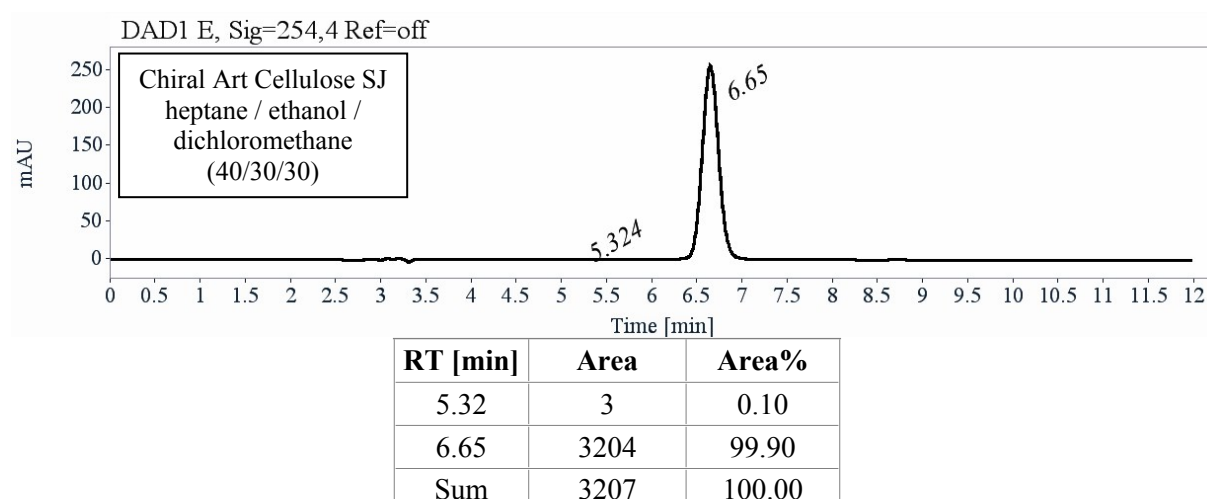
### **Preparative purification for the fraction of *mer*-(*M,Λ<sub>Ir</sub>*)-1a + *fac*-(*M,Λ<sub>Ir</sub>*)-1c**

- Sample preparation: About 5.4 mg of the fraction of *mer*-(*M,Λ<sub>Ir</sub>*)-1a + *fac*-(*M,Λ<sub>Ir</sub>*)-1c is dissolved in 3 mL of dichloromethane.
- Chromatographic conditions: Chiral Art Cellulose SJ (250 x 4.6 mm), hexane / ethanol / dichloromethane (40/30/30) as a mobile phase, flow-rate = 1 mL/min, UV detection at 254 nm.
- Injections (stacked): 6000 times 5 µL, every 7.7 minutes.

- **First fraction: 1.4 mg *mer*-(*M,Λ<sub>Ir</sub>*)-1a**



- **Second fraction: 0.6 mg *fac*-(*M,Λ<sub>Ir</sub>*)-1c**



## I.5. Photophysical studies

Absorption spectra in solution were measured on a Biotek Instruments XS spectrometer, using quartz cuvettes of 1 cm path length. Samples for emission measurements were contained within quartz cuvettes of 1 cm path length modified to allow connection to a high-vacuum line. Degassing was achieved *via* a minimum of three freeze-pump-thaw cycles whilst connected to the vacuum manifold; final vapour pressure at 77 K was  $< 5 \times 10^{-2}$  mbar, as monitored using a Pirani gauge. Luminescence quantum yields were determined using aqueous  $[\text{Ru}(\text{bpy})_3]\text{Cl}_2$  as the standard ( $\Phi_{\text{lum}} = 0.040$ ).<sup>[4]</sup> The luminescence lifetimes of the complexes were measured by multichannel scaling (MCS) following excitation into the lowest-energy absorption band with a microsecond pulsed xenon lamp. The emitted light was detected at 90° using a Hamamatsu R928 photomultiplier tube Peltier-cooled to  $-20^\circ\text{C}$ , after passage through a monochromator. The estimated uncertainty in the quoted lifetimes is  $\pm 10\%$  or better. The spectra at 77 K were recorded in a glass of EPA (= diethyl ether / isopentane / ethanol, 2:2:1 v/v).

**Table SI.2.** UV-vis and emission data for the complexes *mer*-(P)-**1a,b** and *fac*-(P)-**1c**.

Complex	Absorption $\lambda_{\text{max}} / \text{nm}$ ( $\epsilon / \text{M}^{-1}\text{cm}^{-1}$ ) <sup>a</sup>	Emission $\lambda_{\text{max}} / \text{nm}$ <sup>b</sup>	$\Phi \times 10^2$ <sup>c</sup>	$\tau_{\text{phos}} / \mu\text{s}$ <sup>d</sup>	$k_r / \text{s}^{-1}$ <sup>e</sup>	$\Sigma k_{\text{nr}} / \text{s}^{-1}$ <sup>e</sup>	Emission at 77 K <sup>f</sup>	
							$\lambda_{\text{max}} / \text{nm}$	$\tau_{\text{phos}} / \mu\text{s}$
<i>mer</i> -(P, $\Delta_{\text{Ir}}$ )- <b>1a</b>	234 (83426), 270 (83917), 335 (30978), 356sh (29396), 407sh (10269)	542, 583	1.1	31	350	32000	533, 579, 628	1800
<i>mer</i> -(P, $\Delta_{\text{Ir}}$ )- <b>1b</b>	233 (88457), 280 (87415), 355 (30958), 405 (11818)	542, 583, 640sh	3.1	81	380	12000	533, 580, 627, 688sh	1800
<i>fac</i> -(P, $\Delta_{\text{Ir}}$ )- <b>1c</b>	273 (90912), 328 (36430)	491 (Fluo); 538, 579, 635 (Phos)	2.0 <sup>g</sup>	58	340 <sup>g</sup>	17000	532, 577, 623, 703sh	1900

<sup>a</sup> In  $\text{CH}_2\text{Cl}_2$  at  $295 \pm 1$  K. <sup>b</sup> In deoxygenated  $\text{CH}_2\text{Cl}_2$  at  $295 \pm 1$  K.  $\lambda_{\text{max}} = \lambda_{(0,0)}$  in each case. <sup>c</sup> Quantum yields in deoxygenated  $\text{CH}_2\text{Cl}_2$  at  $295 \pm 1$  K were measured for  $\lambda_{\text{ex}} = 430$  nm, using  $[\text{Ru}(\text{bpy})_3]\text{Cl}_{2(\text{aq})}$  as the standard, for which  $\Phi = 0.040$ .<sup>[4]</sup> <sup>d</sup> Phosphorescence lifetime in deoxygenated  $\text{CH}_2\text{Cl}_2$  at  $295 \pm 1$  K, estimated uncertainty in the values is around  $\pm 10\%$ . <sup>e</sup> Radiative  $k_r$  and non-radiative  $\Sigma k_{\text{nr}}$  decay constants estimated assuming that the emissive triplet state is formed with unitary efficiency such that  $k_r = \Phi / \tau$  and  $\Sigma k_{\text{nr}} = (1 - \Phi) / \tau$ . Clearly this approximation, which usually applies well to phosphorescent cyclometalated Ir(III) complexes, is not valid when fluorescence is also observed. The calculated values for **1c** should thus be treated cautiously, but are provided as a guide; they indicate that  $k_r$  is not significantly different in this isomer. The weaker emission and shorter lifetime of **1a** compared to **1b** is seen to be a consequence primarily of the higher non-radiative decay rate in the former. <sup>f</sup> In diethyl ether / isopentane / ethanol, 2:2:1, v/v. <sup>g</sup> Value based on total emission intensity (fluorescence + phosphorescence).

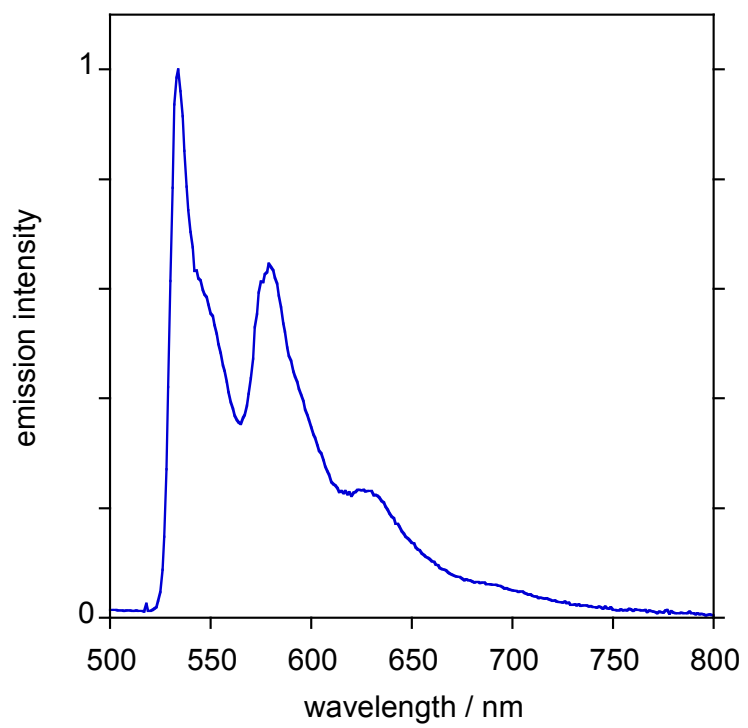
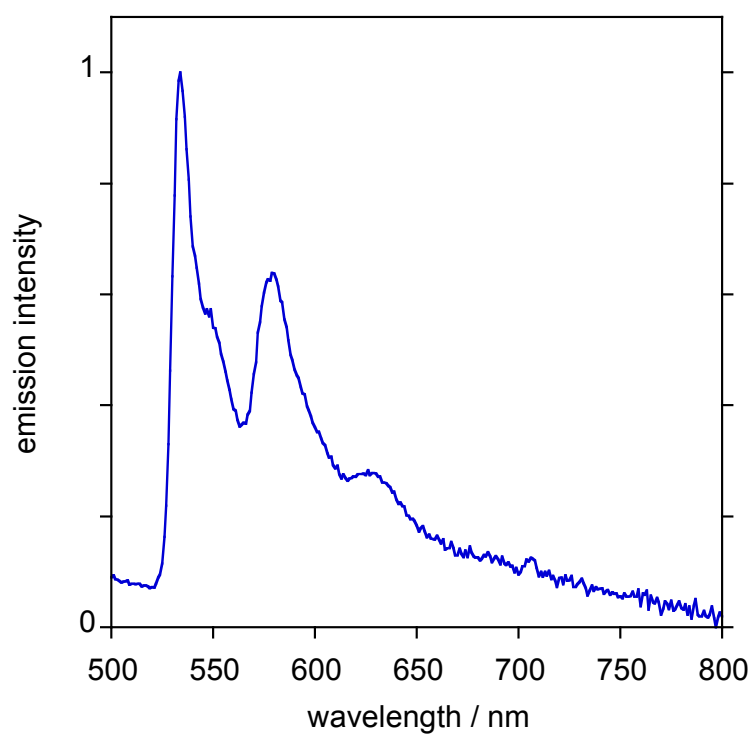


**Figure SI.30.** The emission spectra of mer-( $P, \Delta$ )<sub>n</sub>-1a (top) and mer-( $P, \Delta$ )<sub>n</sub>-1b (bottom) at 77 K in EPA ( $\lambda_{\text{ex}} = 430$  nm).

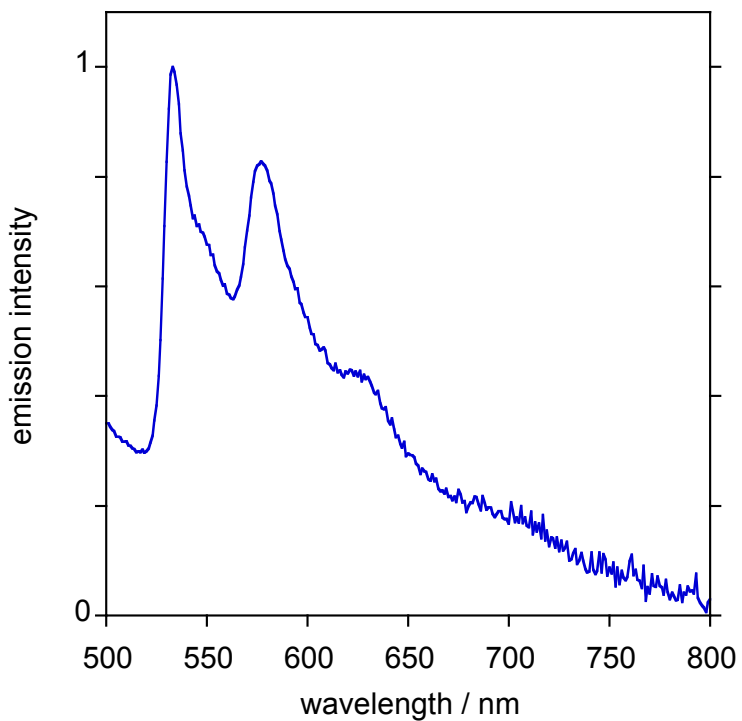


**Figure SI.31.** The emission spectrum of *fac*-( $P, \Delta$ )-Ic at 77 K in EPA ( $\lambda_{\text{ex}} = 430 \text{ nm}$ ),

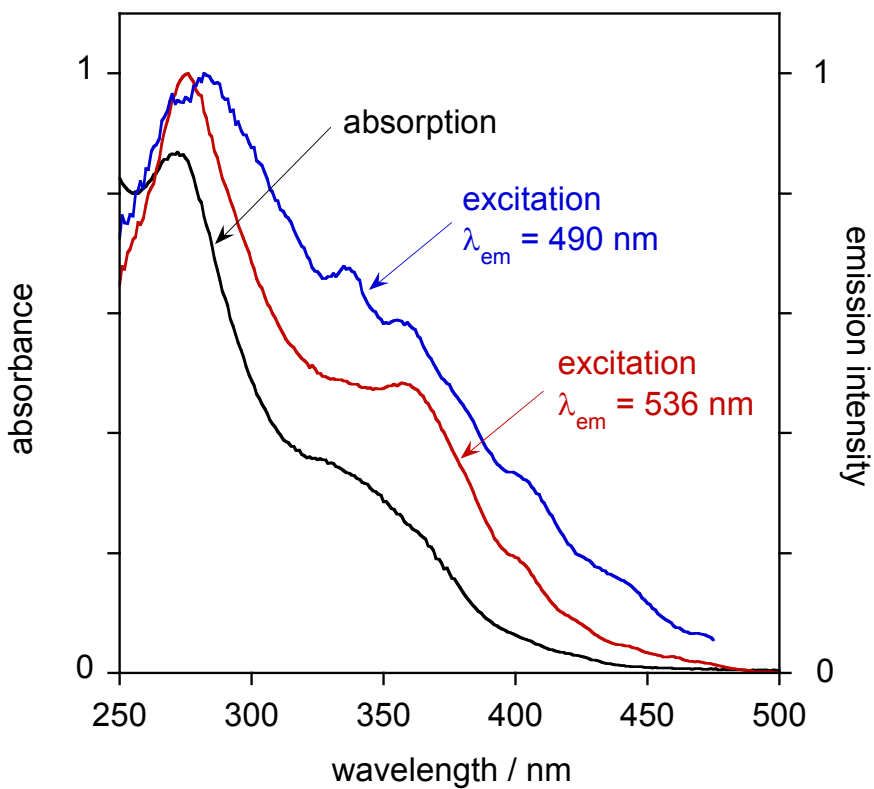


**Figure SI.32.** Absorption (black line) and excitation spectra ( $\lambda_{\text{em}} = 490$  and  $536 \text{ nm}$ , blue and red lines, respectively) of *fac*-( $P, \Delta$ )-Ic in degassed  $\text{CH}_2\text{Cl}_2$  at  $295 \pm 1 \text{ K}$ .

## I.6. Optical rotations

Optical rotations were measured on a Jasco P-2000 polarimeter with a sodium lamp (589 nm) in a 1 or 10 cm cell, thermostated with a Peltier controlled cell holder. Specific rotations are given in  $10^{-1}$  deg·cm $^2$ ·g $^{-1}$ , and molar rotations are given in  $10^{-1}$  deg·cm $^2$ ·mol $^{-1}$ . Specific and molar rotations of the stereoisomers of **1a,b,c** were measured in CH<sub>2</sub>Cl<sub>2</sub> at 25°C at concentrations around 1 with an uncertainty of  $\pm 8\%$  (see also in Table SII.2).

*Table SI.3.* Specific and molar rotations values for **1a,b,c** stereoisomers.

	Concentration (mol·L $^{-1}$ )	[ $\alpha$ ] $^{25}_D$ ( $10^{-1}$ deg·cm $^2$ ·g $^{-1}$ )	[ $\phi$ ] $^{25}_D$ ( $10^{-1}$ deg·cm $^2$ ·mol $^{-1}$ )
<b><i>mer-(M,A<sub>Ir</sub>)-1a</i></b>	$7.2 \times 10^{-5}$	-1839	- 28783
<b><i>mer-(M,Δ<sub>Ir</sub>)-1b</i></b>	$7.6 \times 10^{-5}$	- 1592	- 24908
<b><i>fac-(M,A<sub>Ir</sub>)-1c</i></b>	$4.9 \times 10^{-5}$	- 2047	- 32301
<b><i>mer-(P,Δ<sub>Ir</sub>)-1a</i></b>	$6.1 \times 10^{-5}$	+ 1615	+ 25266
<b><i>mer-(P,A<sub>Ir</sub>)-1b</i></b>	$1.1 \times 10^{-4}$	+ 1875	+ 29342
<b><i>fac-(P,Δ<sub>Ir</sub>)-1c</i></b>	$1.2 \times 10^{-4}$	+ 1784	+ 27921

## I.7. Experimental electronic circular dichroism and UV-visible spectra

UV-visible (UV-vis, in M $^{-1}$ cm $^{-1}$ ) and electronic circular dichroism (ECD, in M $^{-1}$ cm $^{-1}$ ) spectra were measured on a Jasco J-815 Circular Dichroism Spectrometer IFR140 facility. Part of this work has been performed using the PRISM core facility (Biogenouest©, UMS Biosit, Université de Rennes 1 - Campus de Villejean-35043 Rennes Cedex, France).

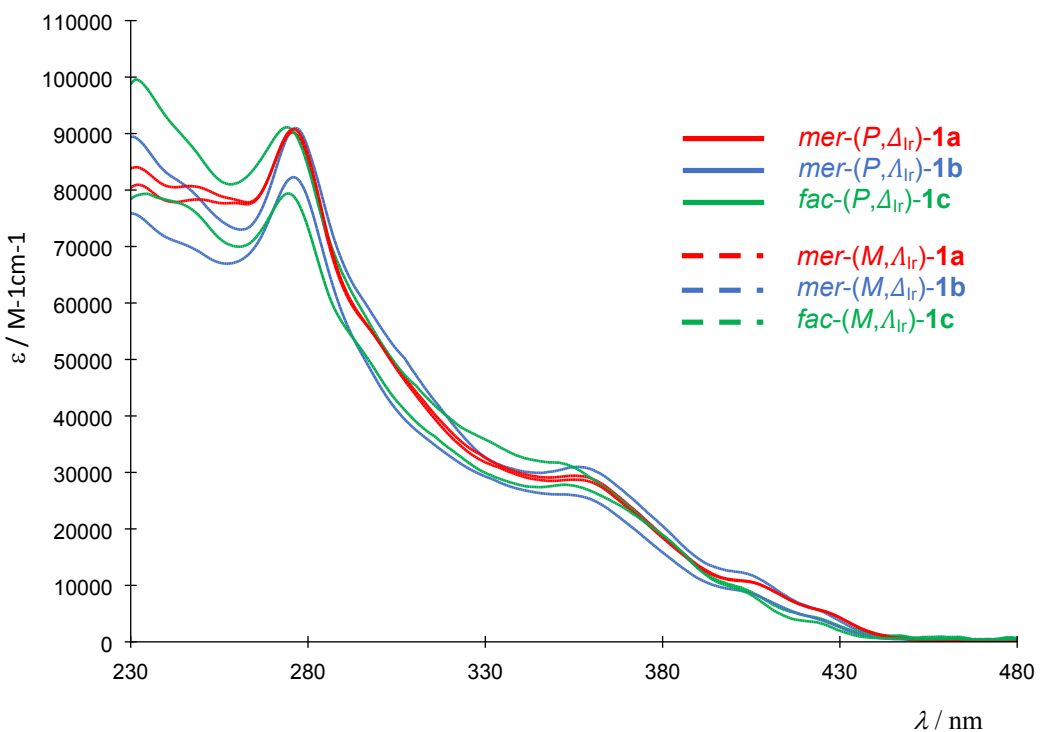


**Figure SI.33.** UV-vis spectra of the tris-NHC-Ir(III) complexes measured in  $\text{CH}_2\text{Cl}_2$  (at  $C = 10^{-5} \text{ mol L}^{-1}$ ) at 298 K.

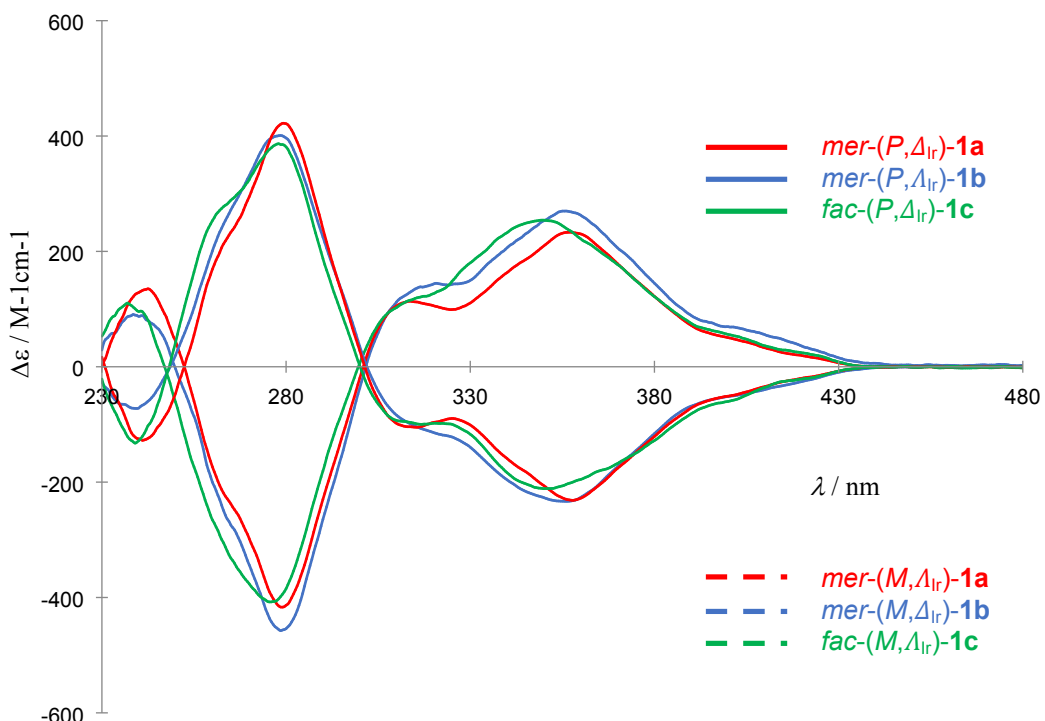


**Figure SI.34.** ECD spectra for the stereoisomers of **1a,b,c** measured in  $\text{CH}_2\text{Cl}_2$  (at  $C \sim 10^{-5} \text{ mol L}^{-1}$ ) at 298 K.

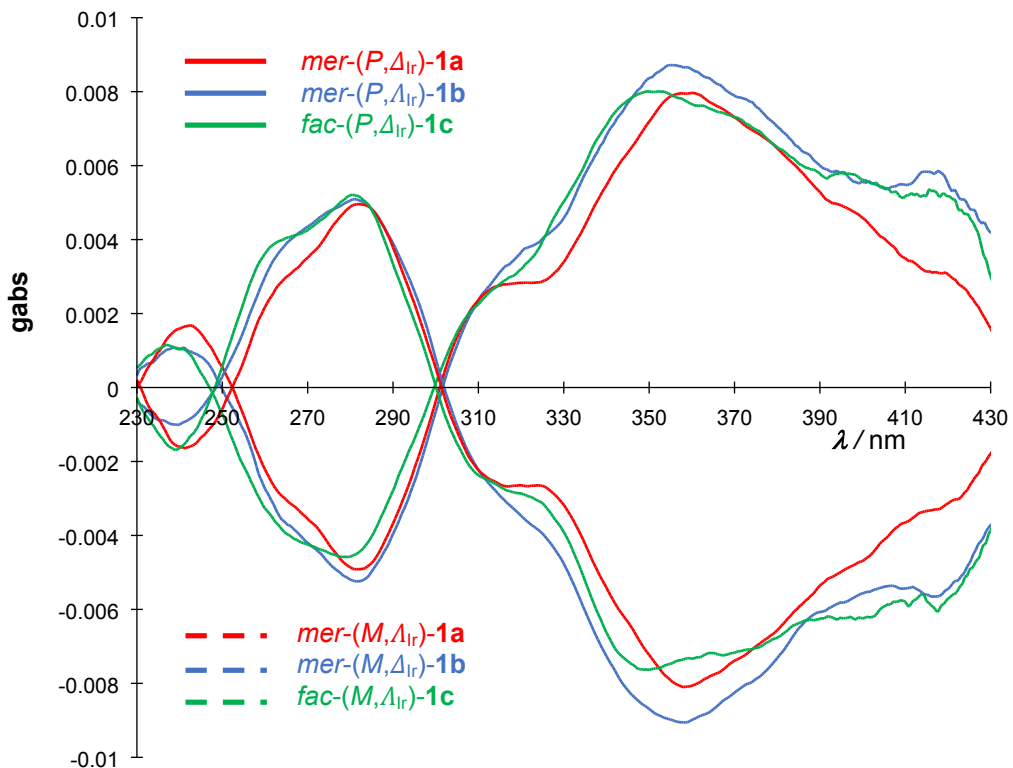


**Figure SI.35.** Absorption dissymmetry factor  $g_{abs}$  spectra of the stereoisomers of **1a,b,c** measured in  $\text{CH}_2\text{Cl}_2$  (at  $C \sim 10^{-5} \text{ mol L}^{-1}$ ) at 298 K.

## I.8. Circularly polarized luminescence spectra

Circularly polarized luminescence (CPL) measurements were performed using a home-built (with the help of the JASCO company) CPL spectrofluoropolarimeter. The samples were excited using a  $90^\circ$  geometry with a Xenon ozone-free lamp 150 W LS. The spectra were measured in  $10^{-5}$  M  $\text{CH}_2\text{Cl}_2$  solution in 1 cm cell under deoxygenated conditions. The solutions were degassed by at least 3 freeze/pump/thaw in a sealed transparent glass apparatus that included the measuring cell whilst connected to the vacuum manifold. The parameters were: emission bandwidth  $\sim 1.0$  nm, integration time = 4 sec, scan-speed = 50 nm/min, accumulations = 10.

The spectra reported below are normalized on the maximum of their corresponding photoluminescence spectra, so that the  $g_{lum}$  values can be directly read on the y-axis at the maximum of each curve.

## I.9. References

- [1] D. A. Lightner, D. T. Hefelfinger, T. W. Powers, G. W. Frank, K. N. Trueblood, *J. Am. Chem. Soc.* **1972**, *94*, 3492–3497.
- [2] N. Hellou, M. Srebro-Hooper, L. Favereau, F. Zinna, E. Caytan, L. Toupet, V. Dorcet, M. Jean, N. Vanthuyne, J. A. G. Williams, L. Di Bari, J. Autschbach, J. Crassous, *Angew. Chem. Int. Ed.* **2017**, *56*, 8236–8239.
- [3] N. N. Dhaneshwar, S. S. Tavale, L. M. Pant, *Acta. Cryst.* **1978**, *B34*, 2507–2509.
- [4] K. Suzuki, A. Kobayashi, S. Kaneko, K. Takehira, T. Yoshihara, H. Ishida, Y. Shiina, S. Oishi, S. Tobita, *Phys. Chem. Chem. Phys.* **2009**, *11*, 9850–9860

## II. Computational Part

### II.1. Computational details

All calculations were carried out employing density functional theory (DFT) methods and its time-dependent variant (TDDFT). No symmetry was imposed in the computations.

DFT geometry optimizations were performed using the Turbomole package, version 7.3,<sup>1,2,3,4</sup> with accounting for dispersion effects *via* the third-generation Grimme's set of semiempirical dispersion corrections with the Becke-Johnson damping, D3,<sup>5,6</sup> and accounting for solvent effects (dichloromethane, CH<sub>2</sub>Cl<sub>2</sub> = DCM,  $\epsilon = 8.9$ ) *via* the conductor-like screening model (COSMO) with the default parameters of the Turbomole/COSMO implementation.<sup>7,8</sup> Structures of *mer*-( $M, A_{\text{Ir}}$ ), *mer*-( $M, \Delta_{\text{Ir}}$ ), *fac*-( $M, A_{\text{Ir}}$ ) and *fac*-( $M, \Delta_{\text{Ir}}$ ) configurations were first optimized using the BP<sup>9,10,11</sup> GGA exchange-correlation functional and a split-valence basis set including one set of polarization functions for non-hydrogen atoms, SV(P),<sup>12,13,14</sup> along with a 60-electron scalar relativistic effective core potential (ECP) for Ir atoms.<sup>15</sup> The resulting BP+D3/SV(P)-ECP/COSMO(DCM)-optimized geometries were then used as starting points for optimizations employing the TPSS<sup>16</sup> meta-GGA functional along with a triple-zeta valence basis set augmented by polarization functions, TZVP,<sup>14</sup> combined with ECP(Ir), that is at TPSS+D3/TZVP-ECP/COSMO(DCM) level of theory, as the TPSS+D3/TZVP method was established as providing a reasonable balance between computational cost and accuracy of structural optimizations.<sup>17,18,19</sup> In order to facilitate the computational efficiency, all these optimizations were performed employing the resolution of identity (RI) approximation with the corresponding auxiliary basis sets taken from the Turbomole basis-set library.<sup>20,21</sup> The subsequent evaluation of the electronic energy for the final RI-DFT TPSS+D3/TZVP-ECP/COSMO(DCM)-optimized structures was carried out *via* single-point energy calculations performed with dispersion-corrected DFT employing the density functionals belonging to different classes of approximation, *i.e.* BP+D3 (gradient), TPSS+D3 (meta-gradient), B3LYP<sup>22</sup>,<sup>23,24</sup>+D3 and PBE0<sup>25</sup>+D3 (global hybrid), the TZVP-ECP basis set, and the COSMO approach to simulate DCM effects.

Following the computational approach that was successfully used in References 26 and 27 for chiral cycloiridated complexes bearing helicenic NHC ligands, subsequent TDDFT linear response UV-vis/ECD and OR calculations for the experimentally observed diastereoisomers **1a,b,c** were performed with the Gaussian 16, version C.01,<sup>28</sup> employing PBE0 and BHLYP<sup>23,29</sup> density functionals and the SV(P)-ECP basis set. Solvent (DCM) effects were modelled with the polarizable continuum model (PCM) using the default parameters of the Gaussian 16 implementation.<sup>7,30</sup> The OR parameters were calculated at the sodium line wavelength  $\lambda = 589.3$  nm. The UV-vis and ECD spectra computations performed with PBE0 / BHLYP covered the 400 / 240 lowest singlet excited states for each system to assure that all transitions with a significant dipole and rotatory strengths in the experimentally observed energy range are included. The presented spectra were simulated as the sums of Gaussian functions centered at the vertical excitation energies and scaled using the calculated oscillator / rotatory strengths with a broadening parameter of  $\sigma = 0.2$  eV.<sup>31</sup> As the calculations were performed for the structures based on *M*-helicenic ligands, the reported ECD spectra are given with the sign

opposite that of the ones calculated to match experimental data for the structures optical antipodes. As indicated by the results presented in Table SII.2 and Figure SII.1, the BHLYP functional appears to provide a better agreement with the experimental OR data, while the PBE0 functional ensures a better reproduction of the experimental ECD spectra; accordingly, the assignment of the spectra was thus based on an analysis of the PBE0/SV(P)-ECP/PCM(DCM) results.

Insight into electronic emission spectra for the experimentally observed diastereoisomers **1a,b,c** was provided *via*  $S_1$  excited-state (**1c**) and  $T_1$  excited-state (**1a,b,c**) geometry optimizations that were performed using the TDDFT method with the Tamm-Dancoff approximation,<sup>32,33,34,35,36,37</sup> TDDFT/TDA, with the PBE0 functional, the SV(P)-ECP basis set, and PCM<sup>38,39</sup> to account for the solvent (DCM) effects. As starting points in these optimizations, structures optimized with unrestricted ground-state DFT (PBE0/SV(P)-ECP/PCM(DCM)) approach and a spin multiplicity of 3,  $T_1^{\{DFT\}}$ , were used since they are supposed to give a good description of the lowest-energy electronic triplet states. All these calculations were carried out with the Gaussian 16 program.

## II.2. Additional computed data

**Table SII.1.** Relative energy values computed for different structures of a chiral iridium(III) cyclometalated complex bearing three N-[6]helicen-2-yl-benzimidazolylidene ligands. Calculations were performed with DFT+D3 employing four exchange-correlation density functionals belonging to different classes of approximation, i.e. BP (gradient), TPSS (meta-gradient), B3LYP and PBE0 (global hybrid), TZVP-ECP basis set and COSMO approach to simulate solvent (dichloromethane = DCM) effects at the geometries optimized with TPSS+D3/TZVP-ECP/COSMO(DCM).

Structure	$\Delta E / \text{kcal/mol}$			
	BP+D3	TPSS+D3	B3LYP+D3	PBE0+D3
<i>mer</i> -( $M,\Delta_{\text{Ir}}$ )- <b>1a</b>	0.00	0.05	0.00	0.26
<i>mer</i> -( $M,\Delta_{\text{Ir}}$ )- <b>1b</b>	4.67	3.33	3.64	3.28
<i>fac</i> -( $M,\Delta_{\text{Ir}}$ )- <b>1c</b>	1.33	0.00	0.56	0.00
<i>fac</i> -( $M,\Delta_{\text{Ir}}$ )- <b>1d</b>	4.03	2.94	2.87	2.82

**Table SII.2.** Experimental and calculated (TDDFT-PBE0 and -BLYP, SV(P)-ECP, PCM(dichloromethane)) optical rotations (specific  $[\alpha]_D$  in  $10^{-1}$  deg  $\text{cm}^2 \text{g}^{-1}$  and molar  $[\phi]_D$  in  $10^{-1}$  deg  $\text{cm}^2 \text{mol}^{-1}$  rotations) of the tris-NHC-Ir(III) complexes **1a,b,c** studied in this work.

System	Calc.				Expt. <sup>a</sup>	
	BLYP		PBE0			
	$[\alpha]_D$	$[\phi]_D$	$[\alpha]_D$	$[\phi]_D$	$[\alpha]_D^{23}$	$[\phi]_D^{23}$
<i>mer</i> -( <i>M,A</i> <sub>Ir</sub> )- <b>1a</b>	-1220	-19097	-1899	-29720	-1839 (+1615)	-28783 (+25266)
<i>mer</i> -( <i>M,A</i> <sub>Ir</sub> )- <b>1b</b>	-2383	-37288	-3631	-56819	-1592 (+1875)	-24908 (+29342)
<i>fac</i> -( <i>M,A</i> <sub>Ir</sub> )- <b>1c</b>	-2066	-32338	-2990	-46785	-2047 (+1784)	-32301 (+27921)

<sup>a</sup> In parentheses, experimental values for the corresponding *mer*-(*P,A*<sub>Ir</sub>)-**1a**, *mer*-(*P,A*<sub>Ir</sub>)-**1b**, and *fac*-(*P,A*<sub>Ir</sub>)-**1c** are listed. See also ‘Optical rotations’ section (section I.7).

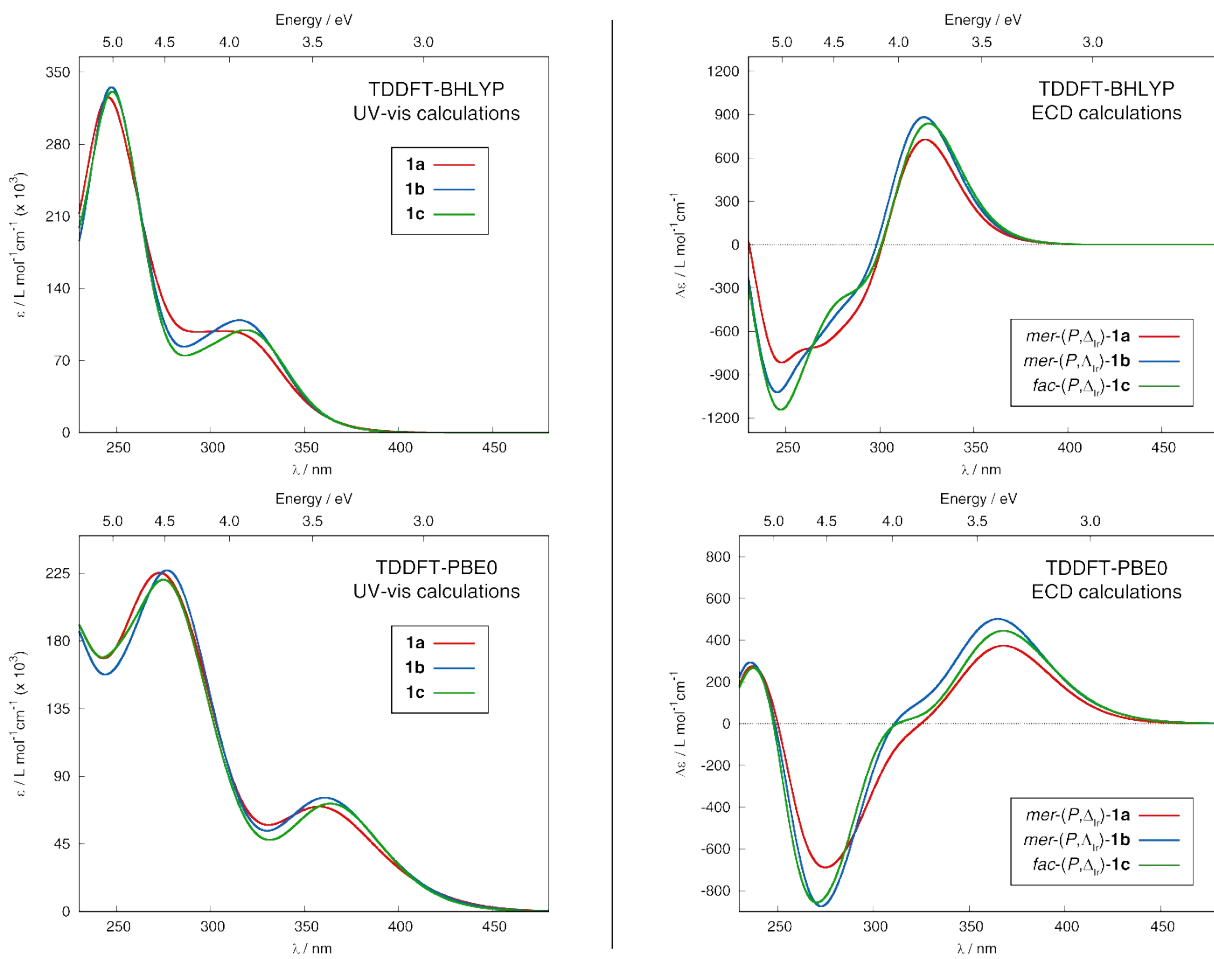


**Figure SII.1.** Simulated (TDDFT-PBE0 and -BHLYP, SV(P)-ECP, PCM(dichloromethane)) UV-vis (left) and ECD (right) spectra for the tris-NHC-Ir(III) complexes **1a,b,c** studied in this work. No spectral shift has been applied. Compare with the spectra presented in ‘Experimental electronic circular dichroism and UV-visible spectra’ section (section I.8).

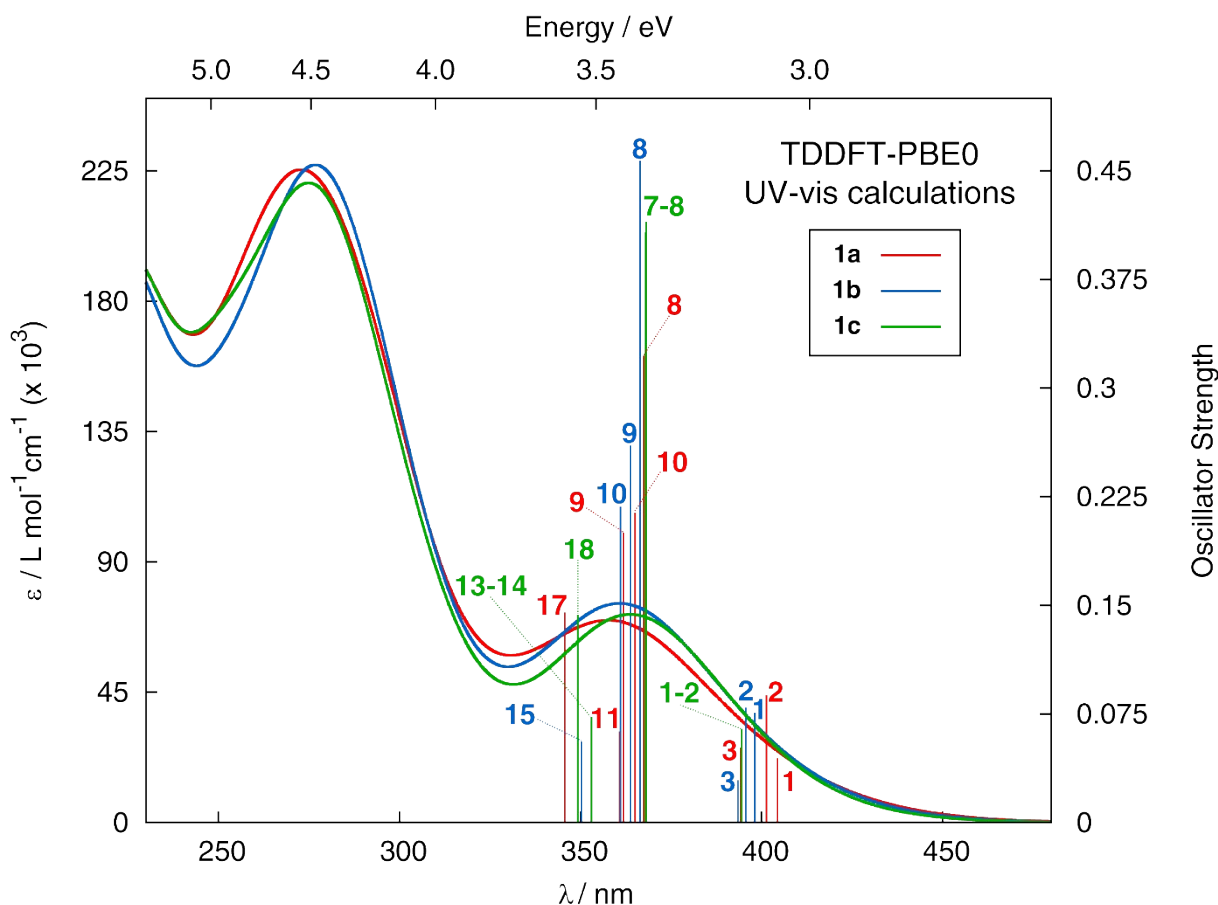


**Figure SII.2.** TDDFT-simulated (PBE0/SV(P)/PCM(dichloromethane)) UV-vis spectra for the tris-NHC-Ir(III) complexes **1a,b,c** studied in this work. No spectral shift has been applied. Selected calculated excitation energies along with the corresponding oscillator strengths, analyzed in detail (see Tables SII.3-5, Figures SII.4-6), are indicated as ‘stick’ spectra.

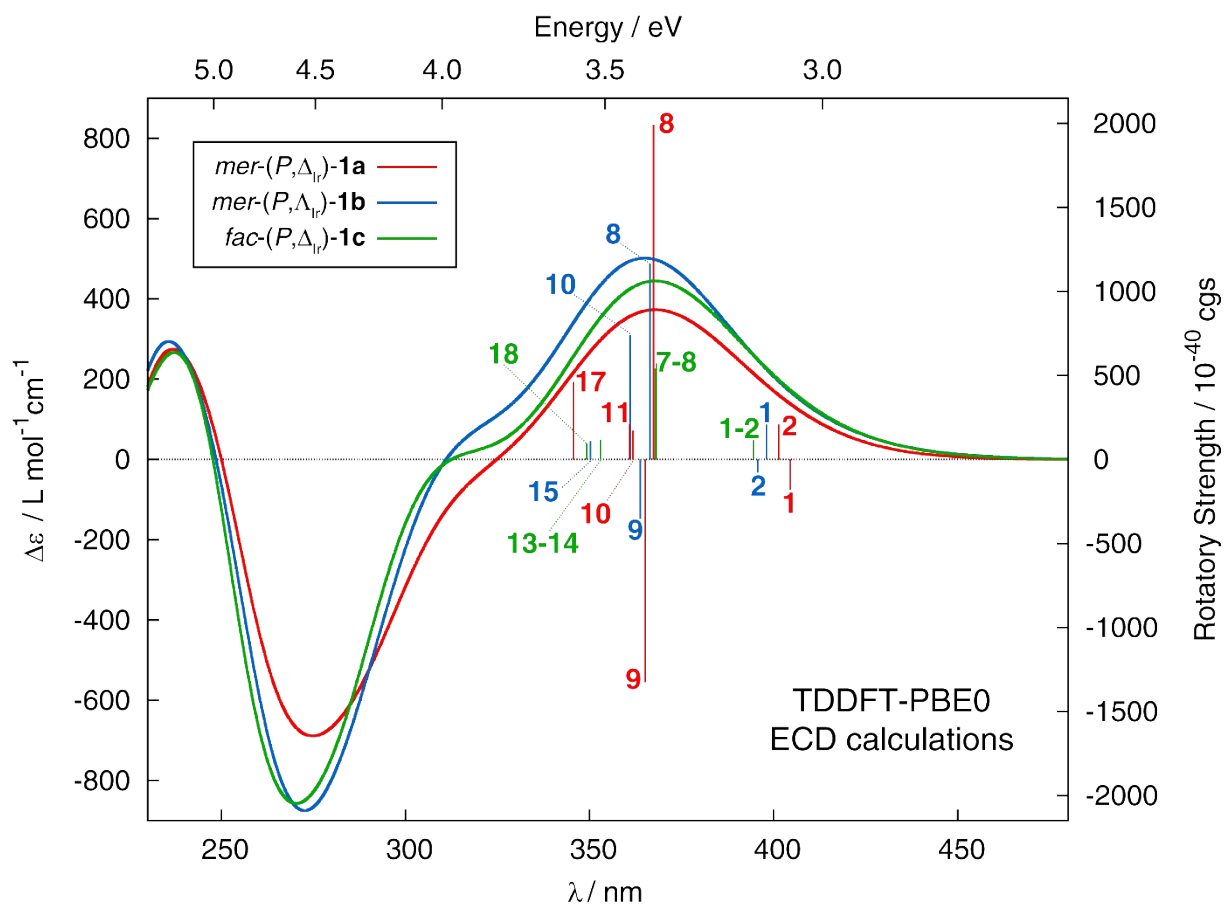


**Figure SII.3.** TDDFT-simulated (PBE0/SV(P)/PCM(dichloromethane)) ECD spectra for the tris-NHC-Ir(III) complexes **1a,b,c** studied in this work. No spectral shift has been applied. Selected calculated excitation energies along with the corresponding rotatory strengths, analyzed in detail (see Tables SII.3-5, Figures SII.4-6), are indicated as ‘stick’ spectra.

**Table SII.3.** Selected dominant excitations and occupied (occ) – unoccupied (unocc) MO pair contributions (greater than 10%) for mer-(P, $\Delta_{lr}$ )-**Ia**. Based on TDDFT PBE0/SV(P)-ECP/PCM(DCM) calculations. See Figures SII.2, SII.3, and SII4.

Excitation	$E$ / eV	$\lambda$ / nm	$f$	$R$ / $10^{-40}$ cgs	occ no.	unocc no.	%
1	3.066	404	0.044	-181.41	367	369	50.7
					367	370	22.3
2	3.089	401	0.088	209.52	367	370	41.9
					367	369	21.5
3	3.145	394	0.052	84.14	366	368	26.2
					365	368	22.3
					362	368	16.4
8	3.375	367	0.322	1992.35	367	372	32.3
					365	369	13.7
9	3.396	365	0.214	-1325.98	367	373	30.9
					366	370	10.1
10	3.426	362	0.200	171.56	366	371	21.1
					366	369	11.3
					364	369	10.0
11	3.436	361	0.063	209.52	366	371	14.4
					364	369	13.3
					366	369	10.3
17	3.587	346	0.145	461.31	364	369	16.1
					363	372	13.9

**Table SII.4.** Selected dominant excitations and occupied (occ) – unoccupied (unocc) MO pair contributions (greater than 10%) for mer-( $P, A_{Ib}$ )-**Ib**. Based on TDDFT PBE0/SV(P)-ECP/PCM(DCM) calculations. See Figures SII.2, SII.3, and SII.5.

Excitation	$E$ / eV	$\lambda$ / nm	$f$	$R$ / $10^{-40}$ cgs	occ no.	unocc no.	%
1	3.114	398	0.076	209.21	367	369	51.8
					365	369	13.7
2	3.133	396	0.080	-77.68	367	370	36.0
					363	370	12.4
3	3.152	393	0.029	74.76	366	368	25.3
					362	368	17.3
8	3.384	366	0.457	1163.77	367	372	25.1
					364	369	12.0
9	3.408	364	0.260	-353.71	367	373	20.0
					366	370	13.2
10	3.434	361	0.218	741.69	366	371	23.2
					362	368	18.5
15	3.540	350	0.056	109.45	367	371	59.4
					362	371	11.0

**Table SII.5.** Selected dominant excitations and occupied (occ) – unoccupied (unocc) MO pair contributions (greater than 10%) for fac-(P, $\Delta_{lr}$ )-**1c**. Based on TDDFT PBE0/SV(P)-ECP/PCM(DCM) calculations. See Figures SII.2, SII.3, and SII.6.

Excitation	$E$ / eV	$\lambda$ / nm	$f$	$R$ / $10^{-40}$ cgs	occ no.	unocc no.	%
1	3.143	395	0.063	109.26	367	369	23.9
					364	369	10.3
					364	368	10.2
2	3.143	394	0.065	113.75	367	370	24.5
					363	368	12.6
					364	370	10.1
7	3.368	368	0.415	571.61	366	371	16.9
					362	372	10.0
					365	371	15.1
8	3.369	368	0.408	540.89	367	369	15.0
					362	373	10.6
					367	370	11.8
13	3.512	353	0.073	110.63	367	372	10.9
					366	370	10.8
					367	369	11.4
14	3.512	353	0.070	116.40	366	369	10.9
					365	370	10.2
					367	373	10.2
18	3.550	349	0.143	95.63	367	371	32.6

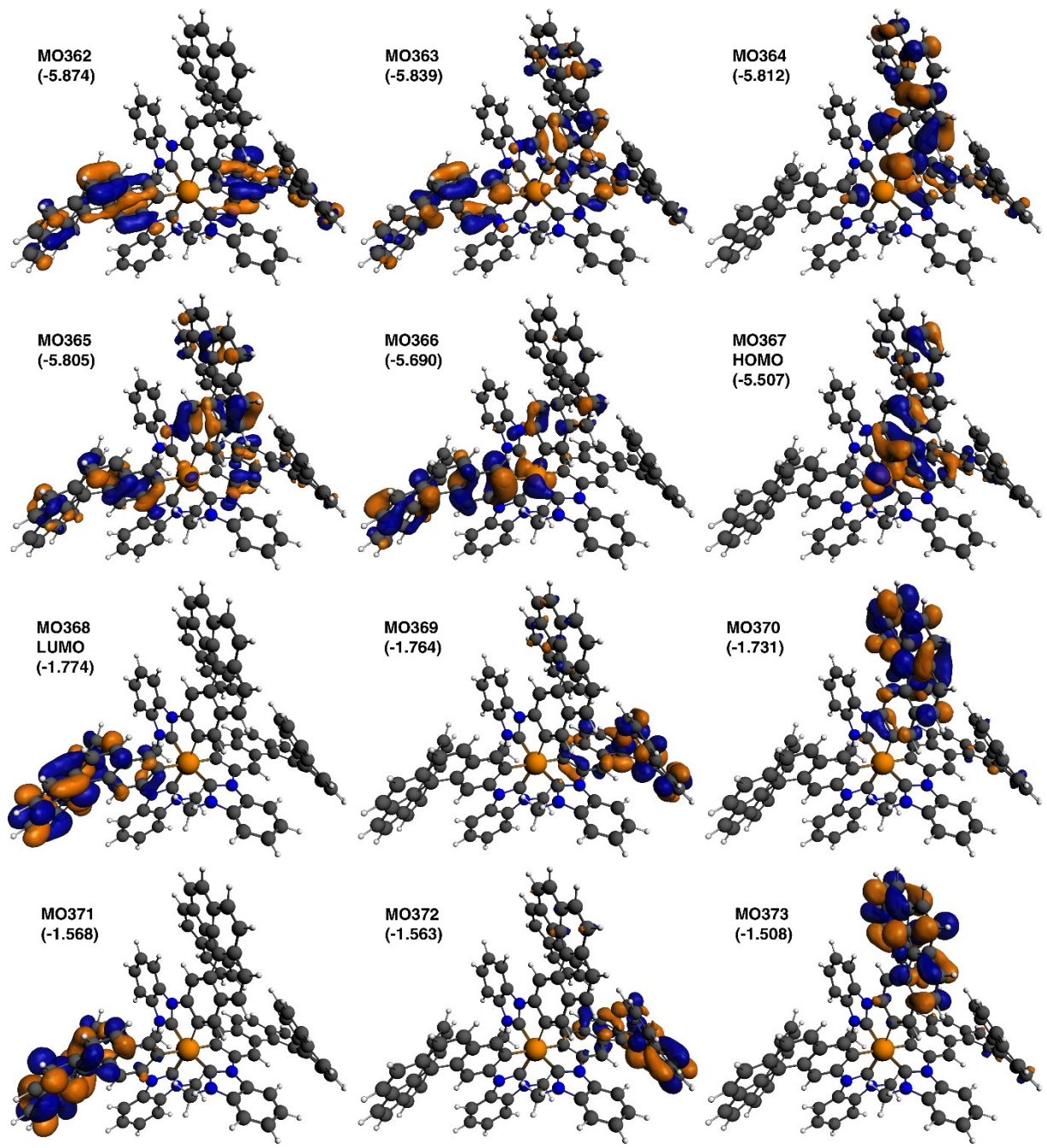


**Figure SII.4.** Isosurfaces ( $\pm 0.03$  au) of MOs involved in selected electronic transitions of **1a**. Values listed in the parentheses are the corresponding orbital energies, in eV.

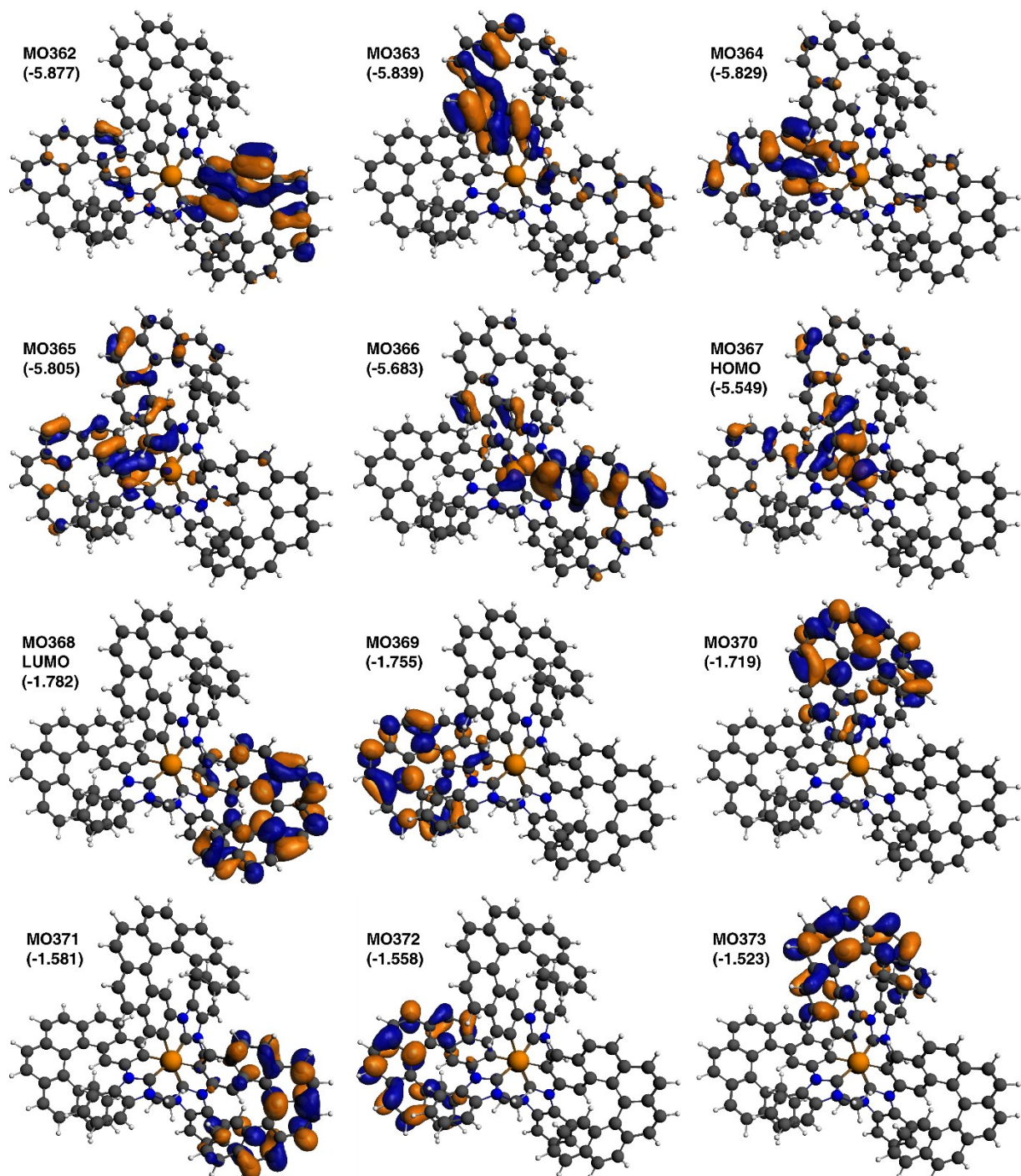


**Figure SII.5.** Isosurfaces ( $\pm 0.03$  au) of MOs involved in selected electronic transitions of **Ib**. Values listed in the parentheses are the corresponding orbital energies, in eV.

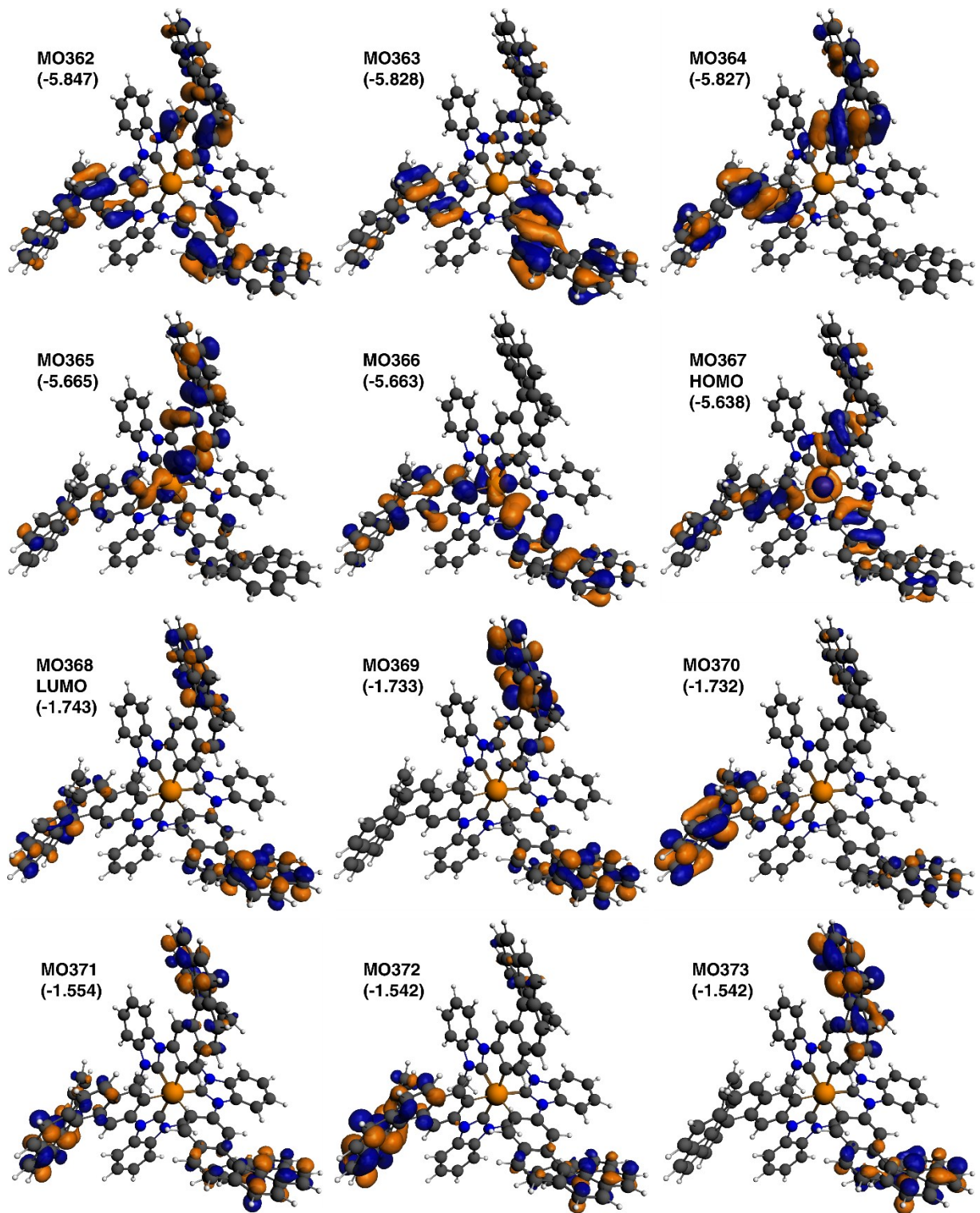


**Figure SII.6.** Isosurfaces ( $\pm 0.03$  au) of MOs involved in selected electronic transitions of **1c**. Values listed in the parentheses are the corresponding orbital energies, in eV.

**Table SII.6.** Experimental and calculated (TDDFT/TDA PBE0/SV(P)-ECP/PCM(DCM)) emission data for the tris-NHC-Ir(III) complexes **1a,b,c** studied in this work.

	<i>mer</i> -(P, $\Delta_{\text{Ir}}$ )- <b>1a</b>	<i>mer</i> -(P, $\Delta_{\text{Ir}}$ )- <b>1b</b>	<i>fac</i> -(P, $\Delta_{\text{Ir}}$ )- <b>1c</b>
Expt. <sup>a</sup>			
295 K	P: 2.288 (542), 2.127 (583)	P: 2.288 (542), 2.127 (583), 1.937 (640)	F: 2.525 (491) P: 2.305 (538), 2.141 (579), 1.953 (635)
77 K	P: 2.326 (533), 2.141 (579), 1.974 (628)	P: 2.326 (533), 2.138 (580), 1.977 (627), 1.802 (688)	P: 2.331 (532), 2.149 (577), 1.990 (623), 1.764 (703)
Calc. PBE0/SV(P)-ECP/PCM(DCM) <sup>b</sup>			
$T_1^{\{\text{TDDFT/TDA}\}}$	2.094 (592)	2.081 (596)	2.100 (590)
Assignment	367-to-368: 67.0	367-to-368: 67.9	367-to-368:
MO-to-MO: %	366-to-368: 12.8	365-to-368: 11.7	77.1
$S_1^{\{\text{TDDFT/TDA}\}}$	—	—	2.800 (443)
$R / f$	—	—	257.70 / 0.288
Assignment	—	—	367-to-368:
MO-to-MO: %	—	—	96.0

<sup>a</sup> Energies, in eV (nm). 295 K: recorded in dichloromethane, 77 K: recorded in EPA. F = fluorescence. P = phosphorescence. See also ‘Photophysical studies’ section (section I.6).

<sup>b</sup>  $T_1^{\{\text{TDDFT/TDA}\}}$ : TDDFT/TDA  $T_1$ - $S_0$  energy difference at TDDFT/TDA PBE0/SV(P)-ECP/PCM(DCM) optimized  $T_1$  geometry, in eV (nm), along with MO-pairs assignment of the corresponding transitions.  $S_1^{\{\text{TDDFT/TDA}\}}$ : TDDFT/TDA  $S_1$ - $S_0$  energy difference at TDDFT/TDA PBE0/SV(P)-ECP/PCM(DCM) optimized  $S_1$  geometry, in eV (nm), along with the rotatory strength  $R$ , in  $10^{-40}$  cgs, and oscillator strength  $f$  values, and MO-pairs assignment of the corresponding transition. For MOs isosurfaces, see Figure SII.7.

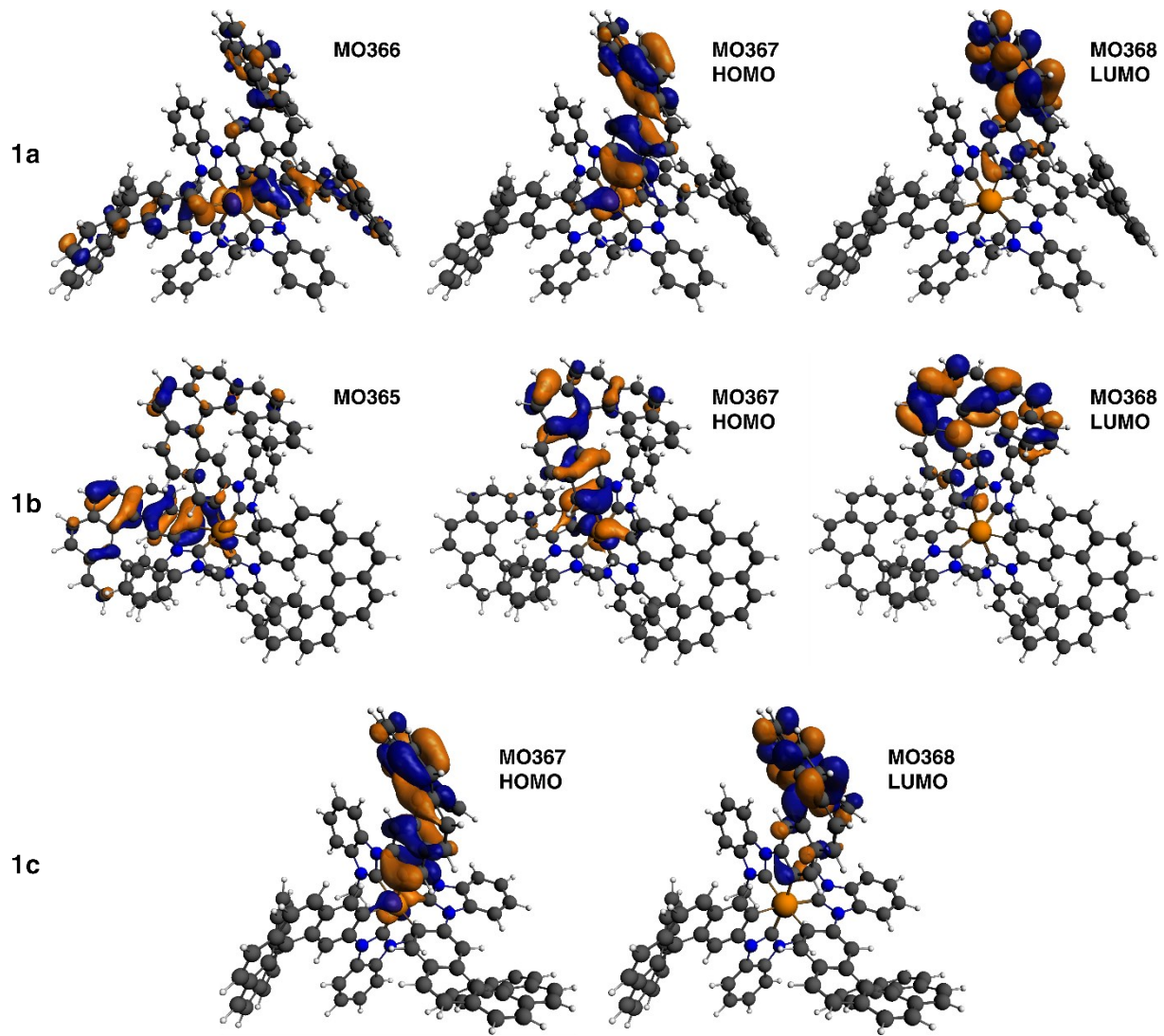


**Figure SII.7.** Isosurfaces ( $\pm 0.03$  au) of MOs of  $S_0$  at  $T_1^{(TDDFT/TDA)}$  excited-state geometry involved in  $T_1 \rightarrow S_0$  emission transitions for the tris-NHC-Ir(III) complexes **1a,b,c** studied in this work. Isosurfaces of the corresponding MOs of  $S_0$  at  $S_1^{(TDDFT/TDA)}$  excited-state geometry involved in  $S_1 \rightarrow S_0$  emission transitions for the tris-NHC-Ir(III) complex **1c** appeared to be very similar and therefore they are not shown.

### II.3. Cartesian coordinates for optimized structures

Optimized (TPSS+D3/TZVP-ECP with the continuum solvent model for  $\text{CH}_2\text{Cl}_2$ ) geometries of tris-helicene-NHC-Ir complexes along with the corresponding absolute energies:

The atomic symbol followed by three Cartesian coordinates, in Å.

*mer-(M,A<sub>Ir</sub>)-1a*

Total energy = -4360.671697 au

C	-1.1404801	1.3201885	-1.8645127
C	-0.7494202	0.2976696	-1.0170093
C	-1.0745766	-1.0171142	-1.4651896
C	-1.6599665	-1.2903543	-2.6828540
C	-1.9432642	-0.2449230	-3.5893926

C	-1.7465172	1.0926877	-3.1242349
C	-2.1934189	2.1857635	-3.9217235
C	-2.8466878	1.9617228	-5.0992202
C	-3.0002909	0.6393501	-5.6174500
C	-2.4257089	-0.4752312	-4.9368126
C	-3.7796828	0.4435743	-6.7913063
C	-4.0496020	-0.8201278	-7.2333538
C	-3.3996479	-1.9436997	-6.6490051
C	-2.4339902	-1.7655321	-5.6058972
C	-3.7297877	-3.2471700	-7.1137369
C	-3.1184741	-4.3482274	-6.5859489
C	-2.0017830	-4.1944325	-5.7181439
C	-1.5636112	-2.8971258	-5.3224315
C	-1.2980314	-5.3640413	-5.2917310
C	-0.1513330	-5.2714340	-4.5633461
C	0.4325931	-3.9949525	-4.3103398
C	-0.2305975	-2.8035828	-4.7467029
C	1.6867809	-3.9078911	-3.6611902
C	2.3140888	-2.6928319	-3.4889854
C	1.7167297	-1.5281628	-4.0053054
C	0.4826532	-1.5855654	-4.6231951
Ir	0.1740858	0.4011583	0.8414610
C	2.0098207	0.6344626	-0.1465785
N	-0.6613622	-2.0292519	-0.5594987
C	0.0623444	-1.6012638	0.5383547
N	0.4931457	-2.7281311	1.1651287
C	0.0262315	-3.8699555	0.5099063
C	-0.7259375	-3.4264932	-0.5982817
C	-1.3532643	-4.3476677	-1.4370745
C	-1.1889180	-5.7033569	-1.1464136
C	-0.4219139	-6.1366517	-0.0563092
C	0.1999002	-5.2203859	0.7945032
C	1.3399478	-2.7438486	2.3526806
C	-1.6744163	0.1735436	1.8387213
C	-1.5863553	0.0069745	3.2520572
C	-2.6729849	-0.2531906	4.0601937
C	-3.9639852	-0.3839965	3.5032946
C	-4.1055076	-0.1433725	2.1023396
C	-2.9542088	0.0966911	1.3118803
C	-5.4125754	-0.0844920	1.5318524
C	-6.5207317	-0.1580455	2.3276056
C	-6.4072586	-0.4169889	3.7289571
C	-5.1327519	-0.6888906	4.3024158
C	-7.5617997	-0.3455055	4.5590895
C	-7.4434435	-0.4594583	5.9169338
C	-6.2079407	-0.8568302	6.5034603
C	-5.0846045	-1.1578447	5.6719931
C	-6.0921208	-0.9499354	7.9194638
C	-4.9188600	-1.3484892	8.4972369
C	-3.8700100	-1.8775369	7.6924055
C	-3.9995536	-1.9072197	6.2755468
C	-2.7097940	-2.4276302	8.3227603
C	-1.7525909	-3.0744809	7.5993856

C	-1.9496164	-3.3190714	6.2064417
C	-3.0987430	-2.7829595	5.5438208
C	-1.0482475	-4.1442988	5.4923705
C	-1.2914138	-4.4935219	4.1799696
C	-2.4626996	-4.0366162	3.5455778
C	-3.3397265	-3.2039013	4.2129847
N	-0.2631195	0.1415782	3.7540939
C	0.7430687	0.3599057	2.8206445
N	1.8856060	0.5074624	3.5480760
C	1.6368763	0.3648222	4.9124632
C	0.2549321	0.1235922	5.0559493
C	-0.2911179	-0.0813519	6.3247136
C	0.5767568	-0.0338660	7.4179933
C	1.9484709	0.2122453	7.2650114
C	2.5033880	0.4169218	5.9999164
C	3.2063011	0.7743956	2.9900502
H	3.1191141	0.7459213	1.9051282
H	3.5558411	1.7585466	3.3153942
H	3.9115086	0.0097803	3.3284233
H	3.5640664	0.6054683	5.8704359
H	2.5896856	0.2412979	8.1406774
H	0.1708855	-0.1990455	8.4112419
H	-1.3395330	-0.2842395	6.4887977
H	-2.5611298	-0.3556514	5.1269448
H	-4.2420282	-2.8792216	3.7105160
H	-2.6809632	-4.3421471	2.5262350
H	-0.6015206	-5.1411042	3.6482581
H	-0.1712429	-4.5228710	6.0119361
H	-0.8578859	-3.4647801	8.0772028
H	-2.6137645	-2.3171471	9.4001042
H	-4.7966881	-1.3473368	9.5772963
H	-6.9456234	-0.6615524	8.5279192
H	-8.2942660	-0.2852557	6.5707032
H	-8.5203283	-0.1192633	4.0987229
H	-7.5157845	-0.0182578	1.9118851
H	-5.5058986	0.0857964	0.4615628
H	-3.1024719	0.2584852	0.2454012
H	1.9961206	-1.8763050	2.3137961
H	0.7332039	-2.7144538	3.2614299
H	1.9404290	-3.6547971	2.3440547
H	0.7891173	-5.5522925	1.6426120
H	-0.3129669	-7.1997880	0.1350038
H	-1.6646827	-6.4363147	-1.7902975
H	-1.9512792	-4.0504395	-2.2871198
H	-1.8759797	-2.3044822	-2.9778116
H	0.0444204	-0.6768152	-5.0164801
H	2.2232359	-0.5756830	-3.8933618
H	3.2725166	-2.6319371	-2.9845791
H	2.1498950	-4.8268822	-3.3101984
H	0.3613422	-6.1603505	-4.2057465
H	-1.7098373	-6.3325136	-5.5647431
H	-3.4175481	-5.3519690	-6.8766177
H	-4.5052391	-3.3435966	-7.8695110

H -4.7370772 -0.9932347 -8.0573970  
 H -4.2146458 1.3131813 -7.2777929  
 H -3.2609115 2.7864633 -5.6742963  
 H -2.0427890 3.1964393 -3.5497256  
 H -0.9792825 2.3576208 -1.5774985  
 C 2.3797466 1.9813844 -0.4393284  
 N 1.4543159 2.9337810 0.0636138  
 C 0.3427809 2.4327362 0.7272053  
 N -0.3888028 3.5209571 1.0902979  
 C -1.6479978 3.4913150 1.8252179  
 H -1.5240404 3.9864884 2.7927150  
 H -2.4209839 4.0071635 1.2487837  
 H -1.9264144 2.4489953 1.9655273  
 C 0.2280947 4.7001430 0.6739601  
 C -0.1645665 6.0263331 0.8252532  
 H -1.0831571 6.2899921 1.3389124  
 C 0.6751723 7.0027219 0.2854692  
 H 0.4056244 8.0502949 0.3787630  
 C 1.8592136 6.6478033 -0.3760193  
 H 2.4923591 7.4248115 -0.7929235  
 C 2.2510940 5.3156559 -0.5241144  
 H 3.1679101 5.0879679 -1.0485182  
 C 1.4163667 4.3329037 0.0105244  
 C 3.5214484 2.3354288 -1.1264179  
 H 3.7641287 3.3708747 -1.2979294  
 C 4.4109537 1.3455520 -1.6003311  
 C 5.6296896 1.6629242 -2.3194762  
 C 5.9603232 2.9777690 -2.8374481  
 C 5.0158656 4.0015497 -3.2449531  
 C 3.6850566 3.7328458 -3.7640472  
 C 3.2601913 2.4450025 -4.1719865  
 H 3.9533277 1.6149897 -4.1080162  
 C 1.9926034 2.2304469 -4.6762063  
 H 1.7035273 1.2372049 -5.0030180  
 C 1.0707787 3.2888216 -4.7795273  
 H 0.0676446 3.0999839 -5.1475839  
 C 1.4655062 4.5641129 -4.4350228  
 H 0.7843571 5.4043456 -4.5467505  
 C 2.7758227 4.8196955 -3.9650874  
 C 3.2128560 6.1617378 -3.7522287  
 H 2.4986658 6.9703657 -3.8830433  
 C 4.5196591 6.4182268 -3.4626123  
 H 4.8840694 7.4399436 -3.3889730  
 C 5.4547380 5.3560128 -3.2552160  
 C 6.8382998 5.6637032 -3.1228676  
 H 7.1447028 6.7064164 -3.1427324  
 C 7.7613250 4.6566671 -3.0827772  
 H 8.8265987 4.8716466 -3.1115219  
 C 7.3490685 3.3000828 -2.9536406  
 C 8.3286809 2.2669384 -2.9358620  
 H 9.3706684 2.5391531 -3.0831951  
 C 7.9548435 0.9620158 -2.7761004  
 H 8.6857512 0.1591492 -2.8326293

C 6.6160365 0.6387571 -2.4164594  
 C 6.2901631 -0.7099397 -2.0754396  
 H 7.0526297 -1.4719967 -2.2184373  
 C 5.0661955 -1.0317000 -1.5632022  
 H 4.8266560 -2.0608070 -1.3051147  
 C 4.1130052 -0.0129444 -1.2659375  
 C 2.9132923 -0.3247914 -0.5794745  
 H 2.7248641 -1.3767150 -0.3691077

***mer-(M, $\Delta$ Ir)-1b***

Total energy = -4360.666441 au

C -0.5217331 -2.9020346 0.5978917  
 C 0.3159290 -2.1058909 -0.1690348  
 C 1.3092295 -2.8136612 -0.9134413  
 C 1.4403425 -4.1874341 -0.9108445  
 C 0.5496274 -4.9883476 -0.1623947  
 C -0.4272453 -4.3166168 0.6362032  
 C -1.2461034 -5.0798581 1.5210932  
 C -1.0102097 -6.4108631 1.7155715  
 C -0.0217056 -7.1025005 0.9496086  
 C 0.6493124 -6.4332662 -0.1129269  
 C 0.3318803 -8.4397220 1.2871057  
 C 1.3719600 -9.0595502 0.6503846  
 C 1.9681546 -8.4676560 -0.4996924  
 C 1.4700965 -7.2265410 -1.0039086  
 C 3.0573734 -9.1140543 -1.1505398  
 C 3.6109815 -8.5786607 -2.2803591  
 C 2.9722449 -7.4902864 -2.9405712  
 C 1.8199565 -6.8828095 -2.3677142  
 C 3.4558012 -7.0602310 -4.2160921  
 C 2.7738914 -6.1412814 -4.9572332  
 C 1.5011698 -5.6667548 -4.5178167  
 C 0.9929398 -6.0677973 -3.2417922  
 C 0.7103498 -4.8560140 -5.3670692  
 C -0.5786351 -4.5080387 -5.0199865  
 C -1.1192845 -4.9811678 -3.8078060  
 C -0.3488889 -5.7299765 -2.9402817  
 Ir 0.4629607 0.0019969 -0.2434029  
 C 0.5704277 2.1031772 -0.3027263  
 N 2.1587534 -1.9591114 -1.6674238  
 C 1.9459865 -0.5935649 -1.5308927  
 N 2.8082256 -0.0010864 -2.4033905  
 C 3.5673662 -0.9519507 -3.0842979  
 C 3.1597775 -2.2175880 -2.6133906  
 C 3.7534540 -3.3757574 -3.1172896  
 C 4.7462193 -3.2244294 -4.0879867  
 C 5.1437994 -1.9622459 -4.5503842  
 C 4.5540372 -0.7979587 -4.0531324  
 C 2.9046478 1.4355284 -2.6315252  
 C -1.0565067 0.3328114 1.1454377  
 C -2.4072220 0.5554017 0.9357071  
 C -3.3112512 0.8845293 1.9770982  
 C -2.8478312 0.9576027 3.3272514  
 C -1.4658660 0.7641456 3.5478274

C	-0.6269285	0.4506454	2.4999579
C	-4.6632253	1.2297226	1.6802491
C	-5.4789880	1.7346100	2.6523404
C	-5.0398165	1.8279316	4.0088536
C	-3.7741062	1.2964696	4.3900578
C	-3.4617922	1.2335988	5.8054224
C	-4.1744803	2.1216500	6.6704902
C	-5.3747170	2.7445837	6.2242766
C	-5.8450247	2.5146724	4.9613494
C	-2.4971697	0.3480802	6.4288202
C	-1.9680546	0.7111513	7.6992722
C	-2.5553211	1.7737285	8.4425381
C	-3.6881580	2.3851704	7.9824809
C	-2.1202482	-0.9515960	5.9011897
C	-1.0246096	-1.6602707	6.4877814
C	-0.3890305	-1.1419891	7.6564111
C	-0.8822920	-0.0272489	8.2669150
C	-2.8403932	-1.6025858	4.8713487
C	-2.4470008	-2.8313526	4.3808450
C	-1.2986794	-3.4715579	4.8864244
C	-0.6122257	-2.8968045	5.9359919
N	0.7656891	0.2274827	2.6616312
C	1.4849015	-0.0463186	1.5101436
N	2.7718355	-0.2300406	1.9129620
C	2.8858174	-0.0898703	3.2971019
C	1.5989367	0.2145208	3.7865627
C	1.4004872	0.4276055	5.1512790
C	2.5105466	0.3195823	5.9912894
C	3.7849766	0.0099802	5.4965442
C	3.9930481	-0.2022695	4.1321551
C	3.8942567	-0.5495835	1.0390420
H	3.6859221	-0.1424972	0.0525626
H	4.7974263	-0.0865689	1.4399052
H	4.0351231	-1.6321650	0.9729316
H	4.9756603	-0.4477069	3.7433022
H	4.6228709	-0.0691754	6.1824243
H	2.3734887	0.4743356	7.0569605
H	0.4337052	0.6567192	5.5753040
H	-1.0797788	0.8910747	4.5459266
H	-3.7298592	-1.1342437	4.4691622
H	-3.0367061	-3.3031920	3.6004625
H	-0.9737825	-4.4211883	4.4717856
H	0.2472111	-3.3974764	6.3752558
H	0.4561228	-1.6819855	8.0749382
H	-0.4612652	0.3253708	9.2052696
H	-2.1363089	2.0250147	9.4135112
H	-4.2212108	3.1085412	8.5944030
H	-5.9220568	3.3734193	6.9218500
H	-6.7994088	2.9220992	4.6370209
H	-6.4780518	2.0906206	2.4122982
H	-5.0070797	1.1501802	0.6512704
H	-2.8117173	0.5250408	-0.0747778
H	2.2965145	1.9339134	-1.8779860

H	3.9471650	1.7534497	-2.5440146
H	2.5304871	1.6805423	-3.6289351
H	4.8521455	0.1833354	-4.4074450
H	5.9190725	-1.8875305	-5.3067539
H	5.2146545	-4.1151020	-4.4949067
H	3.4697441	-4.3682682	-2.7981336
H	2.2367063	-4.6714388	-1.4536918
H	-0.7917281	-6.0894657	-2.0200834
H	-2.1515062	-4.7601057	-3.5511281
H	-1.1826682	-3.9012536	-5.6888636
H	1.1317955	-4.5397809	-6.3181436
H	3.1551227	-5.8015094	-5.9164911
H	4.3806798	-7.4968156	-4.5848841
H	4.4872936	-9.0262591	-2.7419710
H	3.4559087	-10.0243339	-0.7095962
H	1.7353225	-10.0290442	0.9813710
H	-0.1852232	-8.9214314	2.1132618
H	-1.5639822	-6.9716992	2.4647768
H	-2.0164413	-4.5644843	2.0863433
H	-1.2726773	-2.4307669	1.2297969
C	-0.3094773	2.7264701	-1.2374310
N	-1.0023214	1.7953516	-2.0551722
C	-0.7783374	0.4498859	-1.7998099
N	-1.5175020	-0.2263694	-2.7189049
C	-1.5627349	-1.6757503	-2.8624090
H	-1.0693445	-2.1147888	-1.9978707
H	-2.6040309	-2.0053834	-2.9045828
H	-1.0456910	-1.9759413	-3.7774676
C	-2.2002914	0.6533580	-3.5580015
C	-3.0483962	0.4035191	-4.6324436
H	-3.2829920	-0.6082624	-4.9464354
C	-3.5830730	1.5127592	-5.2908851
H	-4.2499588	1.3630981	-6.1344261
C	-3.2666583	2.8154822	-4.8798935
H	-3.6881796	3.6616357	-5.4135310
C	-2.4137770	3.0626753	-3.8021316
H	-2.1868282	4.0828176	-3.5275570
C	-1.8775308	1.9592483	-3.1363454
C	-0.4895943	4.0900099	-1.3333035
H	-1.2000735	4.5095689	-2.0276020
C	0.2221058	4.9667187	-0.4849149
C	0.0610834	6.4050872	-0.5348584
C	-0.6004164	7.1140954	-1.6102567
C	-0.6792232	6.6784993	-2.9904512
C	0.3141159	5.8411034	-3.6419605
C	1.5862949	5.5731980	-3.0805273
H	1.8463415	6.0113963	-2.1253183
C	2.5164422	4.7902117	-3.7351897
H	3.4881350	4.6206702	-3.2798069
C	2.2155670	4.2162060	-4.9862836
H	2.9440791	3.5858457	-5.4886427
C	1.0046420	4.4955164	-5.5852457
H	0.7706675	4.1006405	-6.5709142

C	0.0546602	5.3342721	-4.9544494
C	-1.1288585	5.7299994	-5.6480627
H	-1.3230016	5.3105218	-6.6316266
C	-1.9549671	6.6720318	-5.1107048
H	-2.8087223	7.0472184	-5.6695989
C	-1.7225447	7.2032605	-3.8031902
C	-2.5021108	8.3034816	-3.3452914
H	-3.2886133	8.6883644	-3.9892383
C	-2.1872568	8.9236904	-2.1681182
H	-2.6890346	9.8400599	-1.8674525
C	-1.2239185	8.3582378	-1.2849704
C	-0.8815013	9.0319723	-0.0778700
H	-1.3334871	10.0003470	0.1210362
C	0.0315675	8.4887090	0.7839434
H	0.3583620	9.0322145	1.6670220
C	0.4890240	7.1532695	0.5982505
C	1.3252743	6.5418491	1.5831890
H	1.6886802	7.1589212	2.4015090
C	1.6496068	5.2166885	1.5085679
H	2.2998910	4.7610872	2.2521630
C	1.0614959	4.3812356	0.5117323
C	1.2294885	2.9748717	0.5518210
H	1.8815862	2.5807713	1.3300647

*fac-(M,A<sub>Ir</sub>)-1c*

Total energy = -4360.671831 au

C	-1.3731621	-0.2737110	1.2159774
C	-1.2420783	-0.2605847	2.6362890
N	0.1089630	-0.2646936	3.0755009
C	1.0759164	-0.3207591	2.0845693
N	2.2723371	-0.2697475	2.7340911
C	3.5709957	-0.3050822	2.0723508
H	3.4686729	-0.8772274	1.1515911
H	3.9110816	0.7065731	1.8367823
H	4.2930628	-0.7932435	2.7293303
C	2.0895022	-0.1761300	4.1145759
C	3.0124810	-0.0946165	5.1522568
H	4.0807339	-0.0779634	4.9628070
C	2.5063247	-0.0346153	6.4528583
H	3.1947410	0.0291953	7.2899249
C	1.1252384	-0.0584772	6.6910598
H	0.7578111	-0.0221859	7.7121194
C	0.1995535	-0.1327101	5.6474868
H	-0.8568771	-0.1568661	5.8732650
C	0.6966750	-0.1852784	4.3443454
C	-2.3155866	-0.2377570	3.5003036
H	-2.1702377	-0.2253952	4.5683986
C	-3.6346480	-0.2161462	2.9976785
C	-4.7970462	-0.2328733	3.8595680
C	-4.7577960	-0.5746394	5.2646841
C	-3.7828353	-1.4427119	5.8932647
C	-3.0885482	-2.5227976	5.2123140
C	-3.4868722	-3.0209055	3.9478500
H	-4.3550485	-2.5946979	3.4612334

C	-2.8100183	-4.0539807	3.3295115
H	-3.1493461	-4.4152752	2.3628078
C	-1.6901879	-4.6438720	3.9480997
H	-1.1568727	-5.4512157	3.4545801
C	-1.3026094	-4.2163368	5.2019586
H	-0.4678592	-4.6892873	5.7137240
C	-2.0036015	-3.1832317	5.8698054
C	-1.6812606	-2.8463751	7.2199223
H	-0.8338730	-3.3359620	7.6925927
C	-2.4751266	-1.9867124	7.9199507
H	-2.2945889	-1.7976615	8.9752903
C	-3.5673954	-1.3083004	7.2926228
C	-4.4677376	-0.5377642	8.0828779
H	-4.2869823	-0.4597973	9.1518696
C	-5.5890713	0.0035120	7.5166855
H	-6.3452835	0.4884813	8.1289438
C	-5.7673168	-0.0108052	6.1038648
C	-6.9465185	0.5391381	5.5239540
H	-7.7218932	0.9163175	6.1858844
C	-7.1139479	0.5473803	4.1658187
H	-8.0439027	0.8920520	3.7204297
C	-6.0339111	0.1997622	3.3050090
C	-6.1702325	0.3344273	1.8882668
H	-7.1442176	0.6092522	1.4905524
C	-5.1082426	0.1226245	1.0539481
H	-5.2262749	0.1950280	-0.0249388
C	-3.8032700	-0.1109124	1.5837655
C	-2.6687265	-0.1783328	0.7360538
H	-2.8365541	-0.1180860	-0.3375448
Ir	0.4254573	-0.3378308	0.1515088
C	-0.5733744	-0.3547624	-1.6849204
C	-0.9361686	-1.6460048	-2.1705240
N	-0.5665278	-2.7002986	-1.2927862
C	0.1166138	-2.3312244	-0.1454901
N	0.3374244	-3.4867494	0.5406884
C	1.0398689	-3.5621730	1.8165549
H	1.7979936	-2.7805536	1.8375791
H	0.3449729	-3.4197588	2.6478761
H	1.5192437	-4.5386335	1.9017416
C	-0.1964287	-4.5827081	-0.1393262
C	-0.2124471	-5.9359433	0.1828854
H	0.2265521	-6.3063798	1.1033400
C	-0.8184394	-6.8022813	-0.7300014
H	-0.8516033	-7.8657650	-0.5141925
C	-1.3824438	-6.3181888	-1.9184029
H	-1.8398715	-7.0139231	-2.6150800
C	-1.3703283	-4.9585108	-2.2385018
H	-1.8093513	-4.6260351	-3.1682692
C	-0.7720136	-4.0852652	-1.3287518
C	-1.5829666	-1.8542160	-3.3696246
H	-1.8415043	-2.8480570	-3.6978248
C	-1.9295931	-0.7599221	-4.1915712
C	-2.5673391	-0.9245569	-5.4799494

C	-2.6420239	-2.1823186	-6.1903687
C	-1.6991691	-3.2760243	-6.0684817
C	-0.2984085	-3.1155953	-5.7147171
C	0.3613803	-1.8623646	-5.7189037
H	-0.1884930	-0.9760541	-6.0090967
C	1.6960911	-1.7442611	-5.3835724
H	2.1707050	-0.7672432	-5.4044303
C	2.4438042	-2.8820911	-5.0222414
H	3.4912248	-2.7831593	-4.7522074
C	1.8464211	-4.1259054	-5.0528007
H	2.4190294	-5.0201468	-4.8183732
C	0.4890202	-4.2745310	-5.4271281
C	-0.0778126	-5.5756926	-5.5878110
H	0.5251203	-6.4434550	-5.3336254
C	-1.3226877	-5.7192557	-6.1251557
H	-1.7249193	-6.7062086	-6.3402011
C	-2.1370057	-4.5816077	-6.4240299
C	-3.3649693	-4.7573970	-7.1241616
H	-3.6708651	-5.7649588	-7.3938102
C	-4.0846784	-3.6688203	-7.5340121
H	-4.9562872	-3.7836276	-8.1735586
C	-3.7376966	-2.3611746	-7.0896835
C	-4.4830813	-1.2314916	-7.5342708
H	-5.2794387	-1.3886902	-8.2574035
C	-4.1694304	0.0252855	-7.0929643
H	-4.6817637	0.8993480	-7.4873929
C	-3.2356974	0.2035993	-6.0325242
C	-3.0073222	1.5046626	-5.4857533
H	-3.4864193	2.3542835	-5.9664273
C	-2.2081931	1.6790125	-4.3904672
H	-2.0117280	2.6745020	-3.9986008
C	-1.6863513	0.5527161	-3.6854364
C	-0.9857814	0.7134450	-2.4635063
H	-0.7984403	1.7286605	-2.1191505
C	0.5858347	1.7462875	0.1284346
C	1.7315498	2.2631346	-0.5465586
N	2.5632363	1.2508944	-1.0967988
C	2.1685371	-0.0567310	-0.8676928
N	3.0849814	-0.8368715	-1.5054864
C	3.0515096	-2.2949804	-1.5175276
H	2.6788395	-2.6402384	-0.5540750
H	2.3977193	-2.6578877	-2.3140498
H	4.0632335	-2.6718235	-1.6727900
C	4.0507246	-0.0556021	-2.1425822
C	5.1576987	-0.4148942	-2.9048579
H	5.3929496	-1.4536742	-3.1117639
C	5.9592193	0.6193634	-3.3937465
H	6.8328016	0.3791813	-3.9920908
C	5.6531629	1.9596042	-3.1202871
H	6.2985097	2.7442858	-3.5029143
C	4.5380760	2.3195851	-2.3599617
H	4.3415687	3.3638836	-2.1633494
C	3.7277971	1.2924826	-1.8737005

C	2.0031858	3.6091032	-0.6650178
H	2.8758305	3.9563311	-1.1941653
C	1.1281379	4.5648666	-0.1045805
C	1.3856270	5.9875796	-0.1671120
C	2.6634899	6.5640534	-0.5248891
C	3.9554872	5.9358400	-0.3342059
C	4.2492399	4.9650550	0.7070142
C	3.3916569	4.7309453	1.8094897
H	2.4777312	5.3043698	1.8995155
C	3.7023849	3.8051208	2.7862711
H	3.0234755	3.6578419	3.6215925
C	4.8948483	3.0589320	2.7084961
H	5.1320313	2.3276476	3.4760194
C	5.7771737	3.2945698	1.6735628
H	6.7222657	2.7596281	1.6199980
C	5.4954058	4.2635221	0.6804689
C	6.4753690	4.5940644	-0.3046923
H	7.4031050	4.0283932	-0.3292537
C	6.2752303	5.6510554	-1.1424032
H	7.0537827	5.9699241	-1.8310970
C	5.0407051	6.3739842	-1.1423825
C	4.9200896	7.5633087	-1.9168199
H	5.7679782	7.8814254	-2.5179596
C	3.7958083	8.3360837	-1.8190471
H	3.7400621	9.3057874	-2.3073555
C	2.6508607	7.8649476	-1.1155988
C	1.4913236	8.6849958	-1.0036298
H	1.5252691	9.6894718	-1.4178716
C	0.3798692	8.2299980	-0.3478756
H	-0.4789464	8.8775507	-0.1893269
C	0.2864762	6.8653763	0.0485803
C	-0.9274754	6.3617758	0.6111843
H	-1.7276704	7.0678748	0.8200216
C	-1.0815687	5.0301795	0.8788066
H	-1.9961699	4.6570143	1.3342801
C	-0.0822750	4.0897795	0.4853563
C	-0.2998452	2.6946214	0.6117730
H	-1.2262885	2.3692648	1.0811800

*fac-(M, $\Delta_{\text{lf}}$ )-1d*

Total energy = -4360.667150 au

C	-1.8425799	1.1513255	1.2084151
C	-0.5358870	0.7877145	1.4887939
C	-0.2144907	0.7014059	2.8769076
C	-1.1076485	0.9741850	3.8926631
C	-2.4433630	1.3234078	3.5961894
C	-2.8012598	1.4313062	2.2163934
C	-4.1013690	1.9040694	1.8694925
C	-4.9427792	2.3935636	2.8269597
C	-4.5940801	2.3368284	4.2114154
C	-3.4162080	1.6492486	4.6214046
C	-5.3943577	3.0207408	5.1701350
C	-4.9948741	3.0923022	6.4759612
C	-3.9020127	2.3050560	6.9384713

C	-3.2227924	1.4238711	6.0405877
C	-3.4918366	2.3920441	8.2991906
C	-2.4752410	1.6100608	8.7726663
C	-1.9566406	0.5538772	7.9711172
C	-2.4157889	0.3769094	6.6357253
C	-1.0222862	-0.3668690	8.5412948
C	-0.6222365	-1.4798070	7.8628779
C	-1.2111556	-1.8032760	6.6034379
C	-2.1518905	-0.9055624	6.0068349
C	-0.9104131	-3.0311445	5.9667216
C	-1.5668669	-3.4151677	4.8159730
C	-2.5740569	-2.5843874	4.2875475
C	-2.8514358	-1.3614932	4.8640545
N	1.1320836	0.3195797	3.1183198
C	1.9307991	0.1381668	2.0002114
N	3.1384626	-0.2788050	2.4779721
C	3.1237825	-0.3665945	3.8704959
C	1.8370907	0.0267941	4.2929000
C	1.5261733	0.0575753	5.6528264
C	2.5243717	-0.3188396	6.5541832
C	3.7981256	-0.7148935	6.1245055
C	4.1190518	-0.7460956	4.7655745
C	4.2995785	-0.6084717	1.6609073
H	4.2080884	-0.0828742	0.7129073
H	5.2040748	-0.2789652	2.1759173
H	4.3509705	-1.6863454	1.4824571
H	5.1012120	-1.0562908	4.4247067
H	4.5463100	-1.0035850	6.8563516
H	2.2972778	-0.3072509	7.6155339
H	0.5548229	0.3473691	6.0265496
H	-0.7953685	0.9521632	4.9242555
H	-3.6365140	-0.7468428	4.4423951
H	-3.1472430	-2.9034149	3.4220883
H	-1.3290891	-4.3601998	4.3369171
H	-0.1645625	-3.6792079	6.4205309
H	0.1069040	-2.1635005	8.2894541
H	-0.6440638	-0.1576195	9.5389457
H	-2.1098115	1.7201928	9.7903509
H	-3.9871102	3.1153873	8.9421667
H	-5.5248233	3.7146556	7.1925214
H	-6.2782309	3.5517025	4.8253551
H	-5.8922101	2.8491781	2.5555748
H	-4.3784203	1.9290308	0.8203253
H	-2.1530078	1.2725763	0.1723524
Ir	1.0644213	0.4577695	0.1754581
C	0.7200349	-1.6063664	0.0578002
C	1.6827697	-2.3447927	-0.6940496
N	2.6651412	-1.5224315	-1.3076563
C	2.5741448	-0.1621844	-1.0563986
N	3.5663498	0.4127548	-1.7948599
C	3.8477816	1.8413048	-1.8601621
H	3.4419928	2.3074994	-0.9650905
H	4.9285329	1.9927405	-1.8944851

H	3.3869422	2.2829709	-2.7483060
C	4.2840039	-0.5494638	-2.5061267
C	5.3634961	-0.4171933	-3.3737813
H	5.7826936	0.5540937	-3.6144480
C	5.8831676	-1.5900959	-3.9259561
H	6.7261417	-1.5312613	-4.6076371
C	5.3294859	-2.8391060	-3.6138412
H	5.7473308	-3.7362178	-4.0596010
C	4.2427772	-2.9678900	-2.7460638
H	3.8397184	-3.9491664	-2.5418203
C	3.7160266	-1.8011871	-2.1909331
C	1.6791326	-3.7197944	-0.8099326
H	2.4654845	-4.2322482	-1.3402312
C	0.6593022	-4.4861688	-0.2040829
C	0.6205265	-5.9347031	-0.2686565
C	1.4523418	-6.7422672	-1.1394209
C	1.9750663	-6.3427777	-2.4313676
C	1.3349917	-5.3759469	-3.3064825
C	0.0155534	-4.9062686	-3.1019373
H	-0.5626099	-5.2927369	-2.2722637
C	-0.5628314	-3.9842944	-3.9507249
H	-1.5842524	-3.6644028	-3.7674519
C	0.1555440	-3.4677478	-5.0466105
H	-0.2925924	-2.7169017	-5.6905336
C	1.4198909	-3.9508620	-5.3124428
H	1.9736788	-3.6030621	-6.1810850
C	2.0155876	-4.9318641	-4.4840231
C	3.2657710	-5.5186643	-4.8449701
H	3.7783685	-5.1523783	-5.7305038
C	3.7665341	-6.5626827	-4.1252666
H	4.6730733	-7.0725866	-4.4419637
C	3.1139211	-7.0279478	-2.9406396
C	3.5719681	-8.2211468	-2.3134683
H	4.4420340	-8.7259239	-2.7252810
C	2.8576872	-8.7709829	-1.2856474
H	3.1184621	-9.7462074	-0.8820869
C	1.7759589	-8.0609614	-0.6914568
C	1.0127639	-8.6705637	0.3448196
H	1.2488470	-9.6928043	0.6291975
C	-0.0249744	-7.9964965	0.9266165
H	-0.6671370	-8.4808618	1.6580657
C	-0.2153755	-6.6097112	0.6663568
C	-1.2084960	-5.8827590	1.3920831
H	-1.8876292	-6.4415316	2.0317428
C	-1.2929574	-4.5232752	1.2982350
H	-2.0614360	-3.9752824	1.8342626
C	-0.3183793	-3.7828662	0.5661293
C	-0.2637058	-2.3685746	0.6654407
H	-1.0129704	-1.8791512	1.2845979
C	-0.0673394	0.8839660	-1.5367425
C	-0.0629037	2.2508658	-1.9485060
N	0.6484854	3.1010510	-1.0604289
C	1.2616853	2.4874944	0.0208890

N	1.8155622	3.4991733	0.7489846
C	2.5585509	3.3325824	1.9918526
H	2.9511496	2.3184600	2.0186198
H	3.3848179	4.0459692	2.0132924
H	1.9071369	3.4994233	2.8544727
C	1.5675281	4.7377964	0.1563198
C	1.9353854	6.0207920	0.5491342
H	2.4978115	6.1963451	1.4601401
C	1.5449801	7.0759265	-0.2784957
H	1.8120640	8.0930165	-0.0084003
C	0.8124700	6.8389271	-1.4494868
H	0.5171033	7.6758243	-2.0744328
C	0.4404615	5.5501713	-1.8384741
H	-0.1327349	5.4130777	-2.7438753
C	0.8241597	4.4901152	-1.0162874
C	-0.6701639	2.7104389	-3.0993968
H	-0.5847031	3.7436733	-3.3951579
C	-1.3873564	1.8240955	-3.9328654
C	-2.0213998	2.2451897	-5.1676446
C	-2.2103630	3.6263971	-5.5668312
C	-2.3823194	4.7569249	-4.6753610
C	-2.9524106	4.6656196	-3.3422946
C	-3.6212822	3.5121538	-2.8673254
H	-3.7410949	2.6600885	-3.5242532
C	-4.1474537	3.4555172	-1.5925338
H	-4.6679184	2.5570298	-1.2745072
C	-4.0201623	4.5492449	-0.7141489
H	-4.4053476	4.4860431	0.2991240
C	-3.4319069	5.7122223	-1.1658198
H	-3.3672547	6.5857022	-0.5215282
C	-2.9270546	5.8105200	-2.4844813
C	-2.4417045	7.0581101	-2.9799516
H	-2.4099146	7.9106784	-2.3067172
C	-2.0900143	7.1850082	-4.2910086
H	-1.8015453	8.1507946	-4.6986407
C	-2.0985520	6.0596596	-5.1738118
C	-1.8872014	6.2637738	-6.5668117
H	-1.6756139	7.2695690	-6.9203090
C	-2.0605318	5.2292342	-7.4434363
H	-2.0312349	5.3951036	-8.5174667
C	-2.2456989	3.8993200	-6.9699882
C	-2.4732784	2.8433166	-7.8978635
H	-2.5461404	3.0887932	-8.9542840
C	-2.6468576	1.5609470	-7.4562870
H	-2.9045030	0.7612734	-8.1463668
C	-2.3837294	1.2285274	-6.0971117
C	-2.4248995	-0.1380014	-5.6821416
H	-2.7886680	-0.8782103	-6.3908892
C	-2.0050519	-0.5071570	-4.4365826
H	-2.0570525	-1.5429148	-4.1161664
C	-1.4043354	0.4440647	-3.5601206
C	-0.7548678	0.0194348	-2.3722675
H	-0.7720562	-1.0443173	-2.1431691

## II.4. References

- 
- <sup>1</sup> TURBOMOLE V7.3 2018, a development of University of Karlsruhe and Forschungszentrum Karlsruhe GmbH, 1989-2007, TURBOMOLE GmbH, since 2007; available from <http://www.turbomole.com>.
- <sup>2</sup> R. Ahlrichs, M. Bär, M. Häser, H. Horn, C. Kölmel, *Chem. Phys. Lett.* **1989**, *162*, 165-169.
- <sup>3</sup> F. Furche, R. Ahlrichs, C. Hättig, W. Klopper, M. Sierka, F. Weigend, *WIREs Comput. Mol. Sci.* **2014**, *4*, 91-100.
- <sup>4</sup> S. G. Balasubramani, G. P. Chen, S. Coriani, M. Diedenhofen, M. S. Frank, Y. J. Franzke, F. Furche, R. Grotjahn, M. E. Harding, C. Hättig, A. Hellweg, B. Helmich-Paris, C. Holzer, U. Huniar, M. Kaupp, A. Marefat Khah, S. Karbalaei Khani, T. Müller, F. Mack, B. D. Nguyen, S. M. Parker, E. Perlt, D. Rappoport, K. Reiter, S. Roy, M. Rückert, G. Schmitz, M. Sierka, E. Tapavicza, D. P. Tew, C. van Wüllen, V. K. Voora, F. Weigend, A. Wodynski, J. M. Yu, *J. Chem. Phys.* **2020**, *152*, 184107.
- <sup>5</sup> S. Grimme, J. Antony, S. Ehrlich, H. Krieg, *J. Chem. Phys.* **2010**, *132*, 154104.
- <sup>6</sup> S. Grimme, S. Ehrlich, L. Goerigk, *J. Comput. Chem.* **2011**, *32*, 1456-1465.
- <sup>7</sup> J. Tomasi, B. Mennucci, R. Cammi, *Chem. Rev.* **2005**, *105*, 2999-3094.
- <sup>8</sup> A. Klamt, G. J. Schürmann, *J. Chem. Soc., Perkin Trans. 2* **1993**, 799-805.
- <sup>9</sup> A. D. Becke, *Phys. Rev. A* **1988**, *38*, 3098-3100.
- <sup>10</sup> J. P. Perdew, *Phys. Rev. B* **1986**, *33*, 8822-8824.
- <sup>11</sup> J. P. Perdew, *Phys. Rev. B* **1986**, *34*, 7406.
- <sup>12</sup> A. Schäfer, H. Horn, R. Ahlrichs, *J. Chem. Phys.* **1992**, *97*, 2571-2577.
- <sup>13</sup> K. Eichkorn, F. Weigend, O. Treutler, R. Ahlrichs, *Theor. Chem. Acc.* **1997**, *97*, 119-124.
- <sup>14</sup> F. Weigend, R. Ahlrichs, *Phys. Chem. Chem. Phys.* **2005**, *7*, 3297- 3305.
- <sup>15</sup> D. Andrae, U. Häußermann, M. Dolg, H. Stroll, H. Preuß, *Theoret. Chim. Acta* **1990**, *77*, 123-141.
- <sup>16</sup> J. M. Tao, J. P. Perdew, V. N. Staroverov, G. E. Scuseria, *Phys. Rev. Lett.* **2003**, *91*, 146401.
- <sup>17</sup> M. Bühl, H. Kabrede, *J. Chem. Theory Comput.* **2006**, *2*, 1282-1290.
- <sup>18</sup> M. Bühl, C. Reimann, D. A. Pantazis, T. Bredow, F. Neese, *J. Chem. Theory Comput.* **2008**, *4*, 1449-1459.
- <sup>19</sup> S. Grimme, J. Gerit Brandenburg, C. Bannwarth, A. Hansen, *J. Chem. Phys.* **2015**, *143*, 054107.
- <sup>20</sup> K. Eichkorn, O. Treutler, H. Öhm, M. Häser, R. Ahlrichs, *Chem. Phys. Lett.* **1995**, *240*, 283-290.
- <sup>21</sup> K. Eichkorn, F. Weigend, O. Treutler, R. Ahlrichs, *Theor. Chem. Acc.* **1997**, *97*, 119-124.
- <sup>22</sup> A. D. Becke, *J. Chem. Phys.* **1993**, *98*, 5648-5652.
- <sup>23</sup> C. Lee, W. Yang, R. G. Parr, *Phys. Rev. B*, **1988**, *37*, 785-789.
- <sup>24</sup> P. J. Stephens, F. J. Devlin, C. F. Chabalowski, M. J. Frisch, *J. Phys. Chem.* **1994**, *98*, 11623-11627.
- <sup>25</sup> C. Adamo, V. Barone, *J. Chem. Phys.* **1999**, *110*, 6158-6169.
- <sup>26</sup> N. Hellou, C. Jahier-Diallo, O. Baslé, M. Srebro-Hooper, L. Toupet, T. Roisnel, E. Caytan, C. Roussel, N. Vanthuyne, J. Autschbach, M. Mauduit, J. Crassous, *Chem. Comm.* **2016**, *52*, 9243-9246.
- <sup>27</sup> N. Hellou, M. Srebro-Hooper, L. Favereau, F. Zinna, E. Caytan, L. Toupet, V. Dorcet, M. Jean, N. Vanthuyne, J. A. G. Williams, L. Di Bari, J. Autschbach, J. Crassous, *Angew. Chem. Int. Ed.* **2017**, *56*, 8236-8239.
- <sup>28</sup> Gaussian 16, Revision C.01, M. J. Frisch, G. W. Trucks, H. B. Schlegel, G. E. Scuseria, M. A. Robb, J. R. Cheeseman, G. Scalmani, V. Barone, G. A. Petersson, H. Nakatsuji, X. Li, M. Caricato, A. V. Marenich, J. Bloino, B. G. Janesko, R. Gomperts, B. Mennucci, H. P. Hratchian, J. V. Ortiz, A. F. Izmaylov, J. L. Sonnenberg, D. Williams-Young, F. Ding, F. Lipparini, F. Egidi, J. Goings, B. Peng, A. Petrone, T. Henderson, D. Ranasinghe, V. G. Zakrzewski, J. Gao, N. Rega, G. Zheng, W. Liang, M. Hada, M. Ehara, K. Toyota, R. Fukuda, J. Hasegawa, M. Ishida, T. Nakajima, Y. Honda, O. Kitao, H. Nakai, T. Vreven, K. Throssell, J. A. Montgomery, Jr., J. E. Peralta, F. Ogliaro, M. J. Bearpark, J. J. Heyd, E. N. Brothers, K. N. Kudin, V. N. Staroverov, T. A. Keith, R. Kobayashi, J. Normand, K. Raghavachari, A. P. Rendell, J. C. Burant, S. S. Iyengar, J. Tomasi, M. Cossi, J. M.

---

Millam, M. Klene, C. Adamo, R. Cammi, J. W. Ochterski, R. L. Martin, K. Morokuma, O. Farkas, J. B. Foresman, and D. J. Fox, Gaussian, Inc., Wallingford CT, 2016.

<sup>29</sup> A. D. Becke, *J. Chem. Phys.* **1993**, *98*, 1372-1377.

<sup>30</sup> M. Cossi, V. Barone, *J. Chem. Phys.* **2001**, *115*, 4708-4717.

<sup>31</sup> J. Autschbach, T. Ziegler, S. J. A. van Gisbergen, E. J. Baerends, *J. Chem. Phys.* **2002**, *116*, 6930-6940.

<sup>32</sup> I. Tamm, *J. Phys. USSR* **1945**, *9*, 449.

<sup>33</sup> S. M. Dancoff, *Phys. Rev.* **1950**, *78*, 382.

<sup>34</sup> S. Hirata, M. Head-Gordon, *Chem. Phys. Lett.* **1999**, *314*, 291-299.

<sup>35</sup> M. J. G. Peach, M. J. Williamson, D. J. Tozer, *J. Chem. Theory Comput.* **2011**, *7*, 3578-3585.

<sup>36</sup> M. J. G. Peach, D. J. Tozer, *J. Phys. Chem. A* **2012**, *116*, 9783-9789.

<sup>37</sup> M. J. G. Peach, N. Warner, D. J. Tozer, *Mol. Phys.* **2013**, *111*, 1271-1274.

<sup>38</sup> G. Scalmani, M. J. Frisch, B. Mennucci, J. Tomasi, R. Cammi, V. Barone, *J. Chem. Phys.* **2006**, *124*, 094107.

<sup>39</sup> R. Cammi, B. Mennucci, J. Tomasi, *J. Phys. Chem. A* **2000**, *104*, 5631-5637.